University of Stavanger

Faculty of Science and Technology

MASTER THESIS

Study program/ Specialization: Petroleum Engineering - Well Engineering (PETMAS)	Spring semester, 2015 Open
Writer: Thomas Sharman	…… (Writer's signature)
Faculty supervisor: Mesfin Agonafir Belayneh Bernt Sigve Aadnøy	
Thesis title: Characterization and Performance Study of OBM at Various Oil-Water Ratios	
Credits (ECTS): 30	
Key words: Barite Sag Viscoelasticity Rheology Barite Sag Oil Based Drilling Fluids Wellbore Hydraulics Simulation Cuttings Transport Simulation	Pages: 114 enclosure: 20 Stavanger, 15.06.2015

Master Thesis
PETMAS

Characterization and Performance Study of OBM at Various Oil-Water Ratios

Universitetet
i Stavanger

Thomas Sharman

University of Stavanger

June 15, 2015

Abstract

Drilling fluids are an essential part of the drilling operation. One of the main functions of a properly maintained drilling fluid is to suspend cuttings, as well as weighting materials, in static conditions. Insufficient gel strength or low-shear viscosity can enhance settling of weight material, known as barite sag. Some drilling fluids display elastic and viscous characteristics at low shear rates. This means that the fluid possess solid-like and liquid-like qualities. This is known as viscoelasticity. It is thought that viscoelastic behavior can give an advantageous knowledge about dynamic settlement. This involves studies of drilling fluids viscoelastic behavior at deformation rates far below the conventional viscometer range.

This study assess the influence of increasing water fraction in oil based drilling fluids with the use of viscoelastic measurements, computing of the Unified hydraulics model and cuttings transport simulation. Four different oil based drilling fluids were used in this study. The density was equal for all samples at 1750 kg/m^3 with an oil-water ratio increasing from 60:40 towards 90:10 and at the same time keeping the viscosifying-clay concentration constant.

The experiments conducted in this thesis included dynamic and static sag measurements to asses which fluid was most susceptible for barite sag. In addition to conventional rheological methodology, a total of five different types of viscoelastic measurements was included in the search for a qualitative characterization. Viscosity profiles at shear rates far beyond conventional viscometer was obtained from a shear rate ramp. In the evaluation of yield stress in drilling fluids, a controlled stress ramp was performed.

A performance evaluation has been performed with the use of hydraulic wellbore simulation and cuttings transport simulation. This was performed by computing the Unified hydraulics model and by using Landmark's WellPlan.

The experimental investigations shows that the water fraction in oil based drilling fluids has a significant impact when the drilling fluid was formulated with 7 kg/m^3 organophilic clay. The fluid sample with the lowest water fraction showed a behavior of a viscoelastic liquid, while the remaining samples showed viscoelastic gel characteristics. These characteristics are shown to be time and temperature dependent. The characterizations also included a yield stress evaluation based upon five different measurements techniques, which reveal that the apparent yield stress is much lower than estimated by the Herschel-Bulkley model and Bingham Plastic model. Hydraulic simulation showed that a higher water fraction impose an increase in ECD and pump pressure, while the cuttings transport simulation showed a beneficial effect from the increased water fraction. This is primarily caused by the higher viscosity.

Acknowledgements

First, I would like to express my sincere gratitude to my supervisor, associate professor Mesfin Agonafir Belayneh, for his commitment and guidance throughout this master thesis. I would also thank Kim André Vorland, Head Engineer at the Faculty of Science and Technology at UiS, for his assistance and guidance with the Anton Paar rheometer.

Also, I would like to thank M-I Swaco for providing the drilling fluids used in this thesis.

Table of Contents

List of Figures

List of Tables

Abbreviations

API American Petroleum Institute

BHA Bottom Hole Assembly

BHP Bottom Hole Pressure

DHAST Dynamic High Angle Sag Tester

ECD Equivalent Circulation Density

ES Electrical Stability

H-B Herschel–Bulkley

HTHP High Temperature - High Pressure

lpm Liter Per Minute

LSYP Low-Shear Yield Point

LVE Linear Viscoelastic

N/A Not applicable

NCS Norwegian Continental Shelf

OBM Oil Based Mud

OWR Oil Water Ratio

PV Plastic Viscosity

RPM Revolutions per minute

VSST Viscometer Sag Shoe Test

WBM Water Based Mud

YP Yield Point

Nomenclature

η Viscosity

ρ Density

η^* Complex Viscosity

G' Storage modulus or Elastic Modulus

G'' Loss modulus or Viscous Modulus

G^* Complex modulus

$\dot{\gamma}$ Shear rate

δ Phase Angle

$\tan(\delta)$ Damping Factor

ω Angular Frequency

θ Dial Reading on Viscometer

Ω Share Rate on Viscometer

g Free fall acceleration constant

τ^* Shear stress value corresponding to geometric mean of the shear rate $\dot{\gamma}^*$

$\dot{\gamma}^*$ Shear rate value corresponding to geometric mean of the shear stress τ^*

n Flow behavior index

K Consistency index

τ Shear Stress

A Robertson and Stiff model parameter similar to K

B Robertson and Stiff model parameter similar to n

C Robertson and Stiff model correction parameter

1 Introduction

Drilling fluids plays an essential role in the drilling process. In order to drill a well successfully, the fluid need to carry drilled cuttings out from the well along annular space to the surface. This is controlled by the rheological properties of the drilling fluid. A well conditioned drilling fluid should be able to suspend drilled cuttings, as well as weighting agents, when circulation comes to rest and at the same time have a low viscosity during circulation to avoid excessive frictional pressure. High frictional pressure may induce severe well problems such as lost circulation and well collapse. During static conditions and low fluid velocities, a gel-structure should be established by the fluid to avoid particles to settle out. This is achieved if the gel-structure is developed quickly and has sufficient strength, which do not increase extensively in time. These types of characteristics must be present over a range of pressures and temperatures, from low temperatures at the sea floor to high reservoir temperatures. This has evolved drilling fluids into complex fluids with rheological behavior that is complicated to characterize.

During static and dynamic conditions, weighting agents may settle out of suspension. This phenomenon is known as barite sag and is recognized as a concern during drilling and completion as it can lead to well-control issues, lost circulation and wellbore instability. Barite sag tend to be more extensive in OBM than in WBM, and is most severe in inclined wellbores where fluid velocity is low. Both static and dynamic sag are complex phenomenon which is not fully understood despite the broad amount of research conducted over the past decade.

From rheology modeling it is common to assume that drilling fluids are purely viscous and time independent. This is primarily caused by practical reasons. Current literature states that drilling fluids are both viscous and elastic. This type of behavior cannot be characterized with the use of conventional couette rotational viscometer. In order to study structural behavior of drilling fluids, one need to examine the fluids at shear rates far below of what is achievable with conventional viscometers.

This thesis presents experimental characterization and performance study of four different oil based drilling fluids with constant density and increasing water fraction. The characterization includes rheology, viscoelasticity, and barite sag measurements. Performance evaluation is based upon cuttings transport simulation and computing of a rheology model to obtain wellbore hydraulics.

1.1 Problem Formulation

Due to the above mentioned reasons, adequate knowledge and characterization of drilling fluids is necessary in order to understand the involved mechanisms in drilling fluids. This thesis will attempt to assess the influence of increasing water fraction in oil based drilling fluids with regards to viscoelasticity, rheology and barite sag. Also the question about yield stress in drilling fluids will be investigated. In addition, the performance of each of drilling fluid will be studied to address how the OWR impact wellbore hydraulics and cuttings transport.

1.2 Objectives

The main objective of this thesis is;

- Assess a fundamental understanding of drilling fluids.
- Review literature of drilling fluid behavior in relation to barite sag.
- Perform dynamic and static sag analysis.
- Characterize the behavior of oil based drilling fluid with the use of viscoelastic measurements and conventional rheological measurements.
- Conduct a performance analysis in terms of wellbore hydraulics and cuttings transport simulation.

2 Theory

This section contains fundamental background theory about rheology and viscoelasticity of drilling fluids, which is necessary to understand the content of the experiments performed in this report.

2.1 Rheology

Rheology is the study of structural change under applied force. The most common way to define Rheology is "*the study of deformation and flow of matter*" [1]. The subject of rheology can involve a great deal of mathematical and physical analysis depending if what type of approach is wanted [2]. Rheology measurements in drilling fluids are important in order to characterize fluid flow behavior and the related hydraulics under different temperature, pressure and shear rate. Rheology and hydraulics are interrelated studies of fluid behavior [3]. There are two fundamental flow regimes that can exist, which is depending on the fluid velocity, viscosity, fluid density and flow area.

- **Laminar flow regime** where the fluid moves in a smooth, defined pattern. The flow equations are determined analytically. Such flow regime occurs when fluid is moving with low velocity or when fluid is viscous.
- **Turbulent flow regime** where the fluid moves in a chaotic pattern as it moves along the flow channel. The flow equations are empirical using friction factor concept.

In laminar flow the viscous forces are dominating whilst in turbulent flow inertial forces are dominating [4, 5].

2.1.1 Viscosity

Viscosity can be described as a substance resistance to flow and is the most familiar term used in rheology. On a daily basis a liquid is often referred to as "thick" or "thin", which essential is describing a substance's resistance to flow. Viscosity is defined as [6]:

$$\eta = \frac{\tau}{\dot{\gamma}} \tag{2.1}$$

τ is the shear stress, $\dot{\gamma}$ is the shear rate. In the literature, the shear-rate independent viscosity is often denoted as μ while the shear rate dependent viscosity is often denoted with $\eta = \eta(\dot{\gamma})$. To avoid any misconceptions, the symbol used for viscosity in this thesis is denoted as η. Among the factors that is affecting a pure (Newtonian) liquids viscosity is temperature and pressure, where the temperature effect is predominant. The temperature effect is inverse proportional with viscosity and is more dominant for high viscosity substances than for low viscosity substances. Due to the temperature effect on viscosity it is important to note what temperature the viscosity is measured at and also to be consistent and accurate when doing viscosity measurement. The pressure contribution on viscosity is usually small and can be neglected in most circumstances, nonetheless when the pressures increases the viscosity will increase [7]. Since drilling fluids usually does not have a constant viscosity, a more thorough review about external effects on viscosity is given in section 2.1.5 and section 2.1.7.

The unit of viscosity, η, is given as $\mathrm{Pa}\cdot\mathrm{s}$ in the SI system, or centiPoise in oilfield units, signified cP. For water this unit is only 0.001 $\mathrm{Pa}\cdot\mathrm{s}$ at 20.2 °C, thereof the prefix *milli* is necessary, hence $\mathrm{mPa}\cdot\mathrm{s}$. Numerically, $1\,\mathrm{mPa}\cdot\mathrm{s} \equiv 1\mathrm{cP}$. [5, 7].

2.1.2 Shear Rate and Shear Stress

In any situations where it is flow, we have the concepts of shear rate and shear stress. One may imagine laminar fluid flow as a hypothetical stack of small plates upon each other resting on a stationary plane surface. When a force, F, is then applied on the top plate it will move with a higher velocity than the plate below it due to frictional resistance. In the simplest case the velocity of the plates below the upper one will increase linearly, from zero to **u**, as shown in figure 1.

The force per unit area creating the flow or produced by flow is known as shear stress, τ, and is given as:

$$\frac{F}{A} = \tau = \eta\frac{\mathrm{du}}{\mathrm{dr}} \tag{2.2}$$

Where r is the distance from one plate to another and u is the velocity for the uppermost plate. Shear stress is reported in standard oil field units as pounds of force per hundred square feet required to maintain the shear rate ($\mathrm{lb}/100\,\mathrm{ft}^2$). This is approximately what is read off the viscometer dial readings, (θ), since one degree

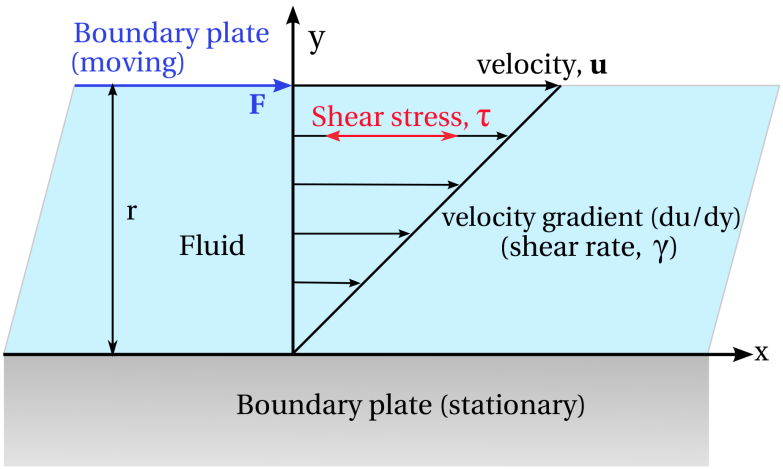

Figure 1: Illustration of shear stress in laminar flow regime for a Newtonian fluid. Adapted from [8]

deflection on the dial reading is equal to 1.067lb/100 ft^2.

$$\tau(\text{lb}/100\,\text{ft}^2) = 1.067 \cdot \theta \tag{2.3}$$

The velocity gradient, or the rate at which one plate is moving relative to the next plate is known as shear rate, often denoted as $\dot{\gamma}$. The unit for shear rate is given in reciprocal seconds (s^{-1}) and is equal to the Fann VG mud viscometer RPM (Ω) multiplied by 1.703 [3, 5, 7].

$$\dot{\gamma}(s^{-1}) = 1.703 \cdot \Omega \tag{2.4}$$

2.1.3 Yield Stress

Yield stress is the amount of stress required to overcome before flow initiates in a liquid. In drilling fluids this is as measurement of the the electro-chemical and/or attractive forces caused by the orientation and concentration of solids (colloidal size) within the drilling fluid [3]. Applying a stress lower than a certain minimum value will cause the liquid to behave elastically and no permanent deformation will occur. Another term for yield stress is *yield point* (YP), where the latter is primarily used for the Bingham Plastic model, which will be discussed in section 2.2.1. There has been considerable discussion in the scientific literature about the yield stress

concept and the modeling of yield stress fluids, mainly caused by limitations in measuring flow at very low applied stress. The models containing a yield stress that are being mentioned in section 2.2 predicts that the liquid will be stationary if the applied stress is below the yield stress and that only elastic behavior is seen [9]. The yield stress concept will be discussed further in section section 3.1.1.

2.1.4 Plastic Viscosity

Plastic viscosity (PV) is a parameter in the Bingham plastic model and is frequently described as the resistance to flow due to mechanical friction. Many drilling fluids engineers find this as an important measure of the drilling fluid because it give an relative indication of solids concentration in the mud. Plastic viscosity is also directly affected by the viscosity of the base fluid for OBM. In oil based mud poor shearing, or poorly emulsified water in oil, can cause water droplets to coalesce and act like fine solids and thus increase the PV. Plastic viscosity is reported in centiPoise (cP) or in Pascal-seconds (Pa s) [6].

2.1.5 Thixotropy and Shear Thinning

Liquids that have a viscosity that decreases with time of shear is called thixotropic. This is a time-dependent flow behavior and should not be confused with shear thinning, which is decrease of viscosity with increase in shear rate. One can expect thixotropic behavior for a shear thinning fluid though they occur due to different effects. Most drilling fluids exhibit thixotropic properties and are highly shear-thinning, due to clay or polymeric viscosifiers used in them. The thixotropic effect is a completely reversible process such that the micro-structure within the fluid is fully restored when the fluid has come to rest [10]. This implies that the fluid has some kind of structural "memory" which is time dependent. During the process of drilling a well, drilling fluid is pumped at high rate through the drill string and passes through the bit before reaching annular space. Due to the shear thinning behavior, the drilling fluid will have a low viscosity at high shear rates for instance when being pumped down the drill string and through the bit. Further the drilling fluid will have a higher viscosity in annular space, which is crucial to carry out drilled cuttings out of the well. When circulation comes at rest, during a connection, the thixotropic behaviour of the drilling fluid will develop a

gel structure which will prevent cuttings to fall out of suspension. One measure of the degree of shear thinning is the yield point to plastic viscosity ratio (YP/PV), the higher the ratio the greater the thinning. Too high gel strength can cause excessive pump pressures when breaking circulation and can also lead to poor solids removal efficiency at surface. Furthermore, when pulling out of hole, high gel strength can reduce the bottomhole pressure (BHP), also known as swabbing. This can be critical if the BHP is reduced below the pore pressure and in this way initiate an influx of formation fluids. On the other hand, if running too fast into the hole where the gel strength is too high can cause excessive surge pressure which can provoke lost circulation. Gel strength is measured usually 10sec and 10min after agitation ceases on a conventional rotational viscometer. In some cases a 30min gel strenght can be taken to ensure that the drilling fluid has a flat gel profile. Progressive gels is a situation where the 30min gel strenght is much larger than 10min gel, and can be used as a indication of ultra fine solids build up in fluid system.
In contrast to thixotropy is rheopexy, or anti-thixotropy in some litterature, which a increase in viscosity over time. This kind of characteristics does not represent drilling fluids and will for that reason not be elaborated any further [3, 5].

2.1.6 Newtonian Fluids

All liquids can be divided as either *Newtonian* or *non-Newtonian* defined by their relationship between shear rate and shear stress. Newtonian liquids have a constant viscosity that will not vary with deformation rate or time, under constant pressure and temperature. The rheological behavior can be described by Newton's law of viscosity. These properties can be formulated by the following equation:

$$\tau = \eta \cdot \dot{\gamma} \tag{2.5}$$

Where η is the viscosity in $\mathrm{Pa} \cdot \mathrm{s}$, τ is the shear stress in Pa and $\dot{\gamma}$ is shear rate in s^{-1}. When shear stress (τ) is plotted against shear rate ($\dot{\gamma}$) it will be a linear plot, which is intersecting through the origin, as seen in figure 2. This kind of plot is also known as a flow curve, or a consistency curve, for a flow model. The slope of the curve will then define the viscosity, η. Since the viscosity is constant, the viscosity determined at an arbitrary steady-state shear rate may be used in hydraulic calculations for flow at other shear rates. Pure fluids such as water, brine and oil exhibits Newtonian

properties. It should be noted that for high enough shear rate, any Newtonian liquid will become non-Newtonian[5, 7].

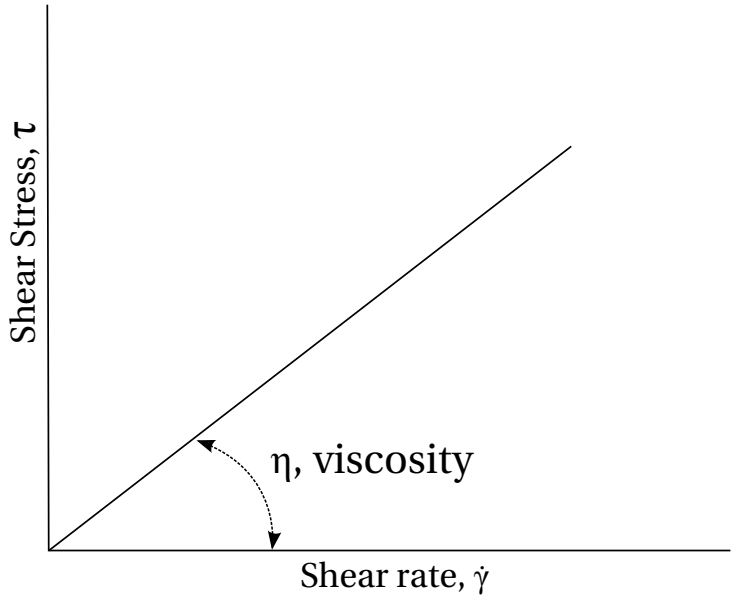

Figure 2: Flow curve of a Newtonian fluid. Adapted from Caenn et al. [5]

2.1.7 Non-Newtonian Fluids

Fluids that do not obey a direct proportionality between shear stress and shear rate are said to be *non-Newtonian* [9]. Unlike Newtonian fluids, the viscosity for non-Newtonian fluids are varying with applied force or shear rate. Non-newtonian fluids are commonly classifies into three categories:

1. Fluid properties are independent of duration of shear.
2. Fluid properties are dependent on duration of shear.
3. Fluid exhibits many properties that are characteristics of solids (viscoelastic).

The classifications are not a clear definition, and fluids might exhibit a combination of these [9]. Drilling fluids are in general non-Newtonian [11]. When determining flow behavior in turbulent flow for non-Newtonian fluid one can use friction factor and Reynolds number concept. However, since the viscosity is not constant, as it is for Newtonian fluids, one may not use a constant value for viscosity at one shear rate for all calculations [5]

2.2 Rheological Modeling

The goal of rheological modeling is to fit experimental data with a mathematical model, which will give a description of the shear stress - shear rate relationship for a particular liquid. The experimental data is collected by the use of a viscometer, which will measure the shear stress for a given shear rate. The data is then plotted on a rheogram (shear stress vs shear rate), which will determine what model that display the best fit. Numerous rheological models has been developed to describe the rheological characteristics. All rheological models requires at least two measurements of shear stress at different shear rates to be able to predict the shear stress at any other shear rate [3]. It is important to emphasize that no rheological models will give an exact description the flow characteristics for all drilling fluids over their entire shear rates range, however, some of them can predict the behavior with high accuracy. When a rheological model is defined, one may use the rheological data to model flow behavior in other geometries, such as pipe flow or annular flow [3]. The mathematical expression by itself may not look complicated; however, the models must be converted to flow equations based on the shear stress at the wall in order to perform pressure loss calculations, which involves advanced mathematical manipulation [12]. Advanced simulation software is available for calculation of circulating hydraulics and hole cleaning efficiency, however the software requires accurate models in order to obtain reliable results. Figure 3 give an visualization of some of the common models used to describe drilling fluids. The following sub-chapters will give an introduction to some of the most common equations used to model non-Newtonian fluids, such as drilling fluids. The Newtonian model has allready been covered in section section 2.1.6 and will thus not be mentioned here.

2.2.1 Bingham Plastic Model

The Bingham plastic model is a two parameter linear model. This model characterize fluids with a yield stress and a constant viscosity for shear stress once the yield stress has been exceeded. The model show good accuracy for the shear-stress/shear-rate relationship for flocculated clay water-base fluids, however most drilling fluids are not Bingham fluids. The shear-stress/shear-rates

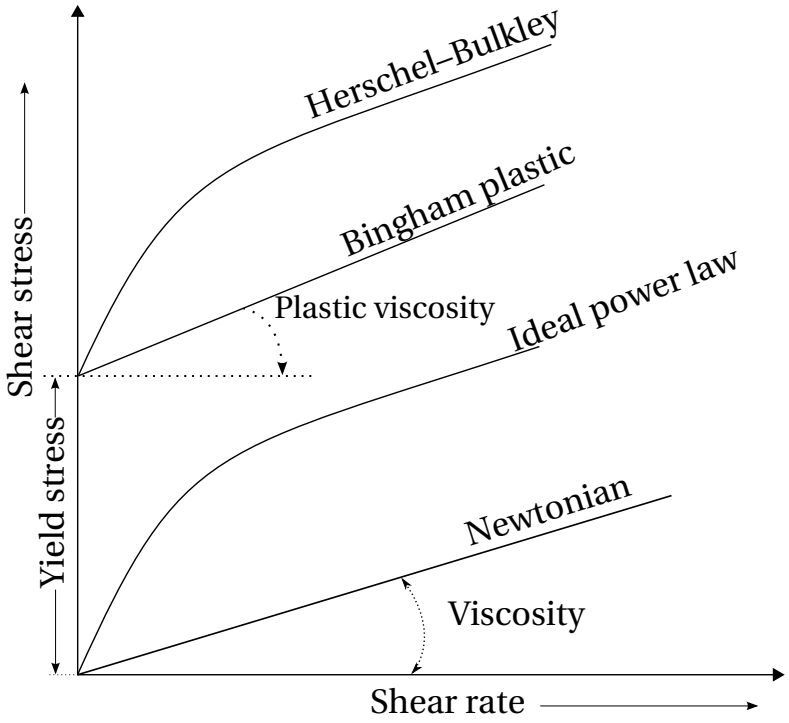

Figure 3: Ideal consistency curves for common flow models. Adapted from Caenn et al.[5]

relationship predicted by the model usually deviate at low and high shear rates. Another limitation of the model is that it commonly overestimates the yield stress. The Bingham plastic model is defined as:

$$\tau = \tau_{yp} + \eta_{pv} \cdot \dot{\gamma} \tag{2.6}$$

Where η_{pv} is the plastic viscosity and τ_0 is the yield point, which is determined from two measurements at shear rates of 600RPM ($1022\,s^{-1}$) and 300RPM ($511\,s^{-1}$). Plastic viscosity and yield point can be calculated as:

$$\eta_{pv} = \theta_{600} - \theta_{300} \tag{2.7}$$

The unit of plastic viscosity is in cP. This is derived from the instrument dimensions and the spring constant. See Caenn et al. [5] for full derivation.

$$\tau_{yp} = 2 \cdot \theta_{300} - \theta_{600} \tag{2.8}$$

Where θ_{600} is dial reading at 600RPM and θ_{300} is dial reading at a shear rate of 300RPM. The model is widely used due to the simplicity, and the two parameters plastic viscosity and yield point are reported as a standard in the mud report on a daily basis in accordance with API drilling fluid report [3, 6].

2.2.2 Power Law

The Power Law model is a two parameter model, which characterizes shear thinning or shear thickening drilling fluids with no yield stress. One of the limitations for the model is that it underestimates the low-shear viscosity, in fact the shear stress for zero shear rate is always zero. Mathematically the Power Law is expressed as followed:

$$\tau = K \cdot \dot{\gamma}^n; \qquad 0 < n \leq 1 \tag{2.9}$$

Where K is the consistency index, and has the unit of [force/area multiplied with time], Pas^n in SI-units, and n is the flow behavior index, which is dimensionless, and $\dot{\gamma}$ is shear rate in s^{-1}. Note that K and n are only of relevance with a specific shear rate. When measurement for a Power Law fluid is plotted with logarithmic scales it will be a straight line where the interception is K and the slope is n.

$$n = \frac{log\frac{\theta_2}{\theta_1}}{log\frac{\dot{\gamma}_2}{\dot{\gamma}_1}} \tag{2.10}$$

The lower the value of "n" the more shear thinning a liquids is. Depending on the value of n, one may characterize what type of liquid one is

n<1; For shear-thinning fluids

n=1; Newtonian

n>1; Shear thickening fluids

The values of the flow index and consistency index are usually determined from the 600RPM and 300RPM dial readings; however, the generalized power-law applies if corresponding shear-rate pairs are defined, ex. θ_6 and θ_3 [3, 6]:

$$K = \frac{\tau_2}{\dot{\gamma}^n} \tag{2.11}$$

2.2.3 Herschel–Bulkley Model

The Herschel–Bulkley (H-B) model includes yield stress into the power-law equation and is for this reason known as the modified power-law. The model is is describing shear thinning drilling fluids with a yield stress. It is considered to be more complicated than Bingham Plastic and Power-law models as it has three parameters. However, it represent a much more realistic flow behavior of drilling fluids. The model has become the model of choice because of the accurate results and it includes a yield stress, τ_y. It is also the recommended model in the current API standard [6]

$$\tau = \tau_y + K \cdot \dot{\gamma}^n \tag{2.12}$$

The consistency index, K, and flow behavior index, n, has the same units as in power law, but they are calculated differently. The value of K in the H-B model is related to the solids content within the fluid in similar way as plastic viscosity is for the Bingham model. In special cases, the H-B model will transform into Bingham Plastic model (n=1), or Power-Law if yield stress is zero [6]. Determining an exact solution for the H-B model is considered to be complex and is mostly limited to computer programs [13]. One way of determine the value of τ_y is to interpolated the shear stress between two known shear rates [14]:

$$\tau_y = \frac{\tau^{*2} - \tau_{min} \cdot \tau_{max}}{2 \cdot \tau^* - \tau_{min} \cdot \tau_{max}} \tag{2.13}$$

Where τ^* is the value of shear stress from the shear rate obtained from the geometric mean of the max and min values, $\dot{\gamma}^*$;

$$\dot{\gamma}^* = \sqrt{\dot{\gamma}_{max} \cdot \dot{\gamma}_{min}} \tag{2.14}$$

2.2.4 Unified Model

Another three parameter rheological model is the Unified model. The model is a simplification based on the H-B model and it was developed with the intention of practical use for field personnel, but still with high accuracy for well hydraulics [13]. Mathematically, the equation is exactly the same as H-B model

defiend in equation (2.12).

$$\tau = \tau_y + K \cdot \dot{\gamma}^n$$

The difference between H-B model and the Unified model is how the values of n and K are determined. One way to determine a value of the yield stress can be done with the use of *low-shear yield point* (LSYP):

$$\tau_0 = 1.067(2 \cdot \theta_3 - \theta_6) \tag{2.15}$$

The "1.067" is an conversion factor from dial readings to the unit $\mathrm{lb}/100\,\mathrm{ft}^2$ as mentioned in section 2.1.2. This was first defined by Bern et al.[15]; however they did not use the conversion factor. Determining the yield stress can be obtain with other measurements. Zamora and Power [13] suggest six different options as usable values of τ_y, where LSYP is among one of them. A comprehensive list of formulas used in the Unified model is shown in appendix E. As an example, the flow behavior index and consistency index for annular flow can be calculated as followed:

$$n_a = 3.32 \log\left(\frac{2\eta_{pv} + \tau_{yp} - \tau_0}{\eta_{pv} + \tau_{yp} - \tau_0}\right) \tag{2.16}$$

And the consistency index:

$$K_a = \frac{\eta_{pv} + \tau_{yp} - \tau_0}{511^{n_a}} \tag{2.17}$$

Where η_{pv} is Bingham PV, τ_{yp} is Bingham YP and τ_0 is defined in equation (2.15)

2.2.5 Robertson and Stiff Model

Robertson and Stiff Jr [16] purposed a three parameter model, which also combine the use of a yield stress with shear-thinning behavior. The model uses thee

$$\tau = A(\dot{\gamma} + C)^B \tag{2.18}$$

Where the parameters A and B are considered to be equivalent to the power law parameters K and n respectively. The last parameter C can be considered as a correction factor to the shear rate. If $B < 1$ then the fluid is shear thinning. It is

not widely used due to the complexity of determining A, B and C [14].

2.3 Viscoelasticity

Viscoelasticity is used to describe materials that are showing viscous and elastic characteristics at the same time when undergoing deformation. Viscosity is describing a fluids internal resistance to flow and can be described according to Newton's law of viscosity, while elasticity is the used in solid mechanics to describe a materials ability to restore its original shape when a load is removed. Drilling fluids exhibit viscoelastic behavior and viscoelastic measurements can be instrumental in order to evaluate drilling fluids performance in drilling operations [17].

A fully elastic solid has the capability to store mechanical energy with no energy dissipation. This means that if a load is applied on a elastic solid, it will restore its shape instantaneous when unloading. In contrast to elastic solids, a viscous Newtonian liquid will dissipate energy with no capability to store energy. By combining the properties from a elastic solid and a viscous fluid it is reasonable to assume that both of these characteristics will be present. From the above definitions one can expect a viscoelastic material will store some of the energy, available for recovery, and dissipate the rest. If we then follow up with the first law of thermodynamics as: "Energy cannot be created nor destroyed, but only transformed" [18].

$$W_{diss} = \begin{cases} 0; & \textit{for ideal elastic solids.} \\ W_{ext}; & \textit{for ideal viscous liquids.} \end{cases} \tag{2.19}$$

Where the work dissipated is denoted as W_{diss}, total work done by external load as W_{ext}. The energy balance will thus be

$$W_{diss} = W_{int} - W_{ext} \tag{2.20}$$

Where W_{int} is work done by internal force.

Viscoelastic *solids* behave different from viscoelastic *liquids*, however both of them show time dependencies upon an applied stress [19]. Among the parameters of interest in order to quantify a materials viscoelastic properties when performing

dynamic rheological measurements are G', G'' and complex viscosity η^*. These parameters are measured in shear. The storage modulus, G′, represent the elastic behavior of the material and is a measure of the energy stored upon shear. If the applied energy is stored, the material will display full recovery and can be considered as a ideal elastic solid. G′ is also known as the elastic modulus. The loss modulus (or viscous modulus), G″, represent the viscous behavior of the material and is a measure of the energy damped, or lost , during shear. Energy is either lost in the process of rearrangements of the materials structure or dissipated as heat into it's surrounding. The lost energy represents an irreversible deformation of a material.The ratio of G″ to G′, known as the damping factor (or loss factor) and is a measure of the viscous to the elastic portion of the deformation represented in figure 4.

$$\tan(\delta) = \frac{G''}{G'}; \qquad 0^\circ \leq \delta \leq 90^\circ \tag{2.21}$$

The loss factor can be used to determine if a material is behaving like a liquid or a solid. An ideal elastic solid is expressed as $\delta = 0^\circ$ and the value of δ will be $\delta = 90^\circ$ for ideal viscous liquid. At the exact balance of viscous and elastic behavior $\delta = 45^\circ$ is an important analysis criteria in gel formation process and yield stress analysis since it represents the transition from solid to viscous behavior.

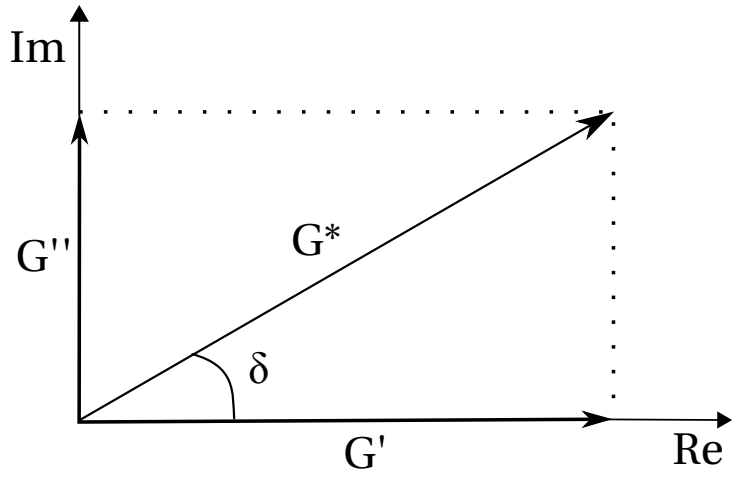

Figure 4: Argand plot of storage modulus, loss modulus and resulting vector of complex shear modulus. Showing phase angle δ. Adapted from Mezger(2002) [19]

The vector sum of G′ and G″ represents complex loss modulus, denoted as G* and

is a measure of the resistance to deformation, or stiffness, of the sample being tested [19]. The magnitude of complex modulus can be expressed as [19]:

$$G^* = \sqrt{(G'')^2 + (G')^2} \tag{2.22}$$

Complex viscosity, denoted as η^*, can be described as a viscoelastic flow resistance of a sample and can be seen as the oscillatory equivalent of shear viscosity. This can be presented in similar fashion as complex modulus, shown in figure 4. The difference is that x axis is now η' and y-axis as $-\eta''$. These represent the viscous component and elastic component respectively. The magnitude of complex viscosity can be expressed as the vector sum of these two

$$|\eta^*| = \sqrt{(\eta')^2 + (\eta'')^2} \tag{2.23}$$

Some materials behave such that complex viscosity and shear-rate dependent viscosity, $\eta(\dot{\gamma})$, has identical shape when plotted in the same diagram. This applies if the measurements are performed withing the linear viscoelastic (LVE) range. The phenomenon is known as the Cox-Merz relation which is an empirically found on the following form:

$$\eta(\dot{\gamma}) = |\eta^*(\omega)| \tag{2.24}$$

The relation is valid if the values of $\dot{\gamma}$ [s^{-1}] and ω [s^{-1}] are equal in size. However, for materials showing gel-like character ($G' > G''$) in the low-shear region, the relation is not useful [19]

Viscoelasticity vs Thixotropy

Thixotropy is change in micro-structure by disruption or recovery- in time, while viscoelasticity is response from the micro-structure in time without being deformed. This holds true as long as the viscoelastic measurements are withing the *linear viscoelastic region*. This is the region where both G' and G'' is independent of stress or strain, and is inevitable in viscoelastic measurements [7], this will be highligted in section 2.3.6.

Viscoelastic measurements of a drilling fluid is not possible be achieved with conventional rheological characterization. Small micro-structural deformation can be measured through dynamic testing, which will be highlighted in the following

sections.

2.3.1 Viscoelastic Models

In order to get a fundamental understanding of the subject of viscoelasticity one may use simple mechanical models. The models consist of springs or dashpots to visualize elastic and viscous elements, respectively. Linear elastic elements are represented as springs that comply with Hooke's law, i.e. force is directly proportional to strain. Viscous elements are represented in similar fashion only using a dashpot to describe the viscous response. A dashpot is a damper that resist motion through viscous friction, and can be described with Newtons law of The simplest model used to describe viscoelastic liquids are the Maxwell model. The Maxwell model consist of a spring and a dashpot in series. If we arrange a spring and a dashpot in parallel we end ut with the Kelvin-Voigt model which is the simples representation of viscoelastic solids. If these two are combined together in a series one end up with a Burgers model.

2.3.2 Viscoelastic Measurements

Some of the fundamental methods in viscoelastic characterization is mentioned in the following sections. The information gained out of these experiment are instrumental for characterization of viscoelastic materials. In connection with viscoelastic measurements one may use either angluar frequency (ω) or frequency (f). To avoid confusion, the term angular frequency is exclusively used in this thesis, which is the angular displacement over one period (T):

$$\omega = \frac{2\pi}{T} = 2\pi f \tag{2.25}$$

2.3.3 Creep Test

Creep testing is one of the fundamental characterization techniques of a viscoelastic material [20]. The elasticity in a sample can be determined form creep and creep-recovery test. Creep test involves to apply a small constant stress to the material being tested over a defined time interval and observe the change in strain. At some time level, defined as t_2 in figure 5, the stress is released and the following

recovery is observed in time. This is know as the recovery phase. The deformation may be elastic or viscous depending on the material being tested.

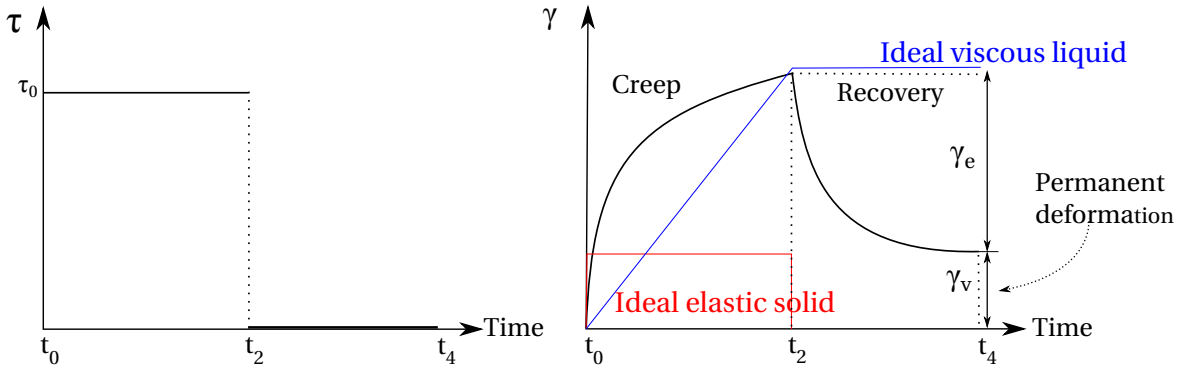

Figure 5: Creep and recovery curve of a viscoelastic, ideal viscous liquid and ideal elastic solid. Left: Constant in time shear stress, τ. Elastic portion represented by γ_e, viscous portion as γ_v. Adapted from Mezger (2002) [19].

One of the parameters that can be obtained from a creep test is zero-shear viscosity, η_0. Zero-shear viscosity is related to deformation at very low shear rate and is determined when the steady-state flow is reached in the end of the test [19]. Furthermore one may determine the limit of (LVE) region through examination of *creep compliance* function, $J(t)$, which is defined in the interval where the sample is being loaded with a constant shear stress. The stres-strain relation can be expressed by the creep compliance;

$$\mathrm{J(t)[Pa^{-1}]} = \frac{\gamma(\mathrm{t})}{\tau_0} \tag{2.26}$$

Creep compliance defines how easily a material can be deformed by a given stress, where a high value indicates that the material is easier to deform. In the LVE range, the creep compliance will be independent of the applied stress. Hence, this can be used to define the yield stress of a fluid by applying an incremental increase in stress over multiple tests. Yield stress can be defined when the J(t) curve starts to be deviate [21]. Another application from the creep test is to analyze the potential for barite sag in a drilling fluid. The settling of barite due to gravity is corresponding to a constant shear stress, which is a similar deformation which occurs in a creep-recovery test [22].

2.3.4 Relaxation Test

In a relaxation test a sudden constant strain is applied and the responding shear stress is observed. It is a measure of the required stress to maintain a constant strain. The sudden strain should be applied in a slow manner so that inertia effects can be neglected [20]. Elastic materials do not relax, hence the observed stress is constant and will stay constant for a infinite time. Viscous fluids, on the other hand, show completely opposite behavior and will relax instantaneous. Viscoelastic materials is thus expected to behave as an intermediate between elastic and viscous, as demonstrated in figure 6 [19].

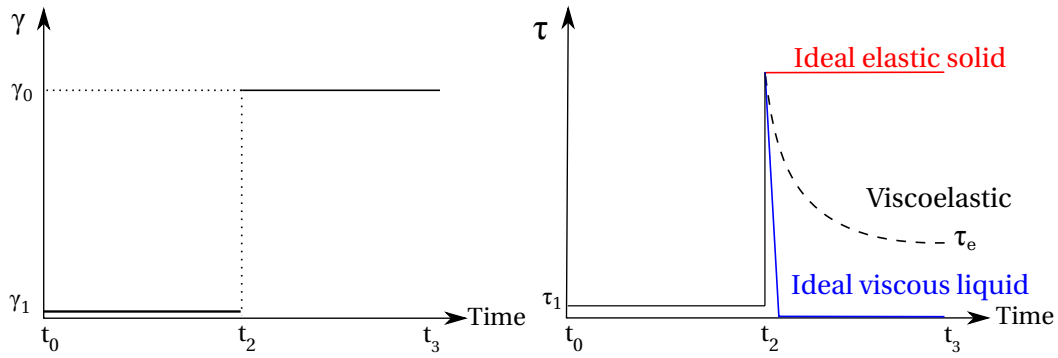

Figure 6: Relaxion test showing responding stress for constant strain, τ_e is equilibrium stress. Adapted from Mezger (2002) [19].

2.3.5 Oscillatory Tests

Along with creep test, oscillatory testing is the most frequently used technique for analyzing viscoelastic behavior [7]. Oscillation can be explained as variation between two states in time. The principle behind oscillatory experiments can be illustrated by a two-plate-model as in figure 7.

A test sample is placed in between a stationary and a movable layer, which is connected to a rotating wheel. Rotation of the wheel will cause oscillatory movement of the upper layer in similar fashion as a sin(x) function. Since the lower layer is immovable, the movement of the upper layer will create a resultant shear stress equal to $\pm\tau$ on the stationary layer. One complete rotation of the wheel corresponds to one complete oscillation period with a angular frequency equal to

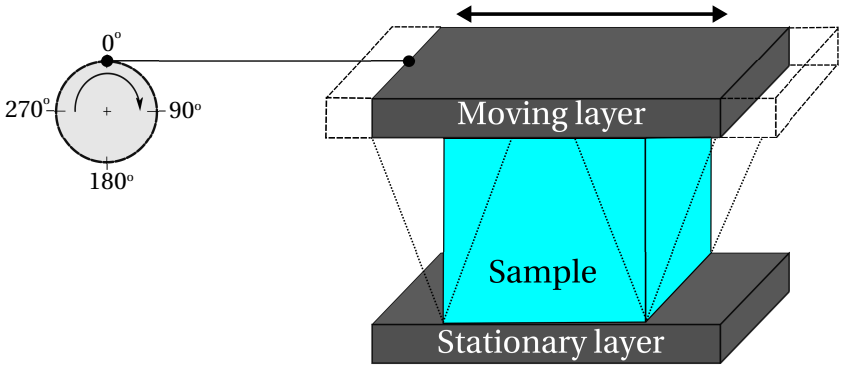

Figure 7: Illustration of the two-plate-model oscillatory test. Adapted from Mezger[19].

ω in units s^{-1} or rad/s. The velocity of the moving layer is equal to the rate of deformation, $\dot{\gamma}(t)$, and will be at its highest for 0° and 180°. The corresponding stress measured from an applied strain depends on the material being tested. A perfect elastic material will show no delay for the stress curve, τ(t), compared with the strain curve, γ(t) [19]. A perfect viscous liquid; on the other hand, will show a delay for τ(t) of 90° for the same experiment, for the same reasons as already discussed in section 2.3.

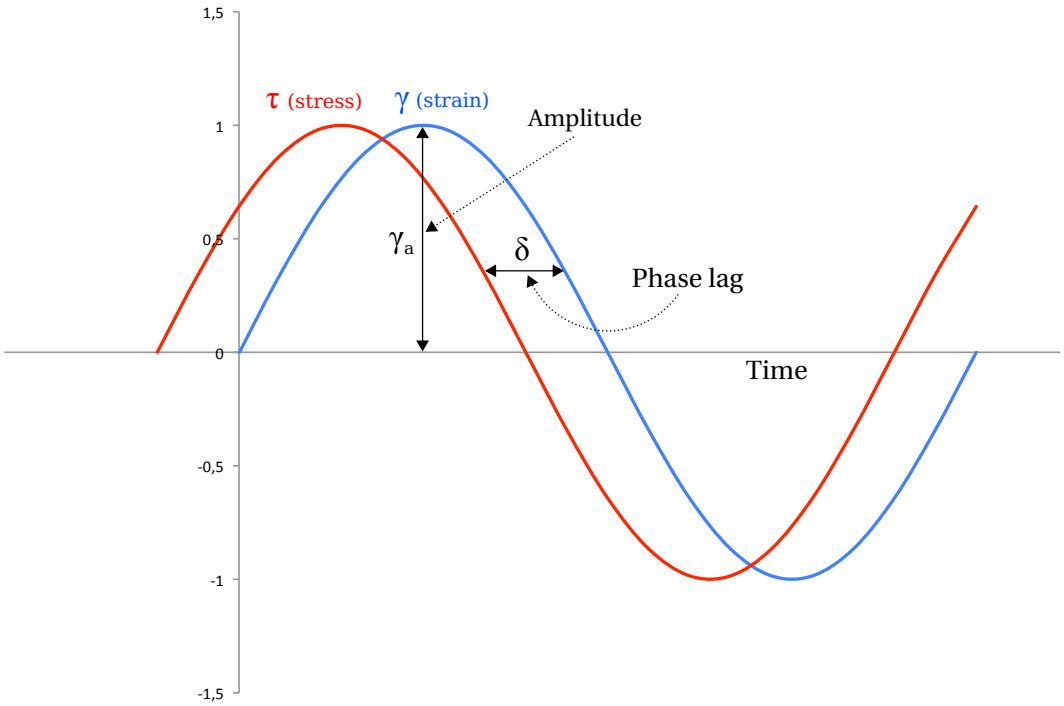

Figure 8: Stress strain response for a oscillatory measurement of a viscoelastic material. Adapted from Mezger (2002) [19].

From figure 8, the applied strain is [17]:

$$\gamma(\mathrm{t}) = \gamma_{\mathrm{a}} \cdot \sin(\omega \mathrm{t}) \tag{2.27}$$

Where γ_a is the strain amplitude, ω is angular frequency in rad/s.

The measured shear stress with controlled strain is;

$$\tau(\mathrm{t}) = \tau_{\mathrm{a}} \cdot \sin(\omega \mathrm{t} + \delta) \tag{2.28}$$

Where and the phase shift angle is denoted as δ, in [°] and τ_a is stress amplitude

If one use controlled shear stress, the applied shear stress is:

$$\tau(\mathrm{t}) = \tau_{\mathrm{a}} \cdot \sin(\omega \mathrm{t}) \tag{2.29}$$

Where $\tau_{\mathrm{a}} =$ constant in Pa, and angular frequency is $\omega = \omega(t)$. And the measured

strain function shifted by δ is thus:

$$\gamma(\mathrm{t}) = \gamma_{\mathrm{a}} \cdot \sin(\omega \mathrm{t} + \delta) \tag{2.30}$$

Storage modulus and loss modulus can be written as:

$$G' = \frac{\tau_a}{\gamma_a} \cos\delta \tag{2.31}$$

$$G'' = \frac{\tau_a}{\gamma_a} \sin\delta \tag{2.32}$$

The response in shear stress as a function of strain can be written as:

$$\tau(t) = \gamma_0 \left[G' \sin(\omega t) + G'' \cos(\omega t) \right] \tag{2.33}$$

$$\tau(\mathrm{t}) = \gamma_{\mathrm{a}} \left[\left(\frac{\tau_{\mathrm{a}}}{\gamma_{\mathrm{a}}} \cos\delta \right) \sin(\omega \mathrm{t}) + \left(\frac{\tau_{\mathrm{a}}}{\gamma_{\mathrm{a}}} \sin\delta \right) \cos(\omega \mathrm{t}) \right] \tag{2.34}$$

2.3.6 Amplitude Sweep

Amplitude sweep test is done in oscillation. The objective with a amplitude sweep is to define the LVE range by keeping the frequency constant and let the amplitude increase with time. This can be performed with either controlled strain or controlled stress. Amplitude sweep is also known as strain sweep or stress sweep. The LVE range is where the structure of a material remains intact for a stress or strain amplitue. The LVE range can be defined by plotting storage modulus (G') and loss modulus (G'') against strain (or stress) using logarithmic scale on both axis. Whenever the amplitude is within the LVE range then G' and G'' are constant, i.e. storage modulus and loss modulus are independent of stress-strain amplitude in the LVE range. For a situation where $G' > G''$ the elastic behavior dominates over viscous behavior and the material is showing a gel character. On the other hand where G'' is greater than G', the opposite is correct, and viscous behavior dominate over elastic behavior, and the material will show characteristics of a liquid even when at rest, i.e. in the LVE range. When the amplitude has reach a certain limiting value, then both G' and G'' will start to diverge from their past constant values and irreversible deformation occur. The LVE is not valid at the point where one of the

curves starts to diverge from its constant value. There are numerous methods of determining LVE range. Usually $G'(\gamma)$ is used to define the LVE range since it tend to diverge before G''. It is imperative that the limiting value for LVE region, in terms of strain, γ_{ys}, is defined for every new, unknown, sample since it defines the limiting value for further analysis. By performing a amplitude sweep one may determine the yield stress, τ_{ys} which is defined at strain equal to γ_{ys}. The flow point τ_{fp} is defined at the crossover point where $G' = G''$ as shown in figure 9 [19, 21].

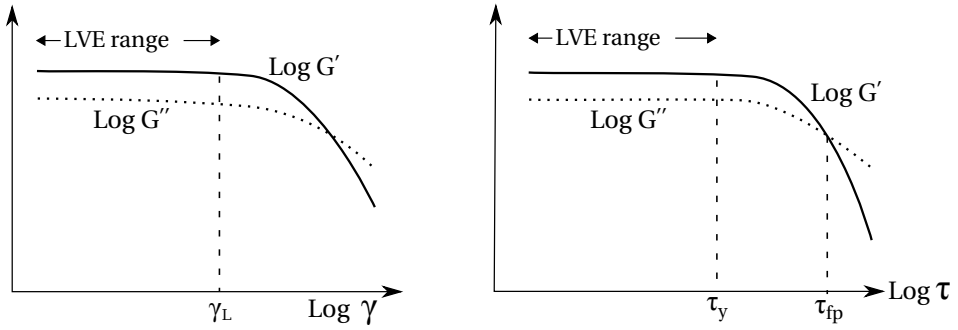

Figure 9: Left:Strain amplitdue sweeps showing gel-like character. Right: Stress amplitude sweep showing yield point τ_1 and flow point τ_{fp}. Limit of LVE range included. Adapted from Mezger [21].

2.3.7 Frequency Sweep

Frequency sweeps are oscillatory tests where the amplitude is kept at a constant value while the frequency vary. The objective of this test is to investigate time-dependent viscoelastic properties. This test is usually performed in such way that the frequencies are descending from high towards low frequencies. Rapid oscillations (high frequency) are representing short-term behavior and likewise are low frequencies used to investigate long-term behavior. The results obtain for the test is usually plotted on double logarithmic axis with G', G'' and η^* on the Y-axis and angular frequency, ω, on the x-axis. In order to perform frequency sweeps one must know the limiting values of the LVE domain. Information on the maximum strain amplitude values to be used is obtained from the amplitude sweep test, hence it is imperative to carry out an amplitude sweep in prior of a frequency sweep [21].

The shear rate values from frequency sweep can be calculated as followed:

$$\dot{\gamma} = \gamma_a \cdot \omega \tag{2.35}$$

2.3.8 Dynamic Time Sweep

Time sweep is used to observe time-dependent behavior of viscoelastic properties. Pre-shearing of the sample at constant temperature in prior of test is required to break the structure of the sample. The test itself is performed within the LVE region at isothermal conditions using constant amplitude and frequency. Time sweep can be used to observe the thixotropic behavior and the following structural regeneration (gel-behavior). The data can be presented on a x-y plot where time is on x-axis and G', G'' and/or η^* is on y-axis in a logarithmic scale[21]. By evaluating the viscoelastic properties over time one may characterize the material's gelling time and settling properties. A drilling fluid with progressive gel-strenght will show an continuous increase in storage modulus over time [17].

2.3.9 Dynamic Temperature Sweep

Temperature sweep are oscillatory test performed at constant amplitude and frequency in each test interval. The only variable is the temperature, where the temperature may be increased in steps or linearly. The objective of temperature sweep is to examine the influence of temperature on a viscoelastic material [21]. For some materials the temperature where the material is transforming from viscoelastic liquid to viscoelastic gel can be determined. This can be valuable information when studying settling of weight materials in drilling fluids [21].

2.3.10 Classification of Materials from Oscillatory Tests

As described through these foregoing sections, interpretation of G' and G'' are important to understand the structural build up when testing a viscoelastic sample. The following is a representation of the calculated and measured values from the applied parameters, while table 1 classify the materials based upon the measurements [21].

- **Applied** : Frequency, strain or stress amplitude
- **Measured** : Phase angle (δ) and ratio of strain and stress amplitude
- **Calculated** : Storage Modulus : Stored energy or elasticity
  - Loss Modulus: Dissipated energy
  - $\tan(\delta)$: Damping
  - Complex Viscosity, η^*: Resistance to flow

Table 1: Classification of Materials from Oscillatory Tests [21]

Ideally viscos flow behavior	**Behavior of a viscoelastic liqids**	**50/50 ratio of the viscous and elastic portions**	**Behavior of a viscoelastic gel or solid**	**Ideally elastic deformation behavior**
$\delta = 90°$	$90° > \delta > 45°$	$\delta = 45°$	$45° > \delta > 0°$	$\delta = 0°$
$\tan(\delta) \to \infty$	$\tan(\delta) > 1$	$\tan(\delta) = 1$	$\tan(\delta) < 1$	$\tan(\delta) \to 0$
$G' \to 0$	$G'' > G'$	$G' = G''$	$G'' < G'$	$G'' \to 0$

2.4 Functions of Drilling Fluids

Drilling fluid is the liquid that is circulated through the wellbore during drilling and workover operations. The drilling fluid system, or more known as the "mud system", is in contact with the wellbore throughout the whole drilling operation and it has multiple important functions in order to drill a well efficient and successfully. Drilling fluids are suspensions of solids containing clay particles and weighting agents such as barite or calcium carbonate with chemical additives as required to modify fluid properties. There are multiple different types of drilling fluids such as pneumatic fluid systems (foam, gas), water based systems, synthetic based and oil based systems, however water-based and oil-based systems are those that are being used on the Norwegian Continental Shelf (NCS) [5, 11]

Drilling fluids are an essential part of drilling wells. The functions are described as tasks that the drilling fluid, or "mud", is capable of performing although not all of them are in the same degree of importance as others. Control formation pressure and remove cuttings out of the well are imperative functions for drilling fluids in every drilling operation. Among the functions mentioned above the most common functions of a drilling fluid are highlighted in the following sections;[3]

1. Control formation pressures.
2. Remove cuttings from the well.
3. Suspend and release cuttings.
4. Seal permeable formations.
5. Maintain wellbore stability.
6. Minimize reservoir damage.
7. Cool, lubricate, and support the bit and drilling assembly.
8. Transmit hydraulic energy to tools and bit.
9. Ensure adequate formation evaluation.
10. Control corrosion.
11. Facilitate cementing and completion.
12. Minimize impact on the environment.

2.4.1 Control Well Pressure

In order to avoid influx of formation fluids, and thus a potential well control situation, it is necessary to have a higher pressure in the well than the formation pore pressure. As formation pressure increases with the vertical depth of the well, the mud weight has to be increased to balance out the formation pressure and maintain wellbore stability. If the wellbore pressure is too high and exceed the fracture pressure of the formation, a lost circulation situation can occur. In the event of lost circulation it is important to refill annulus with drilling fluid to maintain the wellbore pressure in balance with the formation pressure [3]. On the other hand, if the wellbore pressure is reduced below the formation collapse pressure the structural integrity of the wellbore will eventually become unstable which in turn may lead to a mechanical rock-failure mechanism with the associated problems of stuck pipe and loss of well [11]. The hydrostatic pressure exerted by the mud column can be calculated as

$$P = \rho g h_{tvd} \tag{2.36}$$

Where P is pressure in Pa, ρ is density of mud in kg/m^3, g is free-fall acceleration in m/s^2 and h is true vertical depth in meter.

2.4.2 Wellbore Stability

In prior of drilling, the rock strength at some depth is in equilibrium with the in-situ rock stresses. The equilibrium between rock strength and in-situ stresses are however disturbed when a hole is being drilled [11]. Wellbore stability is a function of mechanical and chemical factors. In order to balance out the mechanical forces acting the wellbore, correct mud weight must be within a range. Hydrostatic pressure exerted by the mud column will provide a means of controlling the stresses adjacent to the wellbore other than those exerted by formation fluids [3]. In addition, chemical fluids from the mud are introduced and an interaction process begins between the drilling fluid and in-situ formation. In shales, this chemical differences between drilling fluid and formation will over time cause formation swelling and softening, which will lead to other problems such as sloughing and tight hole conditions. Once wellbore instability has occurred, it will become

weaker and more difficult to stabilize [3, 11]. Aadnoy[4] purposed "*the median line principle*", which is a method of mud weight schedule designed to minimize borehole stability problems. This is obtained by keeping the mud weight close to the in-situ stresses

2.4.3 Cuttings Transport

Along with controlling well pressure, one of the most important function of a drilling fluid is to suspend and transport drilling cuttings along the annulus to the surface where they can be removed by solids equipment. If cuttings are not transported out of the well, it will accumulate in the well and may lead to severe problems such as high torque and drag, stuck pipe, hole packing-off, difficulties of running / cementing casing, and increased bottomhole pressure which again can impose lost circulation [11] [4]. In addition, drilled cuttings will get crushed by the drill string if it is not removed, and high concentration of ultra-fine solids will be incorporated in the mud system. This can result in solids build up in the mud system, which in turn can lead to progressive gel strength and elevated rheology caused by the increase surface area of the particles. Ultra-fine solids (2-44 μm) is not possible to remove with solids equipment and dilution of fresh fluid is the only outcome. The viscosity and rheological properties of the mud system has a significant effect on hole cleaning. Adequate gel strength is required to ensure that the cuttings remain suspended under static conditions when circulation is shut off, however too high gel strength will induce excessive pressures when circulation is broken [3] [11]. A more in-depth review of hole cleaning is written in section 2.7.2.

2.4.4 Seal Permeable Formation

During conventional over-balanced drilling in permeable formation as mentioned in section 2.4.1, mud filtrate will invade the formation, and solids within the mud system will deposit a filter cake on the wall of the formation. A proper maintained mud system should deposited a filter cake on the formation wall that is thin and have a low-permeability in order to minimize filtration invasion. The ability to seal permeable formations is important for successful drilling of the well.

2.4.5 Cooling and Lubrication

During the process of drilling heat is generated by frictional interaction between bit and formation. In addition to heat generated by friction, elevated temperatures from the formation may lead to failure of mud motors, drill bit and bottomhole assembly (BHA) components if not being cooled down. The circulation of drilling fluid from surface down the drill string and up annular space will transport heat away from the source and cool down components. In addition to transporting heat away, the mud will also provide some degree of lubricity and in such way reduce the frictional heat generated. The degree of lubricity will depend on mud type and solids content within the system. In general, oil based mud (OBM) will provide better lubricity than water based mud (WBM), however friction reducers may be added to improve lubricity [3].

2.5 Oil Based Drilling Fluids

Oil based drilling fluids are mixtures of two immiscible liquids: Oil and water. They are invert emulsions since water is broken up into small droplets and uniformly dispersed into the oil, however the word emulsion is commonly used and will be used ahead. The water phase is know as the internal phase while the oil is known as the continuous phase. The volume percentage of oil relative to water is recognized as oil-water ratio and is abbreviated as OWR. For most drilling operations the OWR is in the range of 70:30 to 90:10 and is defined in mud program for each drilling operation. However, oil based drilling fluids are stable at OWR lower than 70:30 as long as there is sufficient emulsifier to form a film around each water droplet and that the droplets are small of uniform size. As a result of water are dispersed into small droplets, a higher water content will increased contact surface area between water and oil. The increased water will affect the stability of the mud as there is less free space for water droplets to move around and will for that reason more easily coalescence into larger water droplets. Furthermore, the water droplets will act much like fine solids are to water based systems, thus increasing the rheology, which will affect the wellbore hydraulics. In order to have a stable emulsion the water must be dispersed into uniform small droplets. This is done by applied mixing energy in the form of shear, which can be obtained through

high pressure mud-guns or when circulating mud in the well where turbulent flow occurs. Unsheared emulsion will have spherical droplets, while they get ellipsoidal when shear is applied before they eventually split in two smaller droplets[23]. Proper shearing of OBM is essential in order to obtain a smooth viscosity profile and non-progressive gel strengths. A relative measure of the stability of an oil based drilling fluid is electrical stability, often abbreviated as ES, which measures the voltage required to induce a current through the sample. Electical stability above 500 V is often considered as a minimum for a stable mud for drilling purposes. Water droplets within the emulsion will form a conductive pathway hence reduce the ES. The larger the water droplets are, the lower the resulting ES will be [3].

The advantages of using OBM compared to WBM are many and is the only choice in some circumstances. Among the benefits of using OBM is shale inhibition, lower equivalent circulating density (ECD), reduced torque and drag, improved wellbore stability, temperature stability, and corrosion friendly. However, OBM is more expensive, it is considered to be more harmful than WBM with respect to healt and environment. Furthermore, treatment of lost circulation is considered to be more difficult with oil based than water based drilling fluids, and discharge of whole mud and cuttings are prohibited in most offshore locations in the world [3, 4].

2.6 Composition of Oil Based Drilling Fluids

The following will give a general overview of the most important composition of a oil based drilling fluid.

Base Oil: The base fluid of oil based drilling fluids are known as the continuous phase. Historically the base fluid for such drilling fluids were crude oil and diesel oil, however these are not used in the modern formulation as they represent a health and environmental risk. Today, non aromatic mineral oil and linear paraffin base oil are examples of base fluid used as the continuous phase.

Weighting Material: Weighting agents are added to the drilling fluid to achieve a desired mud weight. The most used weighting material used in both oil based and water based drilling fluids is barite. Barite is an inert mineral,

$BaSO_4$, which is considered to be cheap and due to the high density it can increase the mud weight quickly. One of the major disadvantages of using barite is that it may damage formation permeability as it is very difficult to remove. Another factor to mention is that barite absorbs gamma rays, which may come in conflict when logging in high density drilling fluids [11]. Other weighting agents with higher density than barite that are available is itabirite and ilmenit [5]. Historically it has been reported that ilmenite is abrasive and casuses erosion; however, recent studies show that this can be avoided by adjusting the particle size distribution of ilmenite and that it give an overall benefit as a weighting material compared to barite [24].

Viscosifier: The primary viscosifier in oil based drilling fluids are surface treated bentonite clay also known as organophilic clay. The surface treatment is required to make the clay dispersible in oil and thus yield. Water and organophilic clay are synergistic in how much it yield. The clay requires water as a polar activator, hence, the effect of clay will decrease as the oil-water ratio increase. Sufficient shear and temperature is also required to ensure that full yield of the clay [3] [25].

Fluid Loss Agent: The primary fluid loss control agent in oil based mud is natural asphalt (gilsonite), amine treated lignite or cross-linked polymers. Asphaltic materials are natural hydrocarbons and are thus naturally oil-wet. They are also more efficient fluid loss agent than amine treated liqnite when used in equal concentrations, however asphaltic materials can damage formation permeability, and as it is a natural hydrocarbon it can give an influence on fluid interpretation when performing reservoir fluid sampling during exploration drilling.

Emulsifier: Emulsifiers are chemicals that reduces the surface tension between two immiscible liquids. They are required in oil based drilling fluids to make it possible to maintain a stable dispersion of fine water droplets into oil. The emulsifier are usually usually long-chain alcohols, fatty acids or polymers. Fatty acids requires lime to form soaps, which will function as a emulsifier. Now days it is common to use an emulsification package, which provide emulsification and wetting agent in one chemical

Wetting Agent: Oil based drilling fluids uses wetting agents to make solids and weighting materials oil-wet. If there is insufficient wetting agent, the solids can get water-wet, which will cause settling of solids out of the drilling fluid.

In addition to the chemicals mentioned above, oil based drilling fluids also include salts, usually calcium-chloride brine in the water phase, which offer inhibition properties for most shales. Ideally the water phase salinity in the drilling fluid will prevent shale to absorb any water by balancing out the formation salinity. Too high salinity may cause dehydration of shale [3].

2.7 Drilling Fluids Performance

2.7.1 Barite Sag

Settling of weight material in drilling fluids is commonly referred to as barite sag. This causes fluctuations in the mud density and is especially prominent in high-angle wells, in particular those exceeding 60° where annular velocity is low and the viscosity for the drilling fluid is low. Sag is recognized as a major concern in drilling and completion operations as it can lead to well-control issues, stuck pipe, lost circulation, and wellbore-instability [3]. The occurrence of barite sag is commonly observed when circulating bottoms up and the resulting mud weight, out of the hole, is lower than the mud weight going into the well. Although Barite sag tend to be more prominent in OBM than in WBM, it can also occur in WBM [26]. One method to avoid barite sag is to use drilling fluids based on heavy brine. These fluids are less subjected to sag since they has a lower concentration of particles, but they do not exhibit the same drilling properties as OBM [27].

Static sag occurs in fluids that are static for a longer period of time. Moreover, if the fluid column is inclined, the settling rate will accelerate significantly. Settling of barite in inclined tubes can be explained as boycott settling. As barite settles out from the suspension zone on the low side, the lighter fluid will travle upwards on the high side. This will create a thin layer of low density fluid on the top of the tube and another just below the upper wall. The particles will then settle out from the sedimention zone and accumulate into a sediment bed on the lower wall as seen in figure 10. The pressure difference over the cross sectional area will create convectional currents, forcing the low density fluid upwards and the sediment bed downwards. The effect of downward flow and sediment bed sliding is called slumping. In deviated wellbores, the flow stream moves along the high side, which will accelerate boycott settling even more. Settling of barite occurs more frequent during circulating than in static situations, hence barite sag is primarily a dynamic settling problem. When drilling under high temperature - high pressure (HTHP) condtions, the mud weight are commonly high and temperatures are high. This causes the viscosity of the drilling fluid to decrease, which in turn can accelerate the potential for sag. These types of wells are specially prone to dynamic barite sag in a

situation where annluar velocity is low, such as when circulating with low flow rate through the choke on the blow out preventer or when running casing [3]. Barite sag in the field is a complex phenomenon with combining factors of pipe eccentricity, annular velocity, drilling fluid rheology, wellbore angle and temperature to mention some.

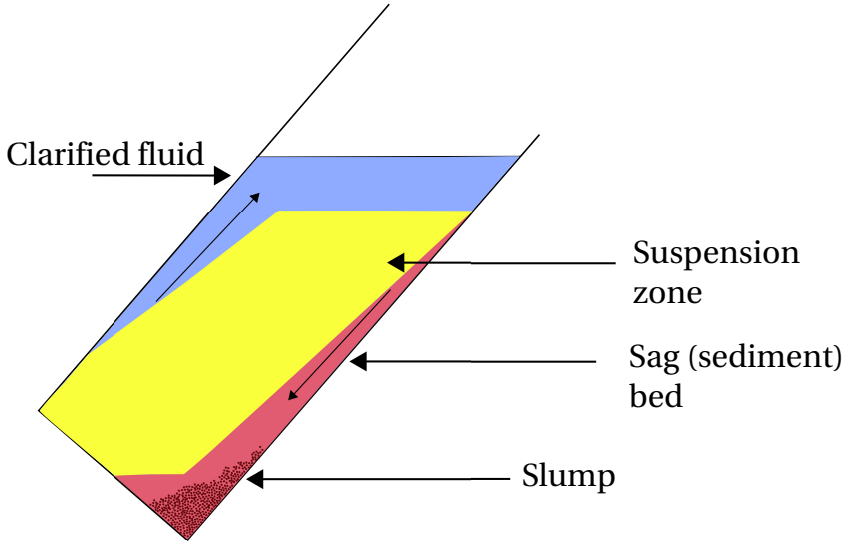

Figure 10: Illustration of boycott settling. Adapted from M-I Swaco([3])

Barite sag potential of a drilling fluid can be analyzed through laboratory testing. However these tests can only give an indication of the settling potential for a particular drilling fluid as they cannot simulate all of the well parameters affecting sag in the wellbore.

Dynamic Testing

Laboratory measurements of dynamic sag performance test can be measured by the use of a conventional viscometer or a flow loop. The viscometer sag shoe test is performed by using a conventional rotational viscometer, a thermocup and a "sag shoe". The upper surface of the shoe is made out of thermoplastic and has a slope with a small collection well at the end of it. The sag shoe is designed in such manner so that it intentionally concentrate settled barite into the collection well. The test is good to observe tendencies of a fluids capability of suspending weighting material under dynamic conditions. It is important to be aware of that this test is a relative

measure of a particular fluids ability to suspend the weighting material and is not a direct measurement of the barite sag under all well conditions. Sag measurements obtained from a flow loop is more accurate on how drilling fluids will perform in the field as they other parameters such as flow rate, eccentricity, pipe rotation and inclination can be manipulated [28].

Static Testing

In this test the drilling fluid is put in a cell (typically 350ml) and then pressured up to prevent fluid of boiling. The cell is then set in a heating oven for a longer period of time for aging, 16hrs or as required, and at a desired testing angle. When the aging is completed, the fluid is separated into five parts and the density of each layer respectively is determined to observe how the weighting material has settled under static condtions. The uppermost layer is typically a free-oil layer which is measured first. Furthermore, the fluid can then be tested in normal fashion to observe how aging has an influence on the drilling fluids properties. The aging testing may also be performed under dynamic conditions by the use of a roller oven.

Under static conditions the only force acting on the weighting material is the gravity force. If sufficient gel strength is obtained, the force acting on the particle must overcome the gel strength minus the buoyancy force in order to settle out the particle. The gel strength can hold back a force equal to:

$$F = \tau_{gel} \cdot A_p \tag{2.37}$$

Where τ_{gel} is the gel strength and A_p is the area of the particle. The equilibrium force is achieved when the gel strength acting on the surface area of the particle is equal to the gravitational force acting on the volume;

$$4\pi r_p^2 \tau_g = \Delta\rho \frac{4}{3} \pi g r_p^3 \tag{2.38}$$

$$\tau_g \geq \frac{(\rho_p - \rho_f)}{6} g D_p \tag{2.39}$$

Where ρ_p is density of settling particle, ρ_f is density of fluid, both in kg/m^3. For API drilling rated barite the density is $\rho_b = 4.200\,\text{kg/m}^3$, 97% of the weight shall be less

than $75\mu m$ and no more than 30% by weight shall be smaller than $6\mu m$ in diameter. If we then calculate the theoretical gel strength required to hold a barite particle of 30 µm in a mud weight of $1500\,\mathrm{kg/m^3}$, the gel strength would then be 0.13 Pa (or $(0.27\,\mathrm{lb/100\,ft^2})$), which is lower than one could measure with a conventional viscometer. In reality, most drilling fluids will sag even with gel strengths much higher than this [6, 29].

The terminal velocity of spherical particles in Newtonian fluids can be expressed by Stokes' law.

$$v_t = \frac{2(\rho_p - \rho_f)}{18\eta} \cdot g D_p^2 \tag{2.40}$$

2.7.2 Hole Cleaning

Hole cleaning is the subject of removing drilled cuttings and transport them out of the well. It is one of the highest concern when drilling a well, and in particular for high angle wells or extended-reach drilling. A thorough understanding of the mechanisms behind hole cleaning is imperative in order to successfully drill such wells. Although the role of fluid rheology is considered to be plays a key role in hole cleaning, there are several other factors, which is of high relevance to achieve good hole cleaning. Among the factors affecting hole cleaning efficiency are;

- Pipe Rotation
- Wellbore Angle
- Flow rate
- Hole size
- Drill pipe eccentricity
- Cuttings size and shape
- Rate of penetration
- Drill string design

Hole cleaning dynamics depends on the hole angle of the well and is commonly separated into three different regimes:

- Low angle ($0° - 45°$)
- Medium angle ($45° - 60°$)
- High angle ($> 60°$)

The main difference with respect to cuttings transportation in vertical wells compared to high angle wells is that the cuttings in high angle wells has a very small distance to travel before reaching the bottom of the well. In horizontal wellbores, the cuttings cannot be suspended even with high flow rates, hence the cutting will fall down on the low side and form a beach. For wellbore angles between $45° - 60°$, the cuttings bed will be more easily brought into suspension during circulation, however when the flow comes to rest, the cutting falls out of suspension and fall on the low side of the well causing a potential slide of cuttings, and form dunes. The fluid velocity for horizontal wells is also different when compared to vertical holes. In vertical wellbores the annular velocity profile is uniform around the drill pipe, however for horizontal wells the velocity distribution is not equally over the cross-sectional area of the well. This is caused by cuttings accumulation on the low side of the well, which will cause much higher fluid velocity on the high side compared to the low side. In fact, the fluid may almost be at rest on the low side. The only way to get the drilled cuttings into the higher velocity area under these circumstances is to apply pipe rotation [30]. The pipe rotation must be above the "viscous coupling" threshold between drill pipe and drilling fluid [31]. The viscous coupling is a fluid film rotating with the pipe, and is a function of fluid rheology and rotational speed of drill pipe, this is illustrated in figure 11. With appropriate fluid rheology the cuttings can then be transported away from its past position until it falls down on the low side again. Without pipe rotation the cuttings will remain stationary on the low side [30].

A primary rheological parameter to monitor a drilling fluids hole cleaning capability is considered to be the low shear rate dial readings, i.e. 6 and 3-rpm on the VG-meter. Mims et al.[30] recommends that the 6-rpm dial reading should be 1 - 1.5 times the hole size when using water based drilling fluids in long horizontal wells, and that it should be slightly less than one when using oil based drilling

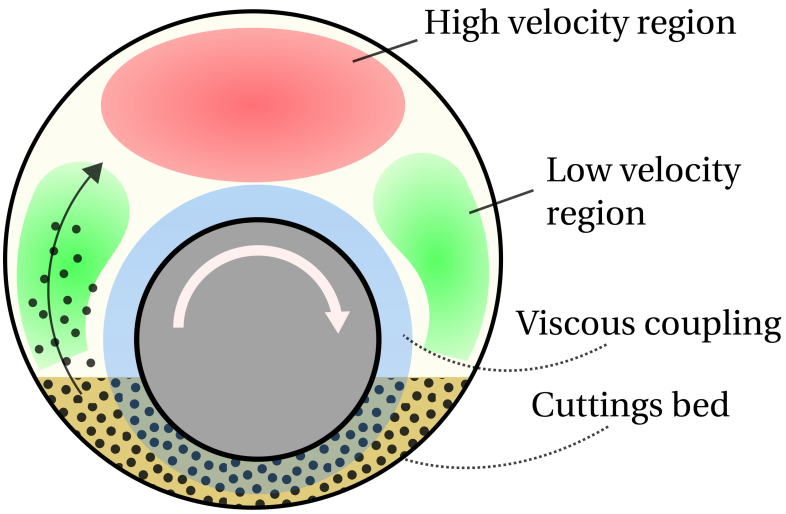

Figure 11: Hole cleaning concept in horizontal well with rotating drill pipe, adapted from Mims et al. [30]

fluids. Furthermore, they also recommend that the oil- water ratio should be kept high when drilling such wells to ensure that the plastic viscosity is kept low and to reduce the ECD. Although the viscosity profile for an oil based and water based drilling fluid might be quite similar, they act differently in respect to hole cleaning. When using water based drilling fluid, there is a risk that the water may react with the cuttings bed and form a gel-structure within the cuttings bed itself. This will not occur in the same way when using oil based drilling fluids as there is less free water to react with the cuttings. This is also why the 10-sec and 10-min gel strength is recommended to be kept low, and that the drilling fluid should only show a low degree of shear-thinning to obtain good hole cleaning [32]. For drilling operations on the NCS, the 3RPM dial reading on a conventional viscometer is a standard rheology specification for each section. This is not one specific number, but rather a small range where the 3RPM readings shall be within for a specific mud system. For top-hole drilling (spudding), the funnel viscosity is typically the rheology specification.

3 Literature Study

This section contains research performed by others as a foundation for the experiments being performed in this paper.

3.1 Viscoelasticity and Barite Sag in Drilling Fluids

It is widely addressed in the literature that rheology of drilling fluids plays an important role in respect to barite sag. Static settlement of barite can be reduced with appropriate gel strength. However, controlling dynamic sag is more complicated than controlling static sag and cannot be predict by standard viscosity measurements. In a situation where static sag is negligible, dynamic sag can be much more severe. Some authors states that dynamic sag may be reduced with elevated gel-strengths and/or low-shear rheology, that is the θ_6 and θ_3 readings on the Fann VG-meter [15], [33], [34]. Bern et al.[15] suggested an alternative method to the Bingham yield point, commonly known as low-shear yield point (LSYP).

$$\text{LSYP}[\text{lb}/100\,\text{ft}^2] = 2 \cdot \theta_3 - \theta_6 \tag{3.1}$$

Furthermore, it is suggest that the LSYP should be be in the range of $7-15$ lb$/100\,\text{ft}^2$ to minimize barite sag [15]. A numerous of studies has tried to investigate the complexity of dynamic sag in drilling fluids. It is thought that viscoelastic behavior can give advantageous knowledge about dynamic settlement. This involves studies of drilling fluids viscoelastic behavior at deformation rates far below the conventional viscometer range.

Hanson et al.[33] conducted more than 70 test on a flow loop in order to study the phenomenon of dynamic sag. The paper present case histories and follow up with ten practical guidelines to minimize sag problems. One of the recommendation is to not thin the drilling fluid too much in prior of running casing as this may promote sag. However, reduced rheology is in general preferred during cement jobs as this increases the mud mobility during the cement job, which is important for a successful cement job. Furthermore, it was also recognized that dynamic sag is more sever under low fluid velocities and that slumping was most extensive in

angles between $40° - 50°$. The paper concludes that sag is primarily caused by enhanced boycott settling due to dynamic conditions and that dynamic sag is more prominent than static sag because of this.

Arild Saasen [29] made a comprehensive article about the theory describing weight materials behavior in emulsions and oil based drilling fluids. This theory argued that the viscosity of these fluids are low when the share rate is ultra low and that a shear-thickening behavior occur over a very small share rate. This low viscosity environment is caused by a crystalline structure of water droplets created by Brownian motion, which is destroyed when the shear rate is increased followed with an increase in viscosity. It is also argued for that static sag of weight material occur in a non-continuous fashion. Initially the particle will settle due to a low viscosity environment caused by the crystalline structure. When the particle accelerate downwards the viscosity around the particle increases, which causes the particle to stop. This process will occur over again, making the particle to settle step-wise . The shear-thickening effect is in contrast to the shear thinning effect observed at higher share rates. Furthermore, possible methods to reduce critical shear rate where this shear-thickening behavior is suggested in order to mitigate sag. One of the methods mentioned is to decrease the oil-water ratio as this reduce the free space for water droplets to move before they collide with nearby water droplets. It is also argued for that reducing the free space between water droplets, without changing the water fraction, would also reduce the onset of shear thickening. This could be done by apply more mixing energy.

Manipulating of the internal water phase composition in oil based drilling was performed by Omland et al.[35], with focus on correlating static sag with fluid composition. This was done by formulating 16 different invert emulsion fluids with same density and water activity. Four different base fluids was used for the continuous phase, and additionally four different salts used for internal phase. The results showed that static sag was higher when a low-viscosity base fluid was used. The paper concludes that the choice of base fluid is imperative in controlling the drilling fluid viscosity and that ammonium calcium nitrate ($NH_4Ca(NO_3)$) salt used as internal phase provided better sag stability when compared to the frequently used calcium chloride ($CaCl_2$).

A similar approach was made by Tehrani et al.[36]. They focused on how viscosifying the internal brine phase of an oil based drilling fluid would affect fluid rheology in connection with dynamic sag. Dynamic sag testing was done with a sag shoe and a Fann 35 model rotational viscometer. All chemical concentration constant where held constant while the type and concentration of viscosifier was altered. Observations showed good correlation between reduction in dynamic sag and the LSYP. When the LSYP was increased, the measure barite sag decreased. Addition of ionic polymer showed a reduction of sag close to 30% in the laboratory tests.

Ehrhorn and Saasen[37] discuss the importance of rheology in connection to barite sag. The paper states that oil based mud does not develop any gel structure as there is no bonding forces between individual particles within the fluid. In the conclusion it is stated that static or dynamic sag can not be prevented, only minimized if the viscosity at low-shear rate is sufficient.

Tehrani et al. [28] investigated the correlation between the rheological properties of invert emulsion fluids and barite sag measured in the lab. This was done by addition of different organophilic clay and polymers in invert emulsions before investigating dynamic sag. From the experiment it was found a correlation between low-shear rate viscosity and dynamic sag behavior down to shear rate of $0.001\,s^{-1}$ for fluids containing clay, where a higher degree of sag was observed for fluids showed lack of low-shear rate viscosity. Viscoelastic measurements was also used in the attempt to correlate dynamic sag measured in the lab with viscoelastic parameters such as G', $\tan(\delta)$, and complex viscosity η^*. Experiments showed that dynamic sag decreased when the elastic properties of the fluid increased, i.e. when the fluid showed behavior of viscoelastic gel or solid. This correlation was obtained when comparing dynamic sag and $\tan\delta$, at a frequency of 1 Hz. Temperature dependency on elastic modulus was also found, and in particular that elasticity was reduced as temperature increased.

Herzhaft et al. [38] study oil based mud formulations used in deep water drilling operations. Several oscillatory measurements at low temperature to study the structural properties at rest. Viscous modulus (G'') and elastic modulus (G') was compared for pre-sheared mud samples and un-sheared mud samples. Their measurements showed that the viscous modulus was not significantly affected by shear, however, elastic modulus showed a lower value when being pre-sheared. The linear viscoelastic range was larger for pre-sheared samples. The paper identified that the interaction between organophilic clay and emulsion droplets was responsible for a solid-like structure at low shear rates promoting elastic structure at rest. This interaction could be described as colloidal particles which is destroyed if mixing energy is high enough. In common with Tehrani et al. [28], it was showed that the level of elasticity decreased for increased temperature. Observations performed suggested an intermediate plateau in shear stress at intermediate shear rates and Newtonian-like behavior at low, and high shear rates. These trends were observed for temperatures from 0 °C to 80 °C. Comparison of between low-shear rate rheometer with the conventional VG-35 was also conducted. It was concluded that the conventional VG-35 viscometer overestimates the viscosity at low shear rates.

In the search for a correlation between rheological behavior of oil based drilling fluids and dynamic sag, Savari et al.[39], performed a series of laboratory tests on five different field mud samples. A Dynamic High Angle Sag Tester (DHAST) was used to study dynamic sag and an Anton Paar high end rheometer for the rheological measurements. From the DHAST measurement, it seems like the sag rate was at the highest for all fluid samples when a shear rate of $10\,s^{-1}$ was applied. Results presented in the paper showed some general trends from the amplitude sweep test where high G^* (complex modulus) and dynamic yield stress show better sag performance. From the frequency sweep test, their measurements showed that the two samples with highest value of $\tan\delta$ (viscous dominance) also showed high ability to sag. Their complex viscosity (η^*) values form the same measurement did not show the same correlation. Their test results were not consistent for all fluid samples, which indicates that several mechanisms are involved in barite sag.

Bui et al. [17] studied viscoelastic properties and their applications in oil based

drilling fluids, primarily in the linear viscoelastic range. The paper provide a comprehensive description on viscoelasticity behavior and testing. Furthermore, it was observed that linear viscoelastic range, gel strenght and dynamic yield stress is dependent on temperature and frequency. All of these decreased when temperature was increased and frequency was decreased. The time to develop a gel-structure was observed to be higher then what is recommended by API to determine the gel-strength. It was also investigated if the samples obeyed the Cox-Merz rule (explained in section 2.3). The results showed that the steady shear viscosity was lower than complex viscosity, and the samples did not follow the Cox-Merz rule.

Saasen et al. [34] performed a research study on static and dynamic sag in water based drilling fluids with the use of viscoelastic measurements and a standard Fann-35 viscometer. The research was introduced by classifying the drilling fluids by plotting the 3-rpm reading versus gel-strength, classified as high or low. This gave four different classifications of the fluids. Furthermore, to quantify the measured barite sag, a sag number was defined based upon a sag cell. When the static sag was plotted, represented by sag number, vs the 3-rpm reading, it was observed a poor correlation - indicating that the 3-rpm reading is not a good measure of sag potential. When the static sag was plotted against 10-min gel strength, a better correlation was obtained. The trend showed that a higher gel-strength reduced gel, however; this was not valid for all fluids. The dynamic sag measurements showed that viscosity may play an important role, given that the fluid has some resistance to static sag. Viscoelastic measurements was also performed, which focused on G' and G'', and in particluar the ratio of these two as this indicates structural build up of the fluid. The results indicates that G'/G'' will provide information about static sag potential. However, it was emphasized that the value of (G'/G'') is dependent on measurement technique with respect to frequency and amplitude. The hypothesis that G'/G'' should be greater than a constant to avoid static sag was thus supported. In the conclusion of the paper, it is mentioned that dynamic sag is related to low-shear viscosity and that gel formation is an important factor in connection to static sag.

The paper from Omland et al. [23] studied how the amount of shear, or mixing energy, affect an invert-emulsion drilling fluids behavior. Barite sag and

viscoelasticity was investigated to observe if the applied mixing energy influenced the properties. When mixing energy is applied to an emulsion, the droplets will become smaller which increase the surface area and reduce the distance between them. The increased surface are will increase the viscosity while the reduce emulsion droplets will increase the storage modulus, which is related to barite sag. Sag measurements taken at different times of shearing showed improvements when the fluid was sheared for a longer period. Also, the crossover point in the amplitude sweep showed improvements when a the fluid was sheared. The paper concludes that increased shear energy is beneficial with regards to sag potential; and that barite sag potential can be predicted from viscoelastic measurements.

3.1.1 Yield Stress in Drilling Fluids

Yield stress has already been defined from the literature in section 2.1.3 as the amount of stress required to initiate a flow in a liquid. Some highly shear-thinning liquids appear to show yield stress characteristics since a rapid drop in viscosity is observed over a small difference in shear stress, as shown in figure 12. Using appropriate measurement techniques for measurements below this value for shear stress, it can be shown that the viscosity is constant, although large, before it drops many orders of magnitude. Therefor It might be better to refer to a "yield stress region" rather than a yield point [7, 40].

In the paper from Barnes [40] it is argued for that the models containing yield stress gives a good description of flow above the critical stress limit, but also that yield stress for non-Newtonian liquids is just an value that is extrapolated from higher shear rates and that yield stress is not a correct measure for the limiting value of flow. Caenn et al.[5] states that most drilling fluids behaves as an intermediate between Bingham plastic and ideal power law fluids, and that drilling fluids have a *indefinite* yield stress that is lower than one would get by extrapolating shear stress values form high shear rates. Jachnik [41] compares current measurement techniques to estimate yield stress in drilling fluids and compared them with a controlled shear stress rheometer. The comparison showed that curve fit methods obtained from conventional viscometer overestimated apparent yield stress unless the fluid contained a high concentration of fine solids, which led to an

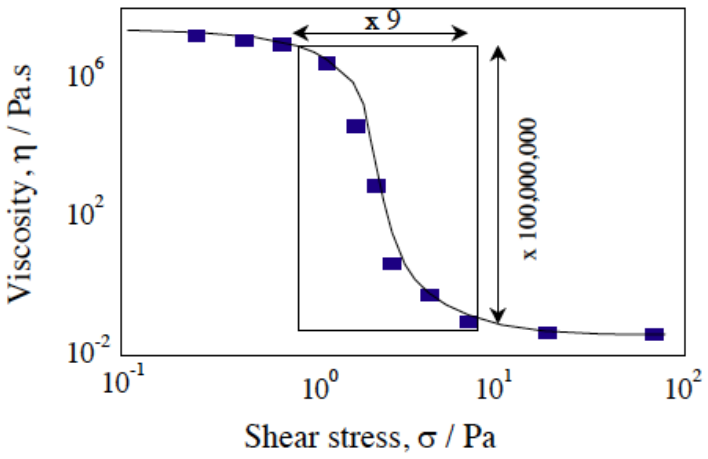

Figure 12: Flow curve of 10% bentonite suspension showing the viscosity drop over a small range of shear stress. From Barnes[40]

underestimation of yield stress. This was also the same for low-shear yield stress, defined in equation (3.1). The paper conclude that viscosity calculated from models are usually underestimated due to the shear rates experienced in parts of annular space ($< 0.01\,s^{-1}$. The paper also emphasizes that the industry relies too much on the Bingham plastic model and suggest that the model should be abandoned, with the exception of monitoring plastic viscosity. Another study emphasizing the yield stress topic is the paper from Maxey et al.[42]. They question what methodology is the most appropriate to as direct measurement of the yield stress. In the research, a controlled shear stress and oscillatory measurement techniques was used to evaluate yield stress. The paper recommend that rheological characterization should be performed at shear rate below $0.1\,s^{-1}$ for more accurate hydraulic predictions, and that the measured yield stress values depended on the measuring technique.

Zamora et al. [43] states in the paper that the yield stress is difficult to determine for a given liquid. The paper suggest that a direct measurement for the yield stress is preferred since yield stress is a property of the liquid, which is independent of any models.

4 Experimental Studies

The oil based drilling fluids used in this thesis were provided by M-I Swaco Norway in accordance with specifications given from the University of Stavanger for this thesis. In order to investigate the oil-water ratio impact on oil based drilling fluids it was essential to keep the concentration for as many as possible chemicals constant for all of the four fluids and let the OWR vary from 60:40 to 90:10. The density of the drilling fluids used in this thesis was 1750 kg/m^3 and had an OWR of 60:40, 70:30, 80:20 and 90:10. Constant density is important in order to characterize the influence of water since solids will affect the fluid behavior. Hence, the only chemicals that are not constant for these fluids are water, baseoil, salt and barite. Salt was necessary to keep as a variable in order to obtain an equal water phase salinity. The formulation of all four drilling fluids is given appendix A.

The rheological measurements were conducted to investigate the fundamental rheological behavior of the drilling fluids at different temperatures. This was performed using the OFI model 800 8-speed, which is a conventional couette geometry, direct-indicating viscometer. These type of instruments are quick and easy to use, but are not as accurate as a high end rheometer. The sag testing was performed under static and dynamic conditions with the use of an alternative static sag test and sag shoe kit, respectively. Observations made in this section will be used in hydraulic modeling and cuttings transport simulation, while the sag observations are to be used in connection with viscoelastic measurements in section 4.4 to investigate for any possible correlations.

4.1 Preprations

Due to the thixotropic behavior of drilling fluids, rheological measurements are dependent of shear history. In order to obtain consistent measurements for all four samples, it was important to define a procedure prior of testing. The preparation included to shear the samples using a Hamilton Beach mixer for 30min prior to performing rheological measurements on the viscometer in order to obtain the same initial state for all samples. This was also done to ensure that a the water was completely dispersed into the oil, and to shear any organophilic clay residues within the drilling fluid. The electrical stability (ES) of the mud was measured before and after shearing as an measure of emulsion stability, given in table 12. Before the rheological measurements were carried out, the drilling fluid was heated to specified temperature using a heating cup, and the drilling fluid was then stirred at high shear rate. The measurements were then performed from high to low shear rates before the 10 s and 10min gel strength was measured.

4.2 Rheological results

The following subsection contains the results obtained from the rheological measurements. The flow curves are represented in oilfield units as this is the most common representation in the oil industry. The y-axis represents the shear stress and is given in dial readings that are not corrected to $lb/100\,ft^2$ and the shear rate is given in reciprocal seconds on the x-axis. The flow curves are represented at 50 °C, with the remaining 20 °C and 80 °C measurements given in appendix B. A comprehensive table for all of the rheological measurements, including gel strengths, are given in table 3.

The measurements are shown in figure 13 and gives an overview in how OWR affect the shear stress measurements. Dial readings decrease when the OWR increase, with a significant difference between the OWR 60:40 sample and OWR90:10. This will lead to increased pump pressure and annular pressure loss, which will be discussed in section 5.1.

The measurements in table 2 shows the ES measurements before and after shearing the mud on a Hamilton Beach mixer for 30min. The ES increasing when the water fraction is decreasing, which is a measure of emulsions stability. The

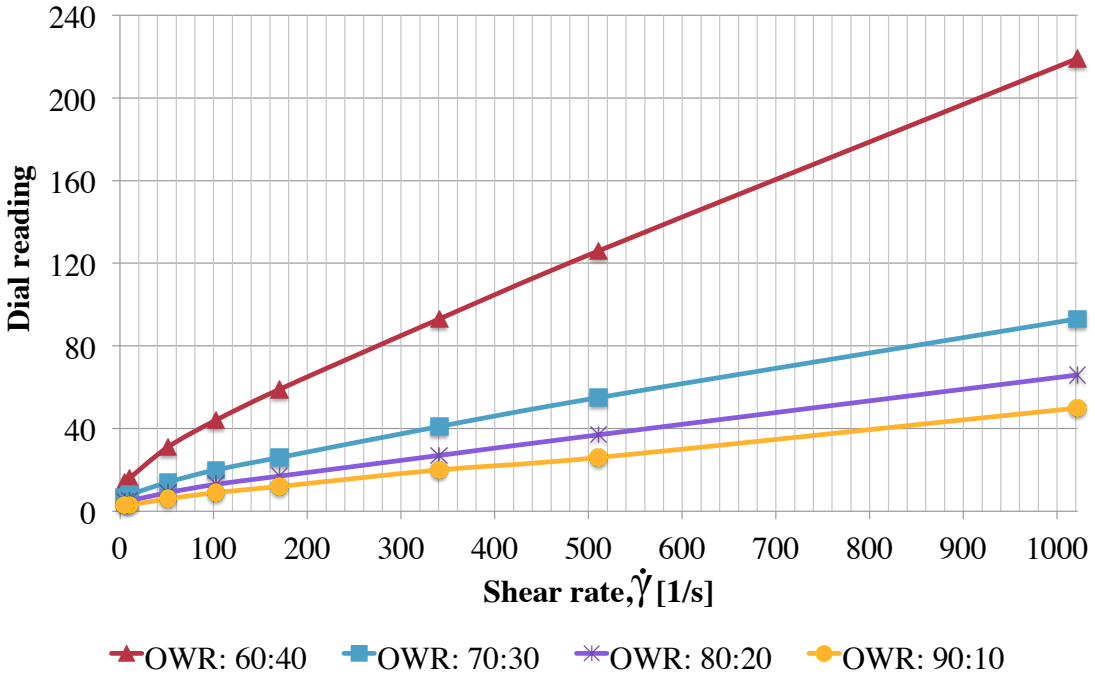

Figure 13: Flow curves for all four samples measured at 50 °C

fluid sample with the largest water fraction has the lowest ES, which is caused by the increased concentration of water droplets within the fluid which creates a conductive pathway between the probes. The 90:10 OWR can be evaluated as the most stabile emulsion based upon the measurements, primarily caused by the very low water fraction.

Table 2: Electrical Stability before and after shearing (50 °C).

OWR	ES before shearing [V]	ES after shearing[V]
60:40	502	598
70:30	699	860
80:20	746	1218
90:10	641	1977

Table 3: Dial reading measurements of all four mud systems on 20 °C, 50 °C and 80 °C. Shear stress not corrected to lb/100 ft^2

Oil Water Ratio	60 : 40			70 : 30			80 : 20			90 : 10		
Temperature	20 °C	50 °C	80 °C	20 °C	50 °C	80 °C	20 °C	50 °C	80 °C	20 °C	50 °C	80 °C
Shear rate[RPM]												
600	278	234	118	131	99	58	85	70	49	62	53	34
300	159	134	74	75	59	37	47	39	29	37	28	19
200	116	99	57	54	44	30	34	29	22	27	21	14
100	71	63	38	35	28	20	21	18	15	15	13	10
60	53	47	30	26	21	16	15	14	12	11	10	6
30	36	33	22	18	15	14	11	10	7	7	6	5
6	19	17	13	10	9	6	5	5	5	3,5	3,5	3,5
3	17	15	11	9	7	5	4,5	4,5	4,5	3	3	3
10sec gel:	14	13	10	7	6	5	5,5	5	5	3	3	2
10min gel:	18	14	11	9	7	6	6	5,5	5,5	4	4	3,5

4.2.1 Model Fit

The rheological modeling was done in order to evaluate which rheological model describes the drilling fluids used in this thesis best. A total of 6 different models was used in this modeling where the rheological measurements in table 3 was used as input. Theses were; Newtonian, Bingham Plastic, Power Law, Herschel Bulkley, Robertson and Stiff, and the Unified model. The Herschel Bulkley, Robertson and Stiff and the Unified model gives the most accurate description of the drilling fluids used here. The Robertson and Stiff model had the highest accuracy with an average deviation from measured values of 1.78% while the other two had a slightly higher deviation. The complete comparison for all models is given in appendix B.1. figure 14 compares the measured rheological values against the rheological models. Values on vertical axis is % deviation from measure values, with average deviation value given to the far right, denoted as "avg". The comparison reveal that the all of the models has an increase discrepancy for the 90:10 OWR drilling fluid.

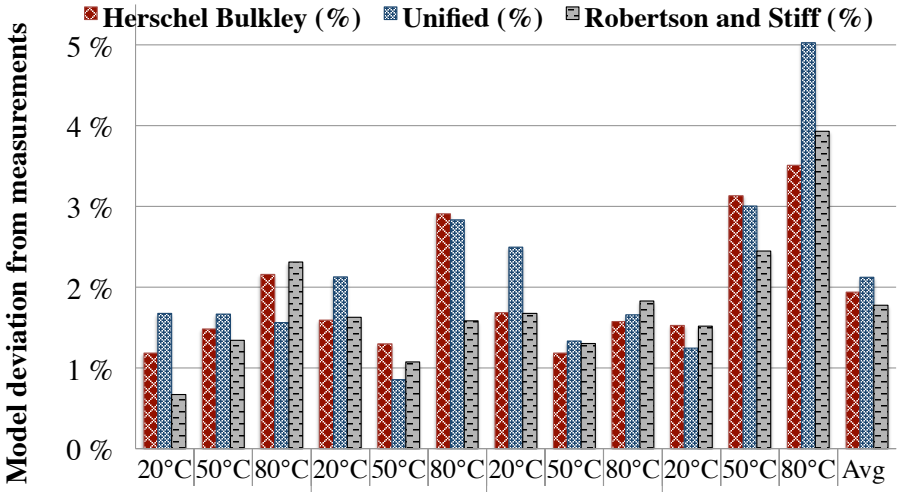

Herschel Bulkley (%)	1,2	1,5	2,2	1,6	1,3	2,9	1,7	1,2	1,6	1,5	3,1	3,5	1,9
Unified (%)	1,7	1,7	1,6	2,1	0,9	2,8	2,5	1,3	1,7	1,2	3,0	5,0	2,1
Robertson and Stiff (%)	0,7	1,3	2,3	1,6	1,1	1,6	1,7	1,3	1,8	1,5	2,4	3,9	1,8

Figure 14: Comparison chart of the rheological models Herschel Bulkley, Robertson and Stiff, and the Unified model. Model deviation against measured rheological valuses, given in %.

4.3 Sag Measurements

4.3.1 Alternative Static Sag Measurement

To measure the rate at which barite settle out of the fluid under static conditions, an alternative static sag test was developed. In addition, it was thought that this method would give insight in the stability of the fluid before taking dynamic oscillatory measurements at approximately static conditions for up to 3 hours.
The method was performed under static conditions at 20℃ with the use of a standard viscometer cup, a steel cylinder submerged into the fluid sample attached to a piece of string, which was hung of from a digital weight. The size of the steel cylinder was; [$H = 2.5\,\text{mm}$ $D = 2.5\,\text{mm}$]. The experiment was performed over a period of 4hrs and weight measurements were taken every 5th minute. The initial setup is illustrated in figure 15.

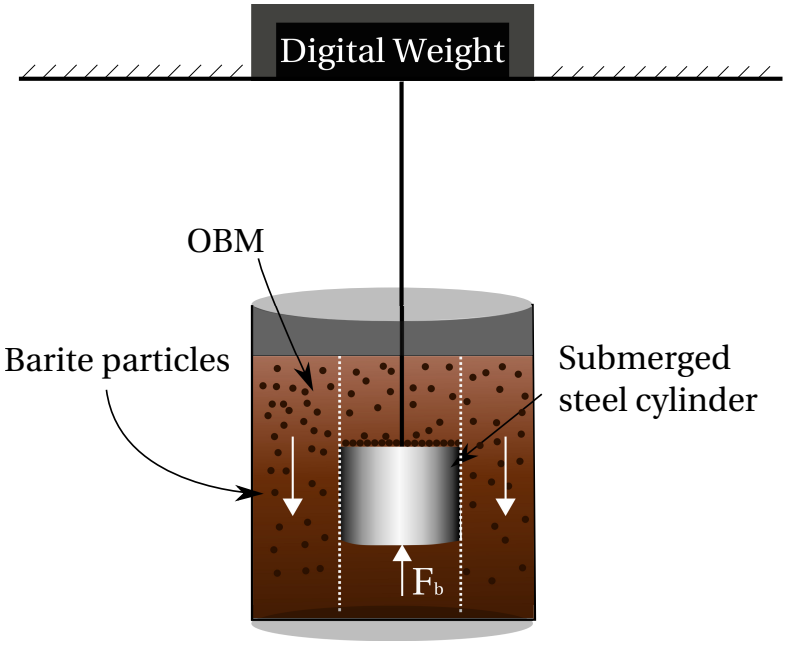

Figure 15: Experimental setup for alternative static sag test

The initial weight measurements of the submerged steel cylinder, for the 90:10 sample, showed a decreasing trend, or equivalent to an increase in force acting upwards, up to 20min. This might be explained by some initial structure in the sample fluid when it comes to rest. The following measurements shows an increase

in weight as an result of barite sag with a linear trend from t = 85 min. The rate at which the barite settles out from t = 85 min to t = 235 min is 0.282 g/h. However, the rate may be have been greater because of the buoyancy is acting in the opposite direction. The same experiment was performed on the fluid with an OWR of 80:20. Now the behavior is very different. A decrease in Δm is seen over a period of 3,5 hours before any weight increase is observed. The results indicate that the 90:10 OWR fluid does not have any structure within the fluid which can prevent settling even at ambient temperature. Due to the observed trend from the 80:20 sample, the remaining 70:30 and 60:40 samples were not tested.

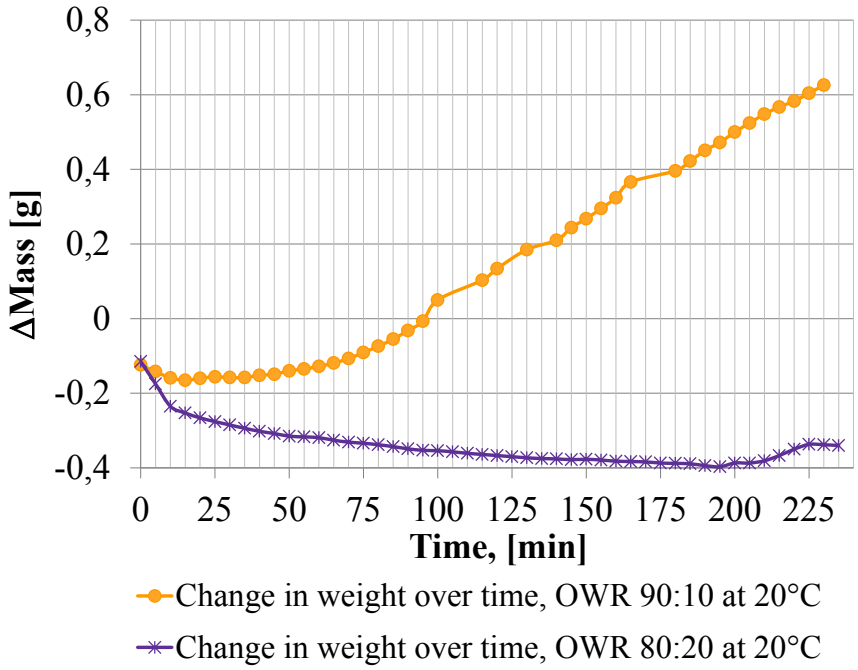

Figure 16: Results from alternative sag test. Change in weight of a cylinder submerged into OBM over time due to barite sag, measured at 20 °C over a period of ≈ 4hrs

4.3.2 Dynamic Sag Measurement

Dynamic sag measurements were performed in order to quantify which of the drilling fluids that was most prone to dynamic sag. The VSST method was chosen to measure this. Prior of measurements, the fluids was sheared with an Hamilton

Beach mixer for 15 minutes. The VSST method was performed at 50 °C with the use of 140 ml fluid. In order to avoid premature saging while heating up the fluid, the initial shear rate was set to 600RPM before a reference weight was taken from the collection well at the end of the sag shoe. This volume was then returned into the heating cup before the shear rate was reduced to constant value of 100RPM for 30min. After the 30min period is over, a new weight measurement is taken. This was conduced with a 20 ml pycnometer and a digital weight. To calculate the change in fluid density with the following formula:

$$\Delta(\rho_{mud}) = \frac{m_{final} - m_{initial}}{\text{Volume}} \quad [\text{sg}] \tag{4.1}$$

The results are illustrated in figure 17

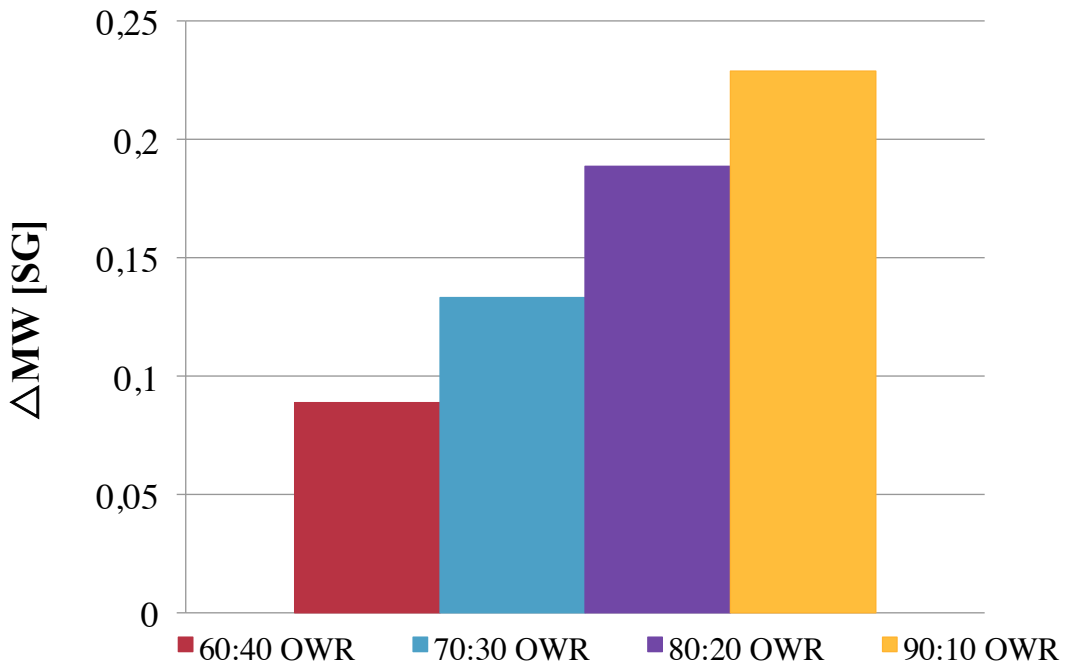

Figure 17: Dynamic sag measurements for all four samples at 50 °C with the use of the VSST method.

The experiment showed that the dynamic sag increase with OWR, and an increase of 0,14sg is observed if we compare 60:40 against the 90:10. This can be seen in connection with the low-shear rheology of the drilling fluids, given section 4.2.

4.4 Dynamic Measurements

The following sections contains the main emphasis in characterization of the drilling fluids presented in this thesis. A total of seven different types of measuring methods were used in the characterization. To avoid a plethora of similar graphical presentations in this section, only the outermost important results are presented while the remaining observations are given in appendix D. The units for stress in the results are given in Pa. Note that the samples are divided by their OWR, meaning that the fluid with an OWR of 60:40 will be denoted as "sample 60:40". The same accounts for the samples with an OWR of 70:30, 80:20 and 90:10.

4.4.1 Experimental Setup

The Anton Paar Modular Compact Rheometer 302 was used for the dynamic measurements. This is an advanced rheometer which can function as both stress-controlled and strain-controlled. The instrument is equipped with a Peltier temperature element, which provides high accuracy temperature regulation with quick response. The following tests were performed in order to characterize the fluids:

- Amplitude Sweep.
- Frequency Sweep.
- Time Sweep.
- Temperature Sweep.
- Creep Recovery Test.
- Controlled Stress Ramp.
- Shear Rate Ramp.

Both non-steady shear and dynamic measurements was performed on all drilling fluids. For the stress ramp and shear rate ramp, a concentric cup geometry was used. The cup geometry was chosen for these measurements to avoid wall slip. The remaining test was performed on a 50 mm parallel plate geometry. The preliminary rheological measurements and sag testing made in section 4.2 and section 4.3.2 revealed wide difference in the fluid characteristics. Due to the fact that testing of drilling fluids is highly dependent on the measurement techniques,

the following procedures was followed on a general basis to minimize measurement error:

- To ensure that reasonable results was achieved from all fluid systems, a temperature of 20 °C was chosen as a test temperature for all isothermal tests.
- All of the test samples was sheared for 10min on a Hamilton Beach mixer prior of starting a series of tests to provide an equal preference for all samples.
- The sample was set to rest for 10min after it was applied on the instrument to achieve a start temperature of 20 °C, and equal start conditions.

4.4.2 Amplitude Sweep - Results

The amplitude sweep test was the first test to be performed in order to define the linear region of the viscoelasticity and to observe the structural characteristics of the liquds. This was, at first, performed with angular frequency of 10 rad/s with the strain varying from 5×10^{-4} % to 50 %. The results from the amplitude sweep test is presented in figure 18.

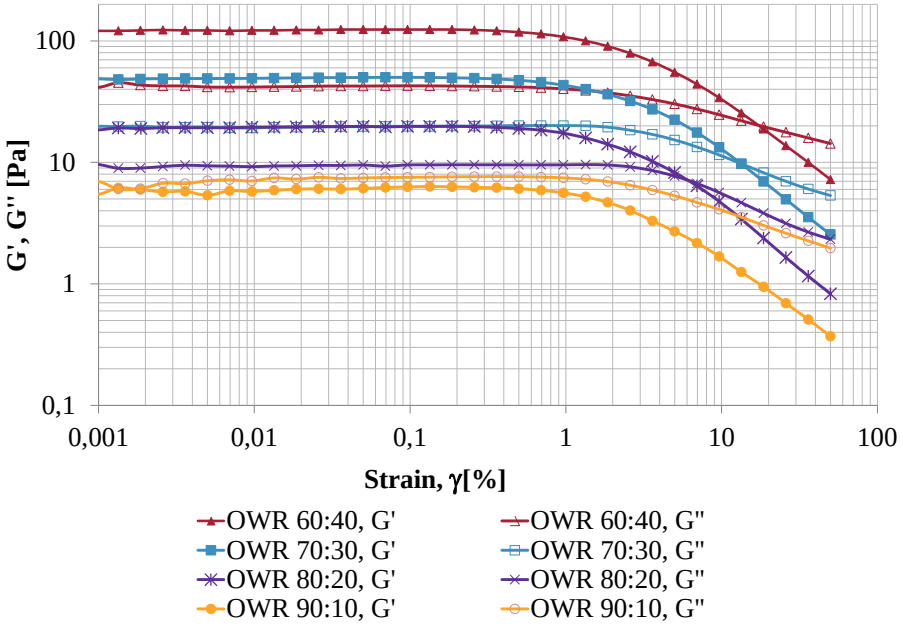

Figure 18: Amplitude sweep test performed on all fluid samples at 20 °C and $\omega =$ 10 rad/s. Note that $\omega = 20$ rad/s for the 90:10 sample.

Figure 18 shows that the LVE region is less than 1% for all samples. For the 90:10 OWR sample, the loss modulus was higher than storage modulus, which is in contrast to what is observed for the other samples. This means that the 90:10 sample exhibit the character of a viscoelastic liquid and that the viscous behavior dominates over the elastic ones. The other samples shows an elastic dominance over the entire LVE region and can thus be characterized as viscoelastic gel. Table 4 defines the crossover point (or flow point) where $G' = G''$, (τ_{fp}), and the maximum LVE range in terms of strain (γ_{ys}) and stress τ_{ys}. The applied strain in further analysis is a smaller value than the γ_{ys} as a safety margin to not exceed the LVE region.

The flow point and the degree of viscoelasticity can be much more easily be presented by plotting phase angle, δ, against shear stress as this is 45° when $G'' = G'$, as shown in figure 19. A low value of the phase angle, δ, represents a greater value of G' compared to G''.

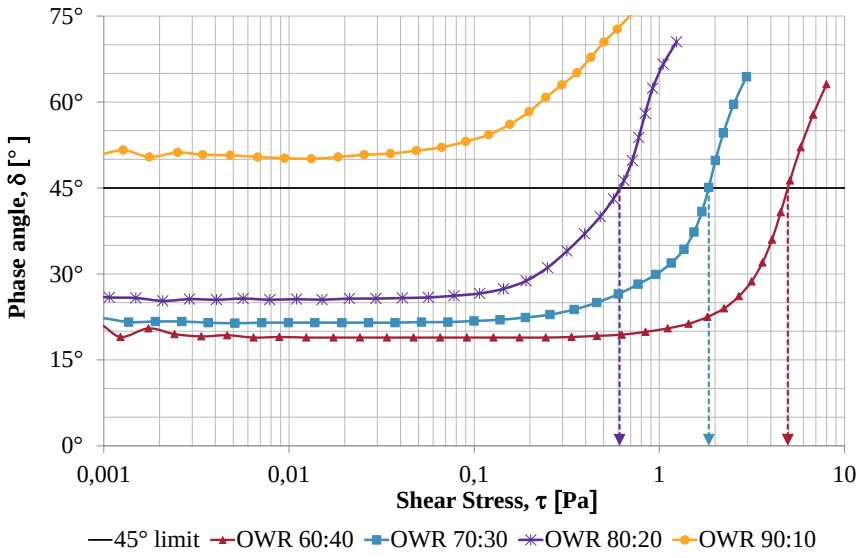

Figure 19: Amplitude sweep test presented with phase angle δ vs shear stress τ to give a better visualization of flow point in terms of stress. Vertical arrows indicating τ_{fp}. Same measurements as in figure 18 and table 4

Table 4: Amplitude Sweep Summary

Sample name	τ_{ys}[Pa]	γ_{ys} [%]	τ_{fp} [Pa]	$G'' = G'$ [Pa]
60:40	0,44	0,34	4,94	20,28
70:30	0,17	0,33	1,85	9,78
80:20	0,07	0,32	0,61	7,11
90:10	N/A	0,28	N/A	N/A

The higher water faction in the 60:40 sample contributes to an elevated storage modulus. This might be due to increased interaction between clay and emulsion droplet. The ratio of G'' and G' decreases with higher water content, meaning that there is a larger degree of elastic behavior.

Additional testing of the 90:10 OWR sample was performed at 1 rad/s, 10 rad/s, 20 rad/s, 50 rad/s and 100 rad/s

Repeatability

The fluid with an OWR of 80:20 was tested at four different times with same parameters in order to observe the reliability of the results obtained in the amplitude sweep. The results showed some discrepancies with two + two in pair exhibit similar behavior. This indicates how important the measurement technique and procedures are. This test could have achieved better results if another fluid with better structure was chosen, for instance the sample with OWR 60:40.

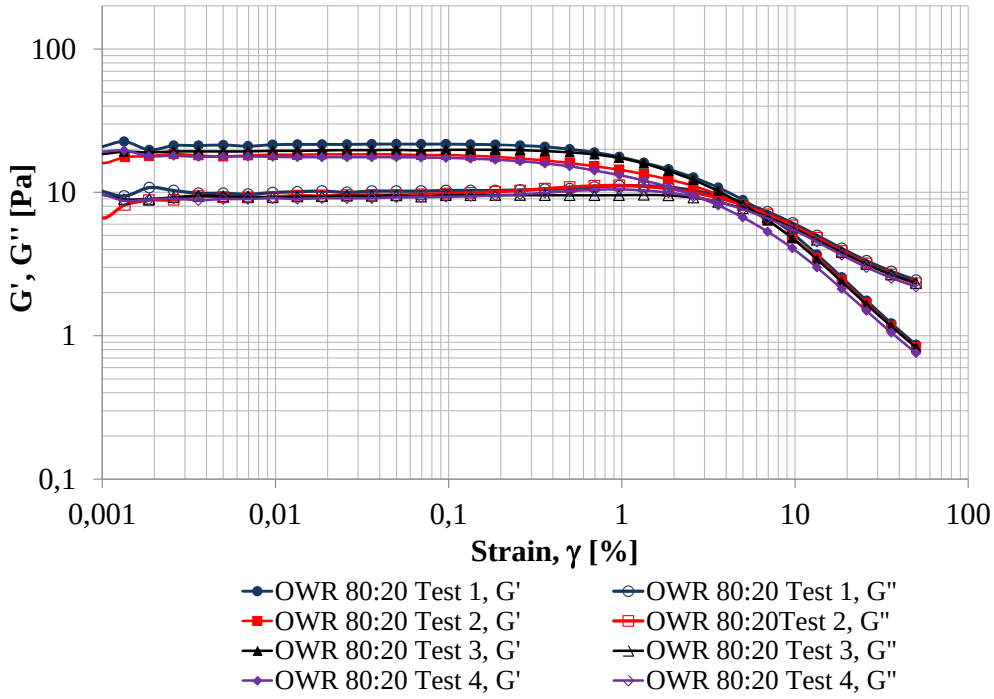

Figure 20: Four different amplitude sweep tests for 80:20 OWR to test the reliability of the amplitude sweep test. Measured at $20°C$ and $\omega = 10\,\text{rad/second}$

The phase angle vs shear stress to observe the flow point, τ_{fp}, in relation to these measurements are given in appendix D.1

Frequency Dependency Another set of amplitude sweeps was performed to investigate the frequency dependency on the LVE range. The same procedure was followed as defined in section 4.4.1, except that the angular frequency was increased from $\omega = 10\,\text{rad/s}$ to $\omega = 50\,\text{rad/s}$. The observation for 60:40, 70:30 and 80:20 is given in figure 21 andfigure 22. The results from this experiment showed that the LVE range is similar with an increased frequency for both the 60:40 and 70:30 samples. Both the storage modulus and loss modulus showed an overall increase for all of the samples; however, the loss modulus increased the most. This can be observed in figure 22 as the phase angle is increasing. The flow point increased for both the 70:30 and the 80:20 samples, while was approximately the same for the 60:40 sample.

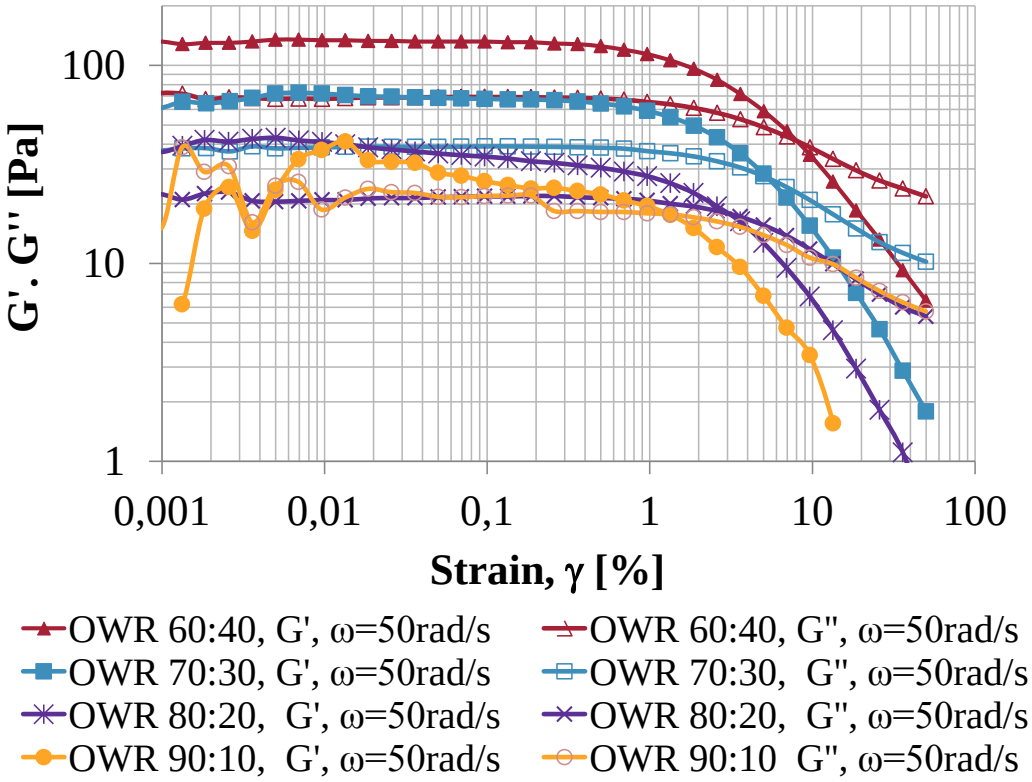

Figure 21: Amplitude sweep performed on all fluids at $\omega = 50\,\text{rad/s}$, $20°C$

The 90:10 sample were more difficult to interpret due decreasing trend of G' at very low strain, indicating that the LVE was not obtained. A total of five different angular frequencies were performed on the 90:10 sample with $\omega = 1\,\text{rad/s}$, $10\,\text{rad/s}$,

20 rad/s, 50 rad/s and 100 rad/s. The observations are given in appendix D.1, which gives a good visualization of the increase in both G' ang G'' with frequency. The experimental results to compare the angular frequency dependency for the remaining samples are shown in figure 22. To illustrate the changes, the phase angle is plotted against the shear stress.

The frequency dependency is an important observation to remember when performing the subsequent tests as they must be tested within the linear region to reveal the viscoelastic characteristics.

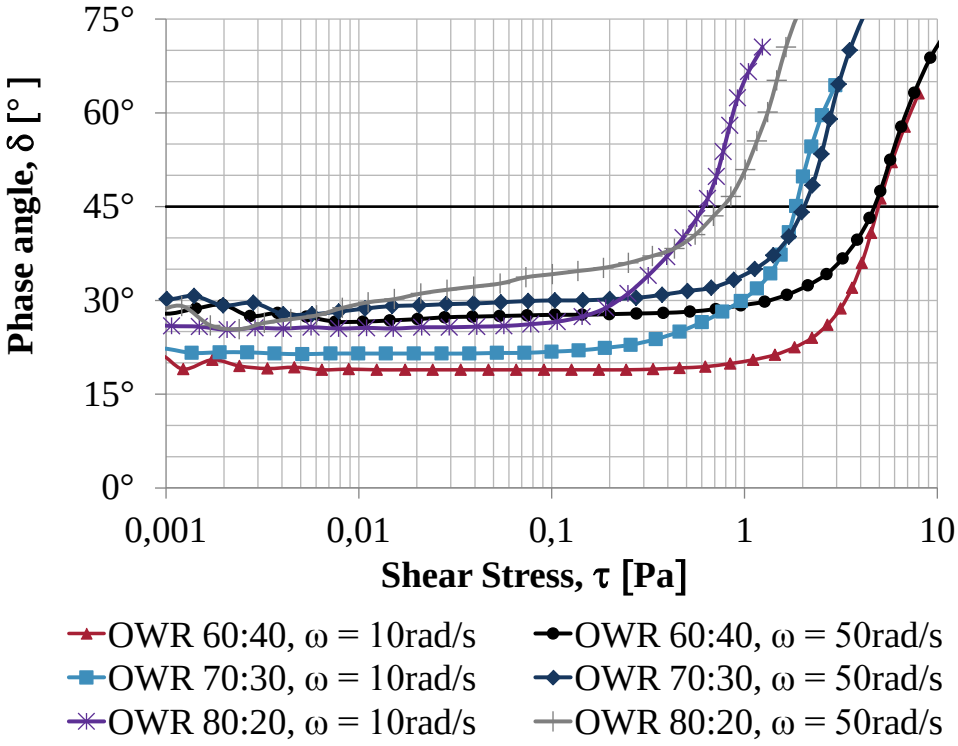

Figure 22: Amplitude sweep performed at 10 rad/s and 50 rad/s

Effect of Shearing In order to investigate how the effect of shearing affect the viscoelastic properties of the fluid sample, an amplitude sweep test was performed on the fluid with an OWR of 60:40. The fluid sample was sheared on a Hamilton Beach mixer for 5min, 20min and 60min. The sample was then set to rest for 10min on the Peltier to reach an equilibrium temperature of 20 °C before the amplitude sweep test was performed with the same parameters as the defined in section 4.4.1.

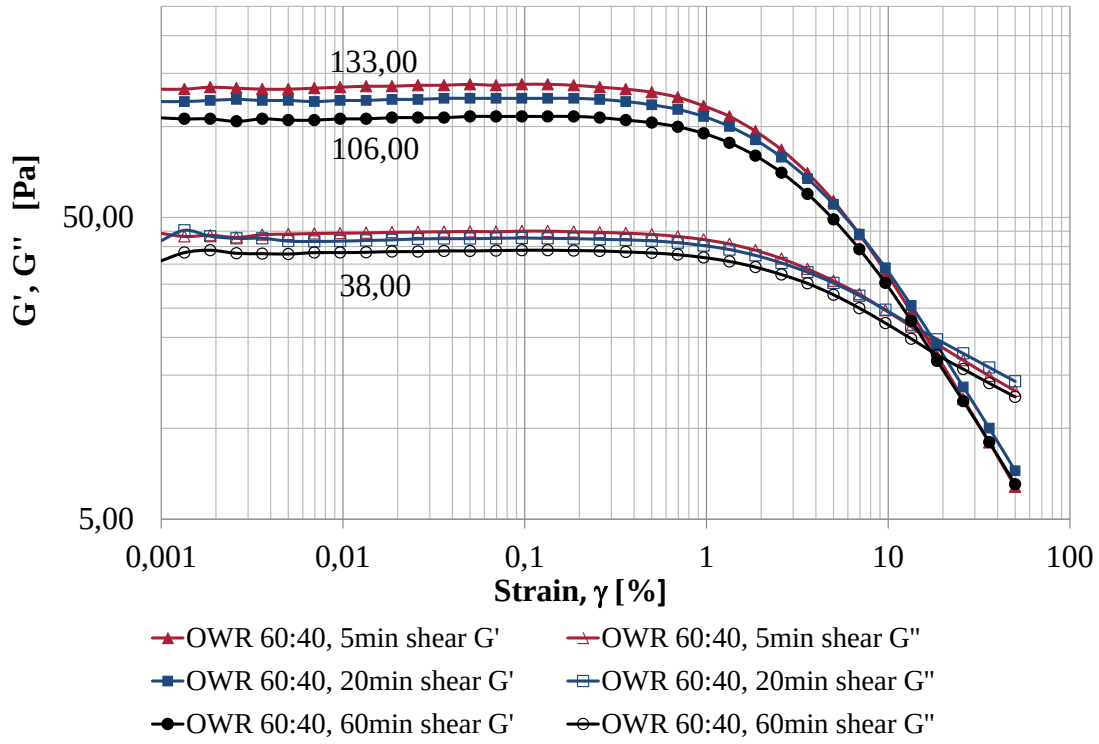

Figure 23: Amplitude sweep test performed on sample with an OWR of 60:40 at 20 °C and $\omega = 10$ rad/s after shearing of 5min, 20min and 60min

The results show a small increase in the ratio of G'' to G' when time of shear increase, from 0.33 for 5min of shear, to 0.34 for 20min of shear and 0.36 at 60min of shear. It can be seen in figure 23 that G'' is not as much affected by time of shear as G' is. This means that the fluid is less degree of elastic dominance when time of shear increase. This observation is not necessarily what one would expect, as more shear would cause smaller water droplets and thus reduce the distance between each of the water droplets, which in theory should increase the storage modulus, as reviewed in the literature study of ref.[23]; however, similar tendency was observed

by [38]. The amount of applied mixing energy with the Hamilton Beach mixer used may also not be sufficient to affect the size of the water droplets significantly. The flow point and LVE region is almost unchanged.

4.4.3 Frequency Sweep

Frequency sweep test was included to test the time dependent deformation response of a material. The angular frequency was set from high to low to avoid settling of weighting material. For the 80:20 and 90:10 samples, the angular frequency was set to start from a lower angular frequency than the other samples because of uncertainty in their LVE region for higher angular frequencies. The input parameters used the sweep is given in table 5. The results obtained can be used to evaluate solid suspension properties of the fluid. The experimental observations are divided into two figures, figure 24 and figure 25.

Table 5: Input Parameters in the frequency sweep test

Sample name	γ [%]	ω [rad/s]
60:40	0,1	0,01 - 100
70:30	0,1	0,01 - 100
80:20	0,036	0,01 - 10
90:10	0,01	0,01 - 10

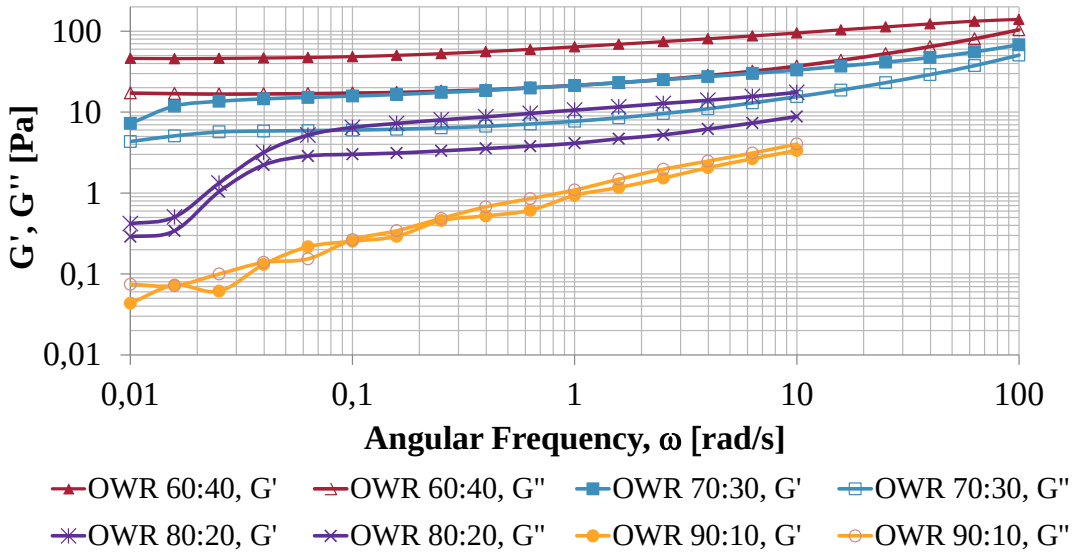

Figure 24: Frequency sweep performed at 20°C, $\gamma = 0.1\%$ for 60:40 and 70:30, $\gamma = 0.036\%$ for 80:20 and $\gamma = 0.01\%$ for 90:10

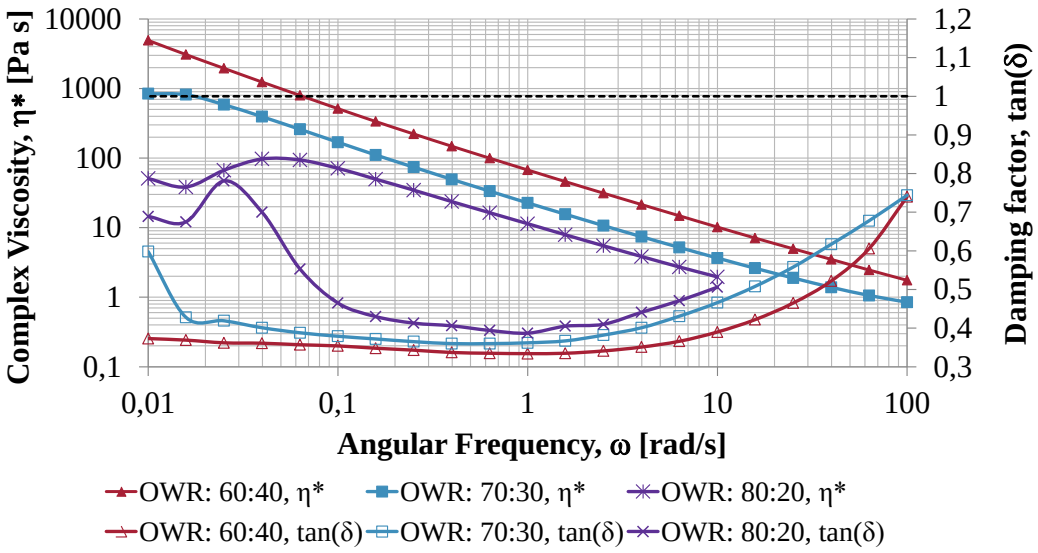

Figure 25: Frequency sweep performed with same parameters as in figure 24. Complex viscosity and damping factor as vertical axis. 90:10 sample not included due to very fluctuating values.

From figure 24, the 60:40 sample display elastic response over the entire range of angular frequencies. The separation of G' and G'' remains almost constant from 10 rad/s and downwards, hence, the behavior can be considered to be independent of the angular frequency below 10 rad/s. When the OWR is decreased to 70:30, similar response is observed; however, a drop in G' and η^* is seen at angluar frequency close to 0.01 rad/s. This may indicate difficulties of keeping barite in suspension. For the 80:20 sample, an elastic dominance is observed from 10 rad/s down to 0.1 rad/s before a significant reduction in both G' and G'' is seen. This is much alike what is observed for the 70:30 sample, with an offset in angular frequency of 0.1 rad/s. The same observations were made at a later stage, given in appendix D.2. From the amplitude sweep test, the 90:10 OWR sample showed viscoelastic liquid behavior. This type of behavior was also observed in the frequency sweep with an viscous-like beavior ($G'' > G'$), confirming its lack of structure.

4.4.4 Time Sweep

The time sweep was performed in order to investigate how the structure of the fluid evolved over time. By observing how the elastic modulus develop over time, it is possible to study development and growth of a gel-like structure. The angular frequency was equal to 10 rad/s, which was the same as in the primary amplitude sweep, where the LVE range was well defined. The fluids were pre-sheared at 1000 s^{-1} for five minutes before the same strain used in section 4.4.3 was used and a total observation time of one hour was set. Time sweep observations is given in figure 26, where the storage modulus against time is shown on the left, and the corresponding damping factor (tan(δ)) is given on the right. Note that the measurements starts after 5 minutes of shear.

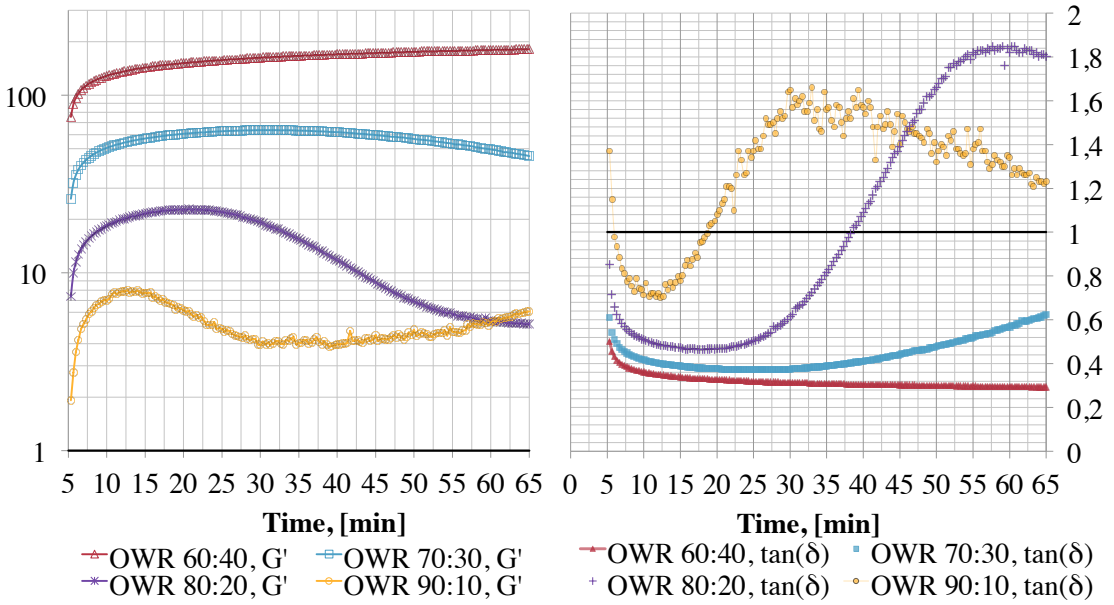

Figure 26: Time sweep of all samples at angular frequency of $\omega = 10$ rad/s, with pre-shear of 1000 s^{-1} for 5min, thereof the start time of 5min.

The initial observation is equal for all of the drilling fluids. An increase in G' and a drop in tan(δ) is observed due to the buildup of a structure. However, the subsequent reactions are very different for each of the samples. The 60:40 sample shows a continuous buildup and has not reached an equilibrium even after 1 hour. In the case of the 70:30 sample, a minimum value for tan(δ) is reached after 30

minutes before an increasing trend is observed over the remaining period. This can be interpreted as a breakdown of structure and barite will start to settle out. This is also observed for the 80:20 and 90:10 samples, although at an earlier stage. The 90:10 sample is showing large fluctuations in the damping factor after 25 minutes, indicating that barite is settling out and free oil moving upwards.

This is much alike what was observed for the 90:10 sample during the "alternative" static sag test in section 4.3.1. First an initial structure is developed before breakdown is observed and barite settle out. The two separate observations may be related. If the shear stress induced by the particles on the fluid in static conditions exceed the strength of the structure governed by the viscoelastic properties, the barite will settle out. If the gel strength is first broken the settling rate will increase even further until an constant rate is reached, as seen in section 4.3.1.

Effect of Angular Frequency:

Due to the observed breakdown of structure over time for all fluids except the 60:40 sample, the angular frequency was reduced to 1 rad/s in order to investigate if the breakdown also occurred at lower angular frequencies. The shear rate for a constant amplitude (γ_a) and angular frequency can be calculated with the equation (2.35)

$$\dot{\gamma} = \gamma_a \cdot \omega$$

Hence, with an reduction in angular frequency from 10 rad/s to 1 rad/s, and with a constant strain within the LVE range, the share rate is now 10% of the previous tests.

Figure 27 shows a comparison between the time sweeps performed at angular frequency of 1 and 10 rad/s in therms of G'. The results reveal that the structural build up is very similar to what was observed in the first time sweep even when the angular frequency is reduced. The main difference is that the values for G' is reduced, which is what one would expect. The same observation can be made if one take the API gel-strength on conventional viscometer. If we use a higher shear rate than 3RPM the shear stress will be higher and vice versa.

From the figure 27, it might appear that the 70:30 sample does not show any structural breakdown; however, it does reach its maximum after 59 minutes, at a value of 48.7 Pa, and start to degrade afterwards. Measurement for 90:10 sample

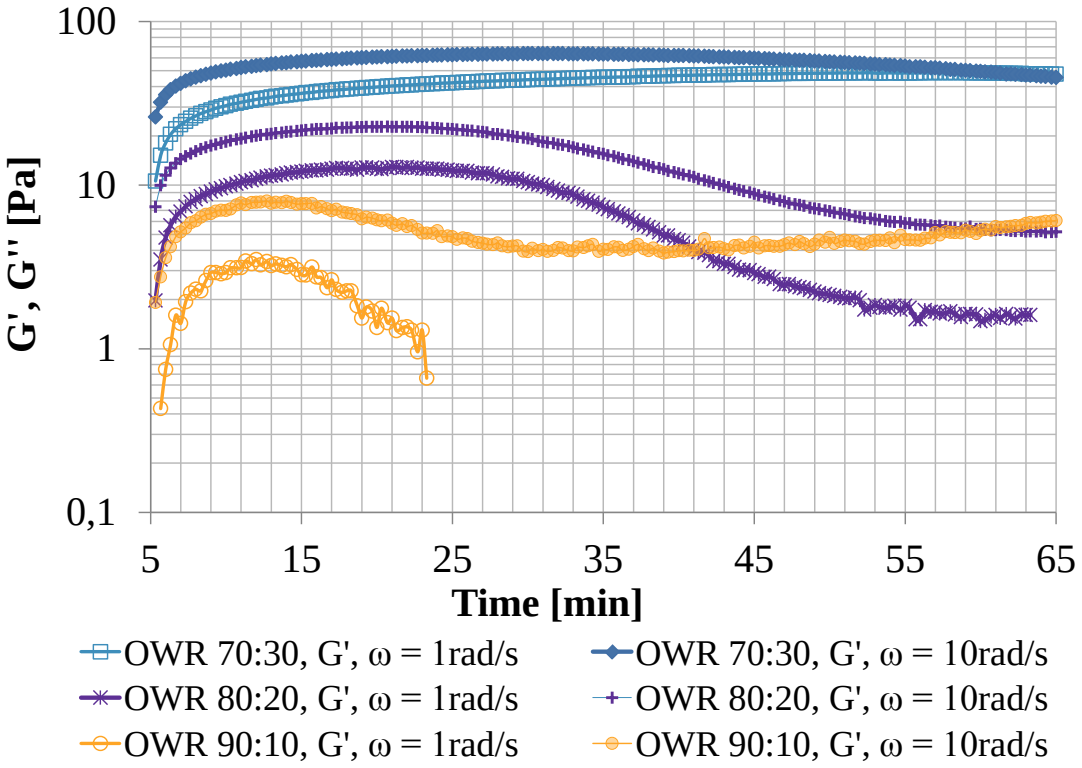

Figure 27: Time sweep of 70:30, 80:20 and 90:10 samples at angular frequency of 1 rad/s and 10 rad/s, showing storage modulus against time.

was aborted once the breakdown was observed. Additional time sweep tests are given in appendix D.3.

4.4.5 Temperature Sweep

Temperature sweep test was performed on all fluid samples. This test was performed in order to evaluate if there existed a temperature at which the fluid changed from being a viscoelastic gel to a viscoelastic liquid. The initial setup was performed with a linear temperature increase of $0,00926°C/s$ from an initial temperature of 4 °C to the end temperature of 80 °C. The angular frequency was set to 10 rad/s with the same strain defined in section 4.4.3. The test sample was let to rest for 10min to reach an equilibrium temperature of 4 °C. The initial setup caused the duration of the measurement to be last for more than two hours, which led to questionable results for the 70:30, 80:20 and 90:10 samples. More reliable results were obtained when a temperature gradient of $0,05°C/s$ per second was used. The observations are illustrated with G', G'' and $\tan(\delta)$. Figure 28 is showing the results for 60:40 and 70:30, while 80:20 and 90:10 are presented in figure 29.

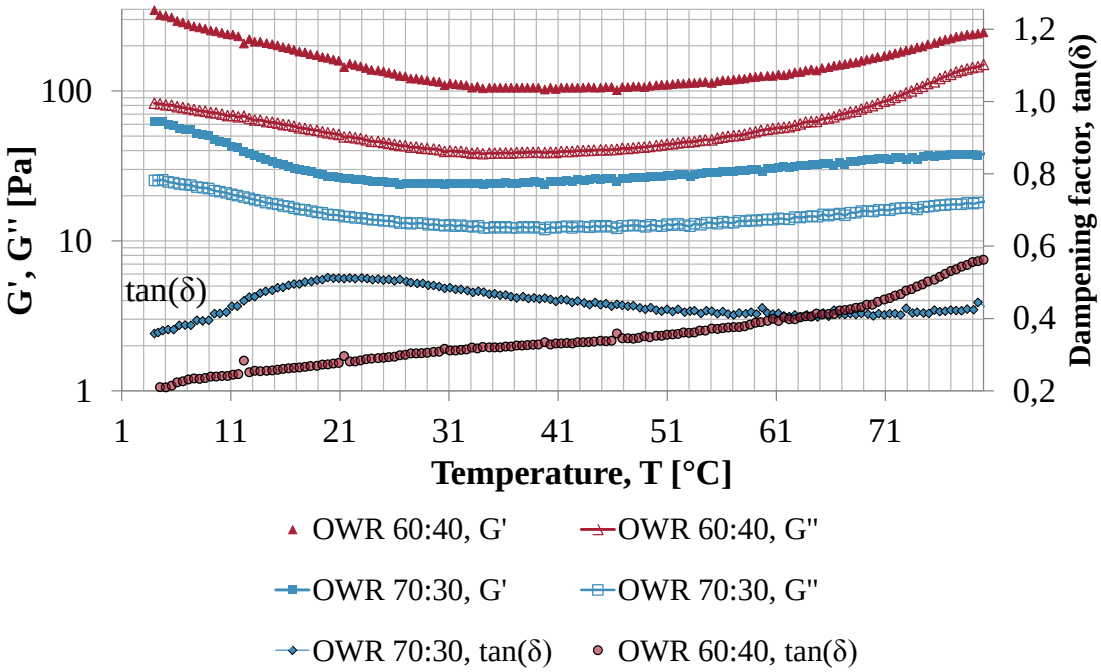

Figure 28: Temperature sweep of 60:40 and 70:30 samples at angular frequency of $\omega = 10\,\text{rad/s}$

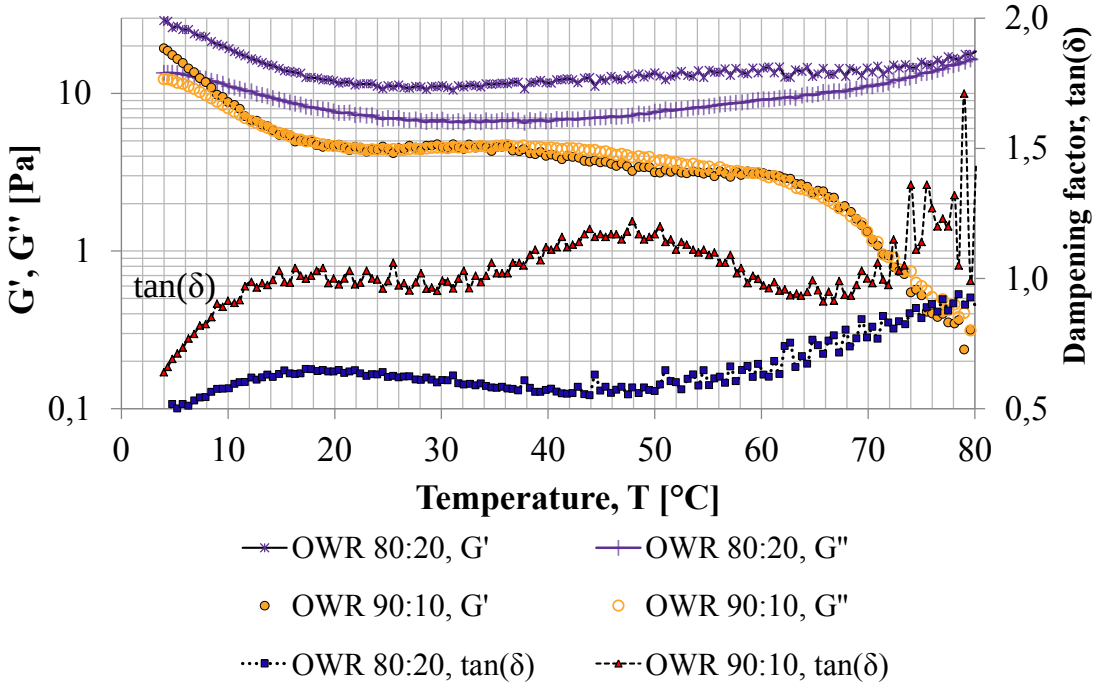

Figure 29: Temperature sweep of 80:20 and 90:10 samples at angular frequency of $\omega = 10\,\text{rad/s}$

All of the samples show same initial behavior for G'. A temperature of 4 °C makes a distinct elastic dominance, followed by a decrease as temperature increase.This is shown by an increase in damping factor from 4 °C to 20 °C in figure 28 and figure 29. Only the 90:10 sample have a cross over point where $G'' > G'$, which occur at temperature close to 17 °C; however, the remaining results for this sample is questionable due to fluctuations in damping factor values at elevated temperatures. For the samples with an OWR of 60:40, 70:30 and 80:20, the elastic modulus is greater than the viscous modulus over the whole temperature range, with no cross over point where $G' = G''$. At the initial temperature, the value of G' is significantly higher than at 20 °C. The 60:40 sample shows an continuous increase in damping factor over the whole temperature sweep. This might indicate that the fluid is showing a decreasing stability and is more prone to barite sag when the temperature is elevated; moreover, the same tendency is not observed for the other fluids. Also, the G' curve is showing the same shape for all of fluids except the 90:10 sample. This means that the shape of the complex viscosity curve (η^*) is similar in shape, which means that the minimum value of η^* is not where the temperature is highest, but

at the minimum point of G'. The results obtained for the samples with an OWR of 80:20 and 90:10, the results are more questionable, at least for temperatures above 45 °C. This is probably caused by a thin layer of base oil raising, which makes only the upper part of the sample subjected to oscillation while the remaining sample is stagnant. The following table defines the minimum value of $\eta*$ ang G' at the corresponding temperature. The 90:10 sample showed its minimum for complex viscosity at the end temperature and is not included in the subsequent table.

Table 6: Min. values for η^* and G' from temperature sweep

	$\eta*$ [Pa s]	G' [Pa]	Temperature [°C]
OWR 60:40:	10,9	102	39,8
OWR 70:30:	2,66	23,6	34,2
OWR 80:20:	1,24	10,5	31,1

This type of test is especially subjected to measurements error due to the temperature increase over time, which may cause evaporation, expansion / contraction, settlements of solids, and phase separation. The latter definitely happened during the measurements with the 90:10 sample when using a temperature increase of $0,00926$°C/s.

Additional tests with increased temperature gradient of $0,00926$°C/s was also performed, see appendix D.4.

4.4.6 Creep-Recovery Test

Creep-recovery test was performed on the fluids that showed a viscoelastic gel behavior. That is the fluids with an OWR of 60:40, 70:30 and 80:20. The 90:10 sample was not tested due to previous testing performed. The initial setup for the creep-recovery test was equal for both the 60:40 and 70:30 samples, while the 80:20 sample was tested with a lower shear stress. The creep recovery test was performed in order to characterize the fluids stability when a small stress is applied. Deformation at constant stress is similar to what happens during static sag. The following procedure was used;

- Preshear sample at 1000 s^{-1} for 3min

- Rest period of 10min
- Teperature was set to 20°C
- Applied shear stres for the 60:40 and 70:30 samples was 0.15 Pa
- Applied shear stress for the 80:20 sample was 0.02 Pa
- In the recovery phase, $\tau = 0$
- Temperature = 20 °C

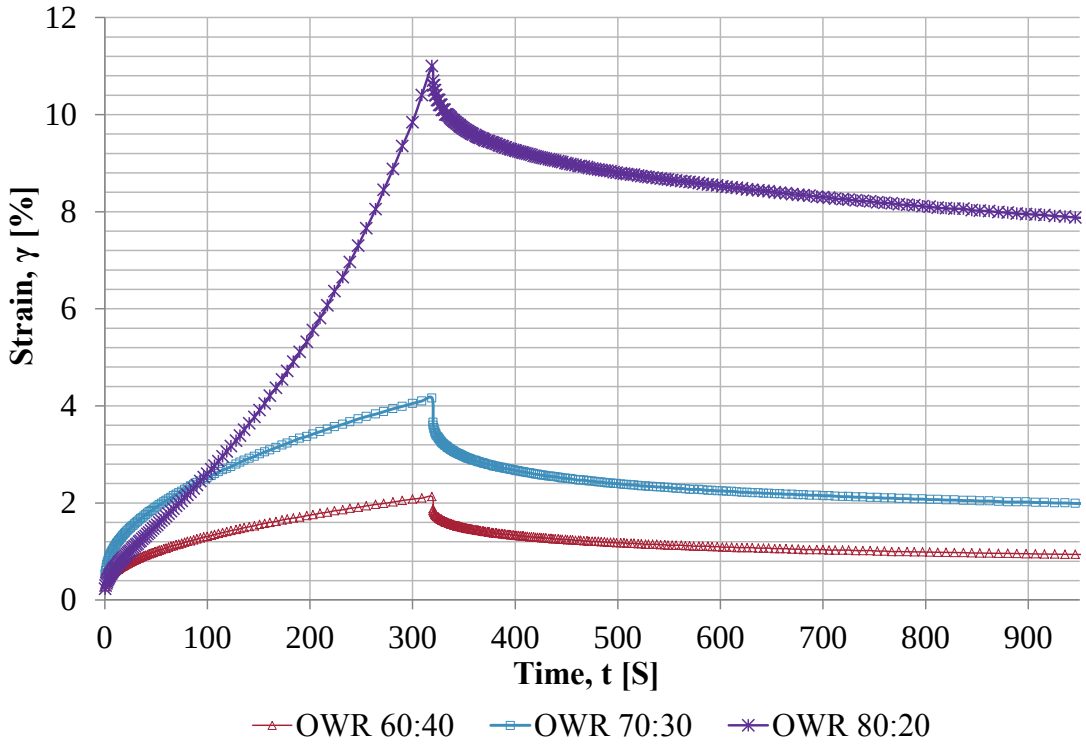

Figure 30: Creep recovery test of 60:40 and 70:30 samples with applied stress at $\tau_0 = 0,15$Pa. Applied stress for 80:20 sample; $\tau_0 = 0,02$Pa

The experimental observation is given in figure 30. When a constant shear stress is applied that is within the LVE region, the sample will deform until it has reached a steady state, or until the stress is released. When an equal shear stress is applied on the 60:40 and 70:30 samples the deformation is largest in the 70:30 sample. In the recovery phase the 70:30 fluid has a larger permanent deformation, which means that the 60:40 sample display a greater elastic behavior. In the case of the 80:20 sample, a significantly larger deformation is observed when a smaller stress

is applied. It also display a large permanent deformation after 10 minutes of rest compared to the two other samples. In other words, the fluid shows a signs of a weak structure, which will cause the fluid to be prone to static sag.

Additional creep-recovery test is given in figure 52, figure 52.

4.4.7 Controlled Stress Ramp

The stress ramp measurements were performed on all fluids with the use of a concentric cylinder measuring set. In this experiment the shear stress was ramped in a linear way from 0.1 Pa to 10 Pa at temperature of 20 °C. Also, to avoid too high shear rates as the stress was ramped, the parameters was set in a such way that the test was terminated if the shear rate exceeded 100 s^{-1}.

This type of test is a quick method to determine the apparent yield stress. Figure 31 shows the viscosity as a function of shear stress, $\eta(\tau)$.

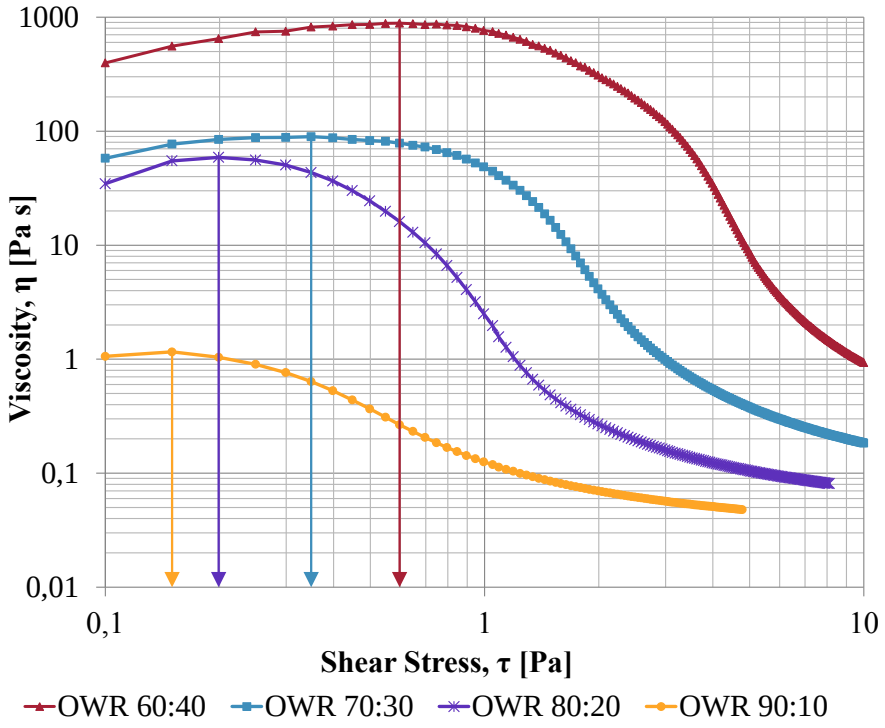

Figure 31: Viscosity vs shear stress from controlled stress ramp measurement showing the maximum viscosity method for determination of apparent yield stress. Measured at 20 °C. The arrows represent the apparent yield stress.

Normally, figure 31 would not have been in a logarithmic scale on the x-axis, however this was done to fit in all the four curves in one plot due to the significant spread maximum viscosity values over a small change in shear stress. When the same plot is presented on a non-logarithmic scale, a rapid viscosity increase is observed before a distinct viscosity peak is observed. Before the viscosity peak is reached, the liquid is undergoing elastic deformation and the peak is observed when this structure is broken (yields) and the fluid starts to flow. The observations made shows that an apparent yield stress exist for the 60:40, 70:30 and 80:20 fluids since a maximum viscosity peak is observed, while the 90:10 sample does not appear to have a distinct maximum value, which confirms the amplitude sweep results. The fluid is not undergoing elastic deformation due to the fact that there is a viscous dominance for this fluid.

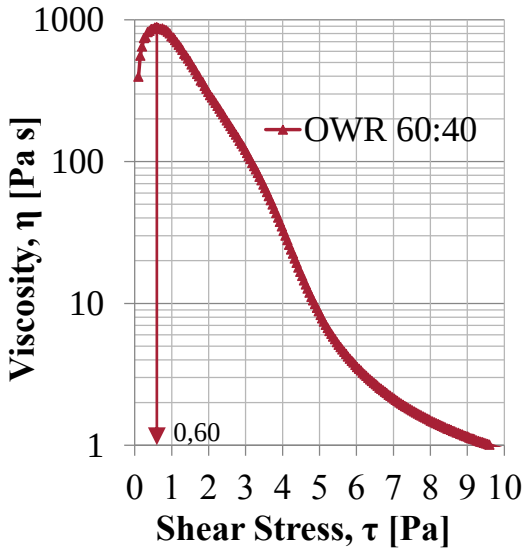

Figure 32: Viscosity vs shear stress for 60:40 sample from controlled stress ramp measurement showing the maximum viscosity. Same measurement as in figure 31

This experiment was also performed with applied stress varied from from 1 Pa to 10 Pa, and from 0.01 Pa to 10 Pa. The plots for these are given in appendix D.6

4.4.8 Controled Shear Rate Sweep

The shear rate ramp was performed in order to obtain viscosity profiles over a wide range of shear rates for each of the drilling fluids being studied. This was conducted by controlling the shear rate in a non-steady state, from 1022 s^{-1} to 0.001 s^{-1}. The sample was first pre-sheared for three minutes at 1022 s^{-1} before the measurements started at a temperature of 20 °C.

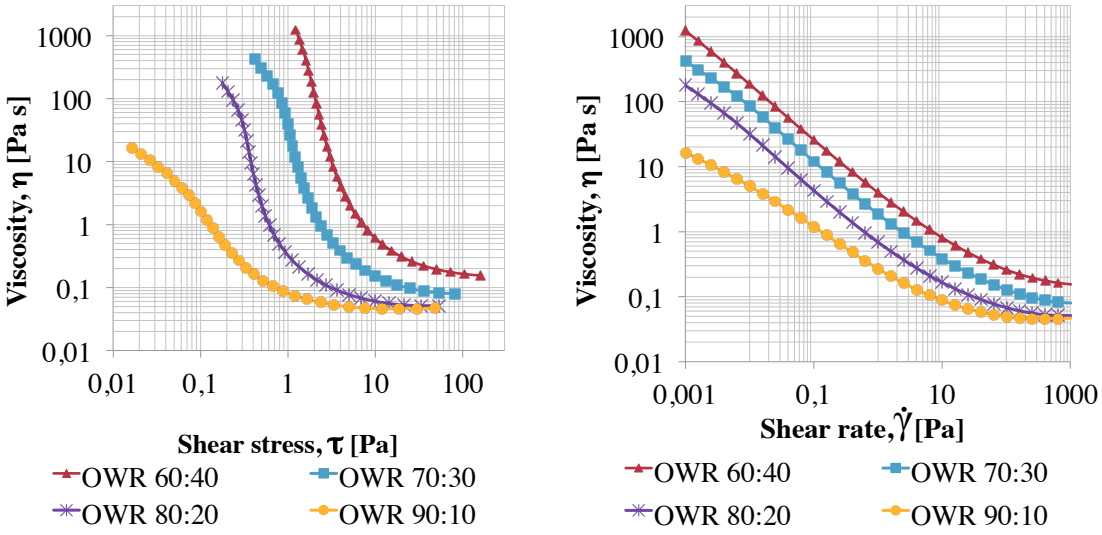

Figure 33: Left: Viscosity vs shear stress. Right: Viscosity vs shear rate - for all four samples, measured in shear rates from 1022 s^{-1} to 0.01 s^{-1} measured at 20 °C

From figure 33, the viscosity for the sample fluid with lowest OWR has a significantly higher viscosity than the sample with highest OWR at a shear rate of 0.001 s^{-1} when measured at 20 °C. The increased water fraction will indeed increase the viscosity. This may be caused by less free space for water droplets to move freely before they collide into nearby water droplets, which in turn increase the overall viscosity, mentioned by [29]. One interesting observation is that the viscosity reduction between the fluid sample with 60:40 OWR and 70:30 OWR is approximately constant for shear rates between 500 s^{-1} and 0.016 s^{-1}. However, the difference increase for lower shear rates, and the same correlation is not observed for the other fluids with a significant viscosity reduction for the fluid with an OWR of 90:10.

The viscosity curves for the remaining fluids is approaching very high values when the shear rate is low. This type of behavior can indicate that the fluids show

yield stress behavior, which can be seen in connection with the controlled stress ramp experiments. This will be discussed in the following section.

4.4.9 Yield Stress Evaluation

A total of five methods has been evaluated in the search of determining the yield stress of the fluid samples. As already discussed in section 3.1.1 the yield stress may not be easily defined with a single point measurement due to the fact that yielding occur over a range of stresses and is rather a process than a single event. However, a single value for yield stress is much more useful when comparing the sample fluids that are being tested. Table 7 summarize the values of yield stress obtained during the foregoing experiments. The 90:10 sample did not show any yield stress under any of the dynamic tests. This is because $G'' > G'$ from the amplitude sweep, and it did not show a pronounced maximum viscosity value from the controlled stress ramp. The Herschel-Bulkley yield stress and Bingham YP is derived from the rheology measurements at 20 °C in table 3. The shear stress form the LVE region, τ_{ys}, and the flow point was defined from the amplitude sweep, the maximum viscosity method was defined from the controlled shear stress ramp. The shear stress values from shear rate of 0.001 s^{-1} in section 4.4.8 is also included, denoted as low shear stress in the table. The figure for these are given in appendix D.7 / figure 55

Table 7: Yield stress evaluation from measurements performed at 20°C.

Sample name	60:40	70:30	80:20	90:10
Bingham YP[Pa]	19,20	9,12	4,32	5,76
Herschel-Bulkley[Pa]:	7.10	3.52	1.98	1.32
Flow point τ_{fp}[Pa]:	4.49	1.85	0.61	N/A
Low Shear Stress[Pa]:	1.23	0.42	0.18	0.016
Max. Viscosity[Pa]:	0.60	0.35	0.20	N/A
LVE, τ_{ys}[Pa]:	0.44	0.17	0.07	N/A

A wide spread in apparent yield stress is seen in the table. The Herschel-Bulkley model estimates a yield stress that is higher than the other types of measurements techniques. This is because it is extrapolated from a shear rate of $\approx 5\,s^{-1}$ to zero. It also estimates that the 90:10 sample has a yield stress whereas viscoelastic measurements showed that the fluid did not have any yield stress. The Bingham YP is also included here because of the wide use of it in the oil industry. It is well documented that this model overestimates the yield stress significantly, which it also does here. The overestimation of yield stress based upon rheology measurements from conventional viscometer, highlight their limitations. Using the flow point ($G' = G''$) from the amplitude sweep as a yield stress measurement is more convenient than using the maximum shear stress value in the LVE region. This is caused by the fact that using the LVE region as a criterion is vulnerable to a subjective interpretation; however, the values of τ_{ys} and τ_{fp} are significantly different. Another measurement technique not included here is multiple creep sweeps. This could have defined the yield stress at a more accurate level.

5 Wellbore Simulation

This section contains the performance study of the drilling fluids used in this thesis. Cuttings transport simulation was performed in Landmarks Wellplan while the hydraulic calculations were performed by computing the Unified rheology model. The simulations and calculations were done one the basis of comparing the performance of the fluids against each other when the oil-water ratio was adjusted.The hydraulic simulation includes pump pressure, annular pressure loss and ECD.

5.1 Hydraulics

The Unified model was used to calculate annular pressure loss and total pump pressure. The ECD was calculated from the annular pressure loss with the following formula:

$$\text{ECD} = \rho_f + \frac{\Delta P_{fric}}{g \cdot h_{tvd}} \tag{5.1}$$

Where ρ_f is the density of the fluid (1,75sg), ΔP is the annular pressure loss, g is the free-fall acceleration and h_{tvd} is the vertical depth of the wellbore. In order to simplify the calculations, the well was chosen to be 8,5" vertical well with a 5,5" drill pipe without a BHA. The depth of the well was chosen to be the same as for the well used in cuttings transport simulation, 3356 m. The density of the drilling fluid is also assumed to be constant at 1,75sg, hence no temperature corrections was performed. In addition, the wellbore is assumed to be cuttings free, with no rotation applied. This will obviously lead to an offset in the pump pressure, annular pressure loss and ECD; however, the simulation was performed with the only purpose to compare the fluids itself. To avoid too many plots on one diagram, only the pump and annular pressures from rheology measurements at 20 °C and 50 °C are included in figure. The remaining results are given in appendix C.

5.1.1 Pump Pressure Simulation

The pump pressure is the sum of frictional pressure loss over the nozzles and in annulus. Simulation shows a significantly higher pump pressure for the fluid with

the lowest OWR, which is primarily caused by the higher rheology. The difference in pump pressure decrease for the remaining three fluids. One interesting observation is the effect of turbulent flow regime for the fluids that has the highest OWR. This is indicated by with a upwards bend in the pump pressure curve seen in figure 34, leading to similar pump pressure for the 80:20 and 90:10 fluids. In a real 8,5"-section drilling operation, the pump pressure would probably be higher than what is simulated here, due to the simplifications made as mentioned above.

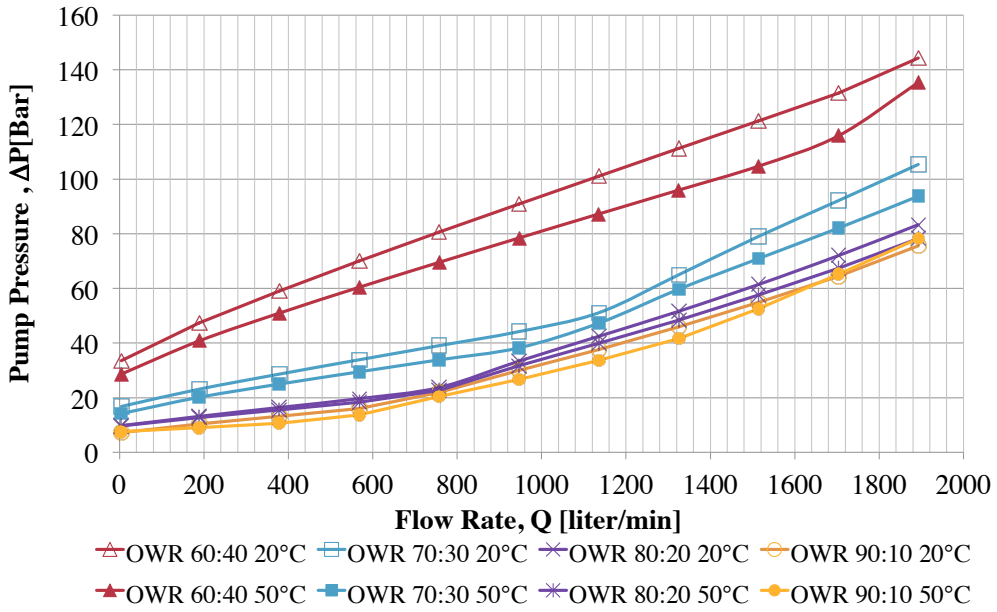

Figure 34: Pump pressure simulationn from the Unified model of a hypothetical 8,5" section. Rheology from all four fluid samples at temperature of 20 °C and 50 °C used as input parameters

5.1.2 Annular Pressure Loss and ECD simulation

The effect of fluid rheology is more distinct when computing the annular pressure loss. Frictional pressure loss for the fluid sample of 80:20 and 90:10 OWR are almost similar in value. The largest difference between these two samples is observed before the onset for turbulent flow regime for the 90:10 sample at 1325 l/min. The largest difference is observed between the drilling fluid with 60:40 and 80:20 OWR at 50 °C and flowrate of 1900 l/min, where the annular pressure loss is in order of 75bar and 22bar respectively. This is shown in figure 35. The difference between the 70:30 and 80:20 sample is in order of 34bar and 22bar at 1900 l/min at fluid rheology of 50 °C. The ECD was calculated from the annular pressure loss and has the exact same curves as shown in figure 35. Again, the increased rheology caused by elevated water fraction in the 60:40 fluid sample lead to an significant increase in the ECD, as shown in figure 36. For the hydraulic simulation with 80 °C display less difference between the pressure losses. This is due to the decrease in viscosity as temperature increase. This is given in appendix C.

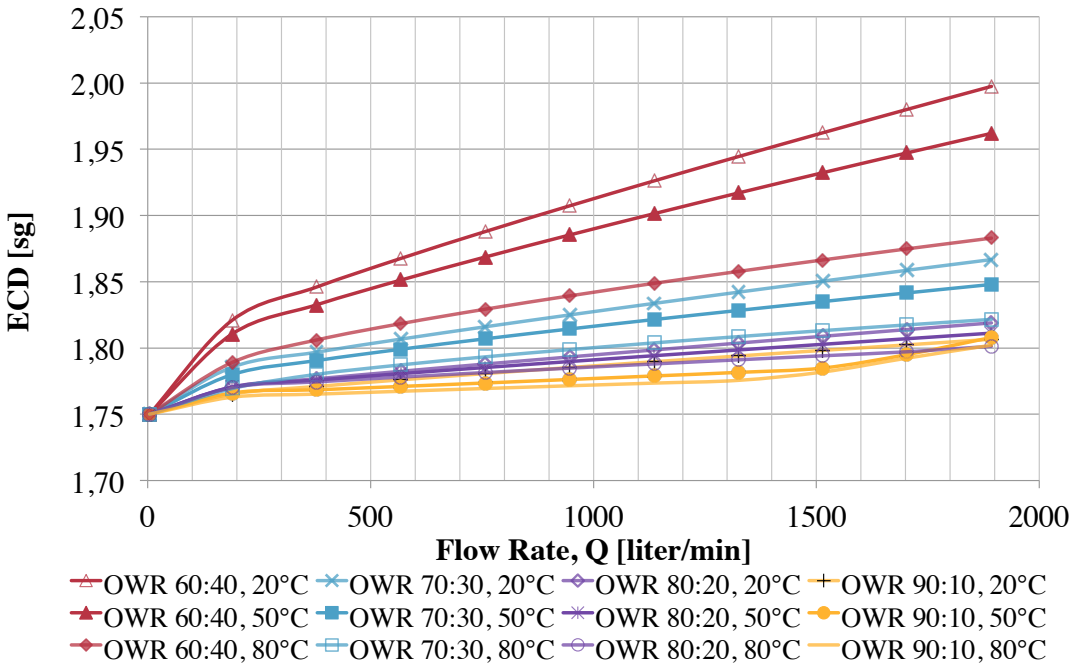

Figure 36: Calculated ECD from annular pressure loss simulation. Rheology data from all four fluid samples at 3 different temperatures used as input parameters.

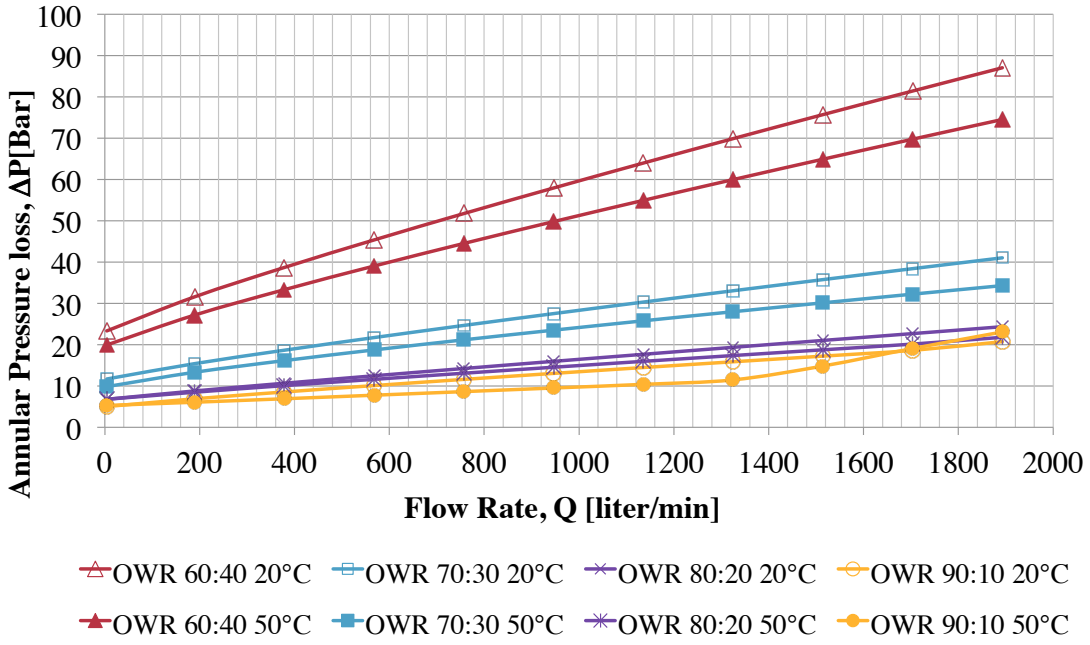

Figure 35: Annular pressure loss simulation from the Unified model for a hypothetical 8,5" section. Rheology from all four fluid samples at temperature of 20 °C and 50 °C used as input parameters.

5.2 Cutting Transport

Cuttings transport simulation was done with two different scenarios. The first simulation is a minimum required flow rate to remove cuttings out of the well, while the second one is minimum flow rate agains wellbore inclination. The wellbore chosen for the first simulation was a 3354 m long well with an maximum inclination of 38° with the section for the simulation was a 8.5" section of 2311 m with the previous casing (13 3/8") sat at 1223 m.
The simulation was done to evaluate the cuttings transport capacity of each of the fluids. Drilling fluid rheology at 50 °C was used for the simulation. The following parameters were used for the cuttings transport simulation.

The minimum required flow rate to remove all drilled cutting was first found, and then a lower flow rate was set for the cuttings bed height simulation in order to give a visualization of the cuttings bed height at that given flow rate. Minimum required flow rate is given in table 9

Table 8: Wellbore simulation parameters for cuttings bed height simulation

Input	Value
Cuttings Diameter:	0,32 [cm]
Cuttings Density:	2,50 [sg]
Bed Porosity:	36,0 [%]
Rate of Penetration:	9 [m/hr]
Rotary Speed	100 [rpm]
Additional Input	
Bit Diameter:	8,50 [in]
Annulus Diameter:	8,50 [in]

Table 9: Minimum required flow rate.

Drilling Fluid	Minimum Flow Rate [lpm]
OWR: 60:40	1667
OWR: 70:30	1667
OWR: 80:20	1892
OWR: 90:10	1863

The cuttings transport simulation is shown in figure 37 where the vertical axis is the measured depth of the well, and the horizontal axis represents cuttings bed height. Cuttings transport simulation was performed at flow rate of 1422 l/min. The fluids transport capacity decrease with increasing OWR. This is seen in connection with the rheology input as discussed in section 4.2. Nevertheless, the fluid with an OWR of 70:30 has a quite similar performance as the 60:40 fluid, while the 80:20 and 90:10 shows a less degree of transport capacity. This is probably caused by the low-end rheology, that is the 3 and 6-rpm dial readings, which is much lower for the 80:20 and 90:10 fluids when compared to the two other fluids at 50 °C, The fluctuations in the cuttings bed height seen in figure 37 is due to the change in inclination with depth.

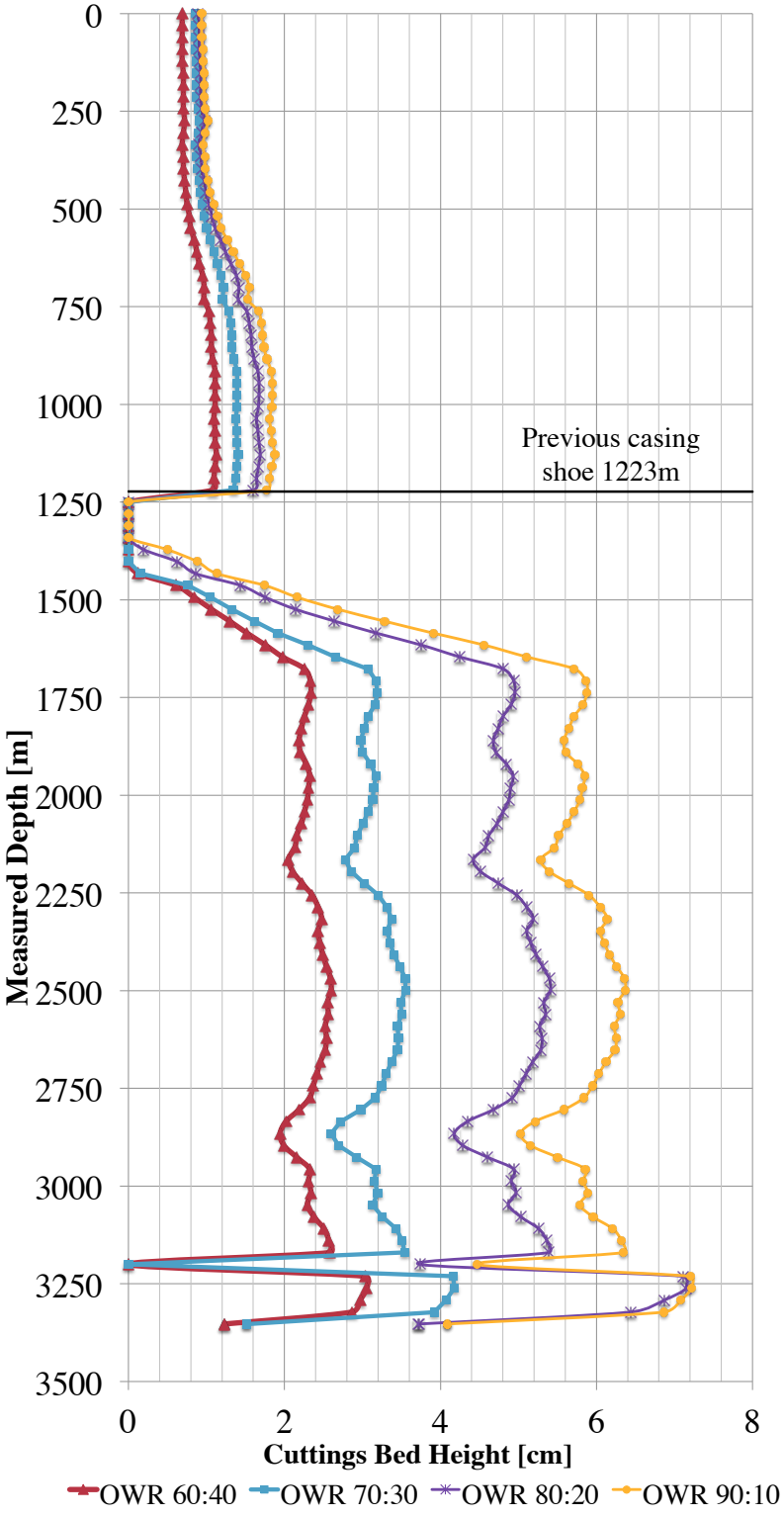

Figure 37: Cuttings bed height simulation at flow rate of 1422 l/min. Simulation based upon fluid rheology at 50°C

Minimum Required Flow Rate

The minimum required flow rate simulation is shown in figure 38. The rheology specifications used in the cuttings transport simulation was also used here. This simulation is based upon a 8,5" well with only a 5" drill pipe as given in table 10 and is a flow-rate vs inclination simulation.

Table 10: Wellbore simulation parameters for minimum required flow rate vs wellbore inclination

Input	Value
Cuttings Diameter:	0,32 [cm]
Cuttings Density:	2,50 [sg]
Bed Porosity:	36,0 [%]
Rate of Penetration:	9 [m/hr]
Rotary Speed	100 [rpm]
Additional Input	
Bit Diameter:	8,50 [in]
Annulus Diameter:	8,50 [in]
Pipe Diameter:	5,00 [in]
Tool Joint Diameter:	5,50 [in]
Minimum Pump Rate:	379 [lpm]
Increment Pump Rate:	357 [lpm]
Max Pump Rate:	3785 [lpm]

The simulation reveals that the fluid with the lowest rheology requires a less flow rate than both the fluids with an OWR of 80:20 and 70:30. Both 70:30 and 80:20 fluid samples showed an increase in the minimum required flow rate at wellbore inclination of 30°. The exact explanation for this for this is most likely because of the early onset of turbulent flow regime caused by the low rheology profile for the 90:10 sample. The 60:40 requires the lowest amount of flow to transport cutting out of the well, which is primarily caused by elevated rheology when compared to the other fluid samples.

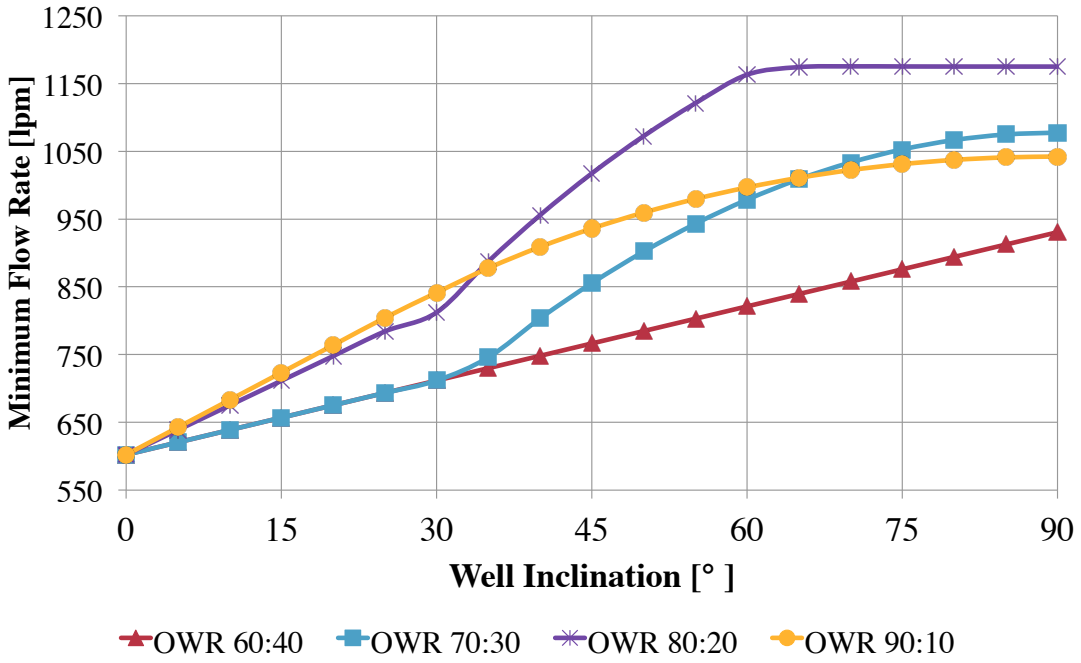

Figure 38: Minimum required flow rate to transport drilled cuttings. Based on fluid rheology at 50°C

5.3 Summary Performace Study

From the cuttings transport and minimum flow rate simulation it may appear that the fluid with OWR of 60:40 has the best performance. However, when including the hydraulics into the evaluation it is evident that this fluid also impose a significantly higher pump pressure and annular pressure loss than the other drilling fluids. An oil based drilling fluid with an OWR of 60:40 is hardly ever used in real drilling operations due to the above observations with regards to hydraulics. Another concern, not studied in this thesis, is the stability of drilling fluids with low OWR.

6 Summary and Discussion

6.1 Characterization of Drilling Fluid

The characterization of the drilling fluids started with rheological measurement performed on a OFI model 800 8-speed conventional rotational direct-indicating viscometer. These measurements were performed at 20°C, 50°C and 80°C, which included gel measurements at 10 s and 10min. Barite sag potential was then investigated at both static and dynamic conditions. The final, and main emphasis in the characterization was performed with an Anton Paar MCR 302 rheometer. A total of five oscillatory and two rotational tests were performed in this investigation. Finally, the hydraulics and cuttings transport simulation was conducted.

Rheological Measurements

The preliminary rheology characterization showed how the temperature and water fraction of oil based drilling fluids influenced the shear stress. The measurements (given in table 3) showed a significant spread in measured shear stress, with a pronounced increase for the 60:40 OWR. This was expected from the literature review, as water will increase the rheology. From model fit analysis it was observed that the Herschel Bulkley, Robertson and Stiff and the Unified model gives a good description of all fluids with an overall average deviation close to 2% from measured values at 20°C, 50°C and 80°C. The Bingham plastic model showed an average deviation of 15,29%.

Barite sag measurements was performed in both dynamic and static conditions. The static sag measurement was performed in a non-conventional fashion in order to observe the rate at which barite settled out and also to observe if there was any static sag at ambient temperature. From the measurement it was observed that barite settled out almost immediately in the 90:10 sample, and continued to settled out with an constant rate of $\approx 0.282\,g/h$. This was in contrary to what was observed for the 80:20 sample where the first indication of settling occurred after 3.5 h. The lack of water in the drilling fluid limits the organophilic clay to fully yield, which consequently results in lack of structure when the water fraction is low, allowing barite to settle out.

Dynamic Measurements

The main investigations in characterizing the drilling fluids was performed in viscoelastic measurements.

Amplitude Sweep

From the amplitude sweep it observed that the drilling fluid with an OWR of 90:10 showed behavior of a viscoealstic liquid. This was observed for angular frequency lower than 50 rad/s at a temperature of 20°C. As water fraction increased the fluids exhibit viscoelastic gel character, as storager modulus was greater than loss modulus over the entire LVE region for the remaining samples. The separation indicates there was some kind of internal structure within the fluid. The separation increased when the water fraction in the drilling fluid increased, meaning that there was observed a larger degree of elastic behavior when OWR decreased. It is difficult to determine if this increased elastic behavior is actually caused by clay that is yielding due to increased water concentration or if its caused by an interaction between the clay and emulsion droplets as reported in [38]. From the literature review it is also plausible that the water droplets are contributing to this effect. When the results from amplitude sweep are seen in connection with the dynamic sag measurements, it seems like the dynamic sag is reduced when the elastic properties are increase, as reported by [28]. The clay concentration is equal for all of the drilling fluids making reasonable to assume that the water droplet interaction with clay may be the primary cause for this elevated elastic behavior.

Effect of Angular Frequency: Additional amplitude sweep was performed by increasing the angular frequency from 10 to 50 rad/s. An increased value of loss modulus was observed indicating a lower degree of viscolastic gel behavior with increased frequency. The LVE region did not change significantly for any of the fluid samples, nor did the stress at the at the end of LVE region. The flow point increased when the angular frequency increased for both 70:30 and 80:20, while it was approximately the same for the 60:40 sample.

Effect of Shearing: Additional experiments were performed to study the influence of shearing. The experiment revealed that both storage -and loss modulus decreased when time of shear increased. Storage modulus was more effected than loss modulus when time of shear increased, showing more viscous dominance. The observation is of same tendency as Herzhaft et al.[38] observed.

Frequency Sweep

The observations made in the frequency sweep experiment revealed that all of the sample, except 90:10 sample, showed elastic dominance over most of the applied frequencies. The 60:40 sample showed independent behavior for all frequencies, while a drop in storage modulus was observed for both 70:30 and 80:20 at low frequencies. This could indicate difficulties of keeping barite in suspension, and that they are frequency dependent. The 90:10 sample showed viscoelastic liquid like behavior over all frequencies being applied, confirming what was observed in the amplitude sweep.

Time Sweep

Time sweep experiment revealed that the structural behavior with increasing OWR was time dependent. Initial structure build up was observed for all fluid samples. The 60:40 sample showed a continuous structural growth over the whole testing period, while the other sample showed a structural breakdown. The time of structural breakdown decreased with an increased OWR, where the 90:10 sample showed first tendency of breakdown after 13 min. This could indicate lack of structure, which could rise the potential of barite sag. Additional testing with lower frequency was also performed. The same observations were made although breakdown was then observed at a later stage.

Temperature Sweep

The temperature sweep was performed from 4°C to 80°C on all fluid samples. This experiment showed that the fluid sample with an OWR of 60:40, 70:30 and 80:20 behaved stable over a wide range of temperatures. This was analyzed through the elastic dominance being present over the whole temperatures region being tested for. Only the 90:10 showed a crossover point from being viscoelastic gel to viscoelastic liquid. This was found to be at 17∘C. The initial response was

equal for each of the fluid samples with a pronounced elastic dominance at 4°C. This behavior can be related to deep-water drilling where sea floor temperatures are close to 0°C. The fluid close to the wall of the riser would exhibit a strong elastic dominance, which may induce a higher BHP when pumps are started after a period of rest. The 60:40 sample showed a continuous increase in damping factor indicating lack of stability at elevated temperatures. The experiment also revealed that complex viscosity $\eta*$ had its minimum when the temperature was far below maximum.

Creep-Recovery Test

Experiments performed with the creep-recover method showed that the degree of deformation when the applied stress was constant. The observations made showed that the degree of deformation increased with OWR. Deformation at a constant stress is thought to give a better representation of barite sag. The 80:20 sample displayed the largest deformation, indicating that the structure was weak, which consequently increase the potential of barite sag in static conditions.

Controlled Stress Ramp

Controlled stress ramp was used to evaluate if the fluids had a yield stress. The fluid sample was subjected to a constant stress increase until a shear stress of 10 Pa or a shear rate of 100 s^{-1} was reached. The yield stress was then evaluated from the maximum viscosity method. From this method it was observed that the all samples except 90:10 exhibited elastic behavior before a viscosity peak was observed. The shear stress at this viscosity peak was evaluated as the yield stress.

Controlled Shear Rate Sweep

From the controlled shear rate sweep the viscosity profiles from each of the fluid sample was obtained. The experiment showed that the viscosity was higher when OWR decreased for all shear rates, which was expected from the literature review. The 90:10 sample showed the lowest degree of shear thinning, which is a primarily caused by lower fraction of water. In static conditions the water droplets are spherically and become ellipsoidal when the fluid is subjected to shear. Also the droplets will tend to align themselves in the direction of the flow, causing any structure to deform, causing shear thinning.

6.2 Performance Evaluation

The performance evaluation was performed with two different approaches. First, a wellbore hydraulic simulation was performed at 20°C, 50°C and 80°C with the use of the Unified rheology model. The simulation was based upon the rheology measurements form table 3. Secondly, a cuttings transport and minimum required flow rate simulation was performed with the use of Landmark's Wellplan. These simulations were conducted in order to evaluate the performance of oil based drilling fluids when the water fraction was altered.

Wellbore Hydraulics

Wellbore hydraulic simulation showed that a lower OWR imposed a higher pump pressure for all temperatures being tested for. The onset of turbulent flow regime decreased with lower water fraction and higher temperature. This is seen in connection with the lower rheology these fluids display. In fact, the difference in pump pressure from the 80:20 and 90:10 fluid sample is almost negligible for all temperatures, due to turbulent flow. The 60:40 sample display the highest pump pressure at all temperatures.

Due to the fact that annular pressure loss is included in the pump pressure calculation, the simulation of annular pressure loss showed same type of behavior as for the pump pressure. However, the fluid sample with an OWR of 60:40 display a significantly higher pressure loss at 1900lpm, all in laminar flow regime. Due to the early onset of turbulent flow regime, at 1300lpm, for the 90:10 OWR fluid sample, the annular pressure loss at 1900lpm is higher then what is observed for the 80:20 fluid. Wellbore hydraulics can seen in good correlation with the rheology for the fluids simulated with. The ECD simulation showed exactly the same behavior as the annular pressure loss as ECD is directly proportional to this.

Cuttings Transport

Cuttings transport simulation was performed to evaluate the cuttings transport capacity for each of the fluids. The rheology at 50°C was used for the simulation. From the simulation is was observed that the cutting transport performance decreased with increasing OWR. This is, again, in direct correlation with fluid rheology, where a higher rheology impose a better transport capacity. The cuttings transport capacity of the 60:40 and 70:30 fluids is not significantly different, whereas

the 80:20 and 90:10 are showing lack of carrying capacity when the flow rate was at 1422lpm. The minimum required flow rate to remove *all* drilled cuttings from the wellbore was shown to be equal for both 60:40 and 70:30 at 1667lpm. The min. required flow rate for 80:20 and 90:10 fluids was 1892lpm and 1863lpm respectively. The lower flow rate required for the 90:10 was due to the onset of turbulent flow regime.

6.3 Weaknesses and Limitations

This subsection contains potential weakness and limitations of the experimental work performed in this study. The hydraulic simulations had several simplifications stated in section 5; however, the simulation was used to compare each fluid system against each other. The simulation was not intended to represent a 100% realistic scenario.

Viscometer Measurements

The experiments performed with the conventional viscometer were all performed with equal methodology to minimize any potential source of error. Nevertheless, when measuring the sample with an OWR of 90:10 at 80 °C, it was evident that fluid was prone to barite sag. After the measurements was performed at 80 °C a distinct barite slump was observable in the bottom of the heating cup, indicating that barite had settled. This may have influenced the rheological measurements, which in turn affects the hydraulic calculations. This could also explain why all of the rheology models had a higher deviation for the 90:10 sample than for the other samples. From the flow curves obtain in section 4.4.8 at 20 °C one may also evaluate the reliability of the viscometer at low shear rates. For the 90:10 sample at a shear rate equivalent of 3RPM the shear stress is 0.59 Pa, which is equivalent to 1,23 lb/100 ft^2 $\approx$ 1° dial reading on the viscometer, while the viscometer dial reading showed 3,5°. However, the shear rate used on the rheometer was continous (non steady state), whilst the viscometer is a steady state measurements. This will influence the measurements due to the thixotropic behavior of drilling fluids and may thus not be compared directly. The suspicion that the viscosity is over estimated at low shear rates for conventional viscometers was also review in the literature study, from [38].

Rheometer Measurements

Measurements made with the Anton Paar MCR 302 are in particular sensitive to erroneous measurements when performed in oscillation. This was most prominent when conducting temperature sweep for the fluids with low water fraction i.e 80:20 and 90:10. The temperature sweep is prone to measurement error due to long measurement time with increasing temperature. This will increase sag potential during the experiment. In addition, when the temperature increase, the sample can expand which will affect the filling. This could have been avoided if normal force control on the rheometer was activated. Elevated temperature makes the sample vulnerable for phase separation, evaporation and drying of sample. Phase separation (free oil) occurred with the 90:10 sample during the temperature sweep when performed with an temperature increase of $0,00926°C/s$, as seen in figure 39. The results from that measurement can be observed in figure 51, appendix D.4. In the picture there is a clear separation with free oil on top. One may also observe barite particles on the left hand side while fluid loss material (black particles) is floating on the edge of the free oil in the center. This was the reason why the rate of temperature was set to a faster rate, as shown in the results.

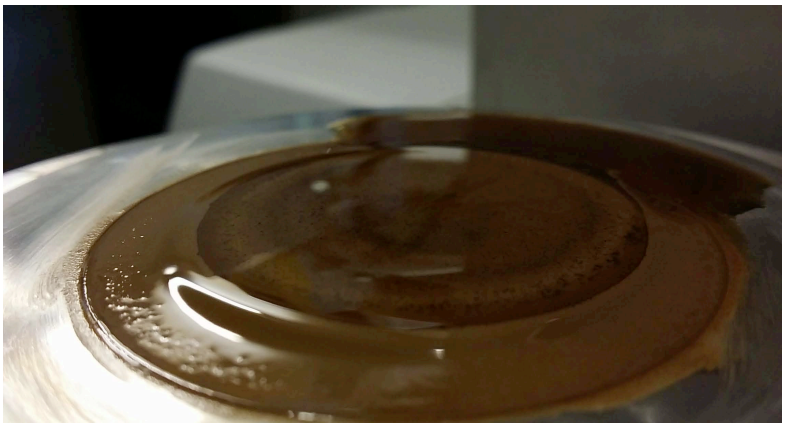

Figure 39: Phase separation after temperature sweep of 90:10 sample.

As previously described in the introduction to section 4.4, the preparations is of high importance when performing viscoelastic measurement at very low shear rates. This was also the reason why equal procedures was followed for each of the samples being tested. The following steps in the measurement which can influence

the results.

- Shear history
- Sample trimming prior of starting experiment
- Rest period before experiment started
- Stability of drilling fluid

Observations made in the time sweep tests reveal change in fluid behavior in time, which makes accurate and reproducible measurements more difficult. The fluid samples were at first used in a series of measurements without being changed. This method was changed to new samples for each measurement technique due to questionable results for the 80:20 and 90:10 samples. Repeatability test performed with the amplitude sweep on the 80:20 sample showed that exact repetitive results are difficult to obtain.

Barite Sag Measurements

The static barite sag measurement was performed with an alternative methodology. The more common and known procedure is to measure static sag is to use an aging cell of 350 ml and let the drilling fluid at isothermal temperature over a longer period. This test was planned for; however, due to limited fluid volumes and uncertainties in how this influenced the properties of the drilling fluid it was decided to perform this measurement at last. The test was not conducted due to limited amount of volume and time. This could have given more data on static sag potential for each of the fluid.

7 Conclusion

This thesis has studied the influence of increased water fraction in oil based drilling fluids. This has been done through extensive testing, with main emphasis in viscoelastic characterization. A thorough literature study has been performed showing little research on this particular subject.

The main observations made in characterizing the drilling fluids can be summarized with the following conclusions:

- Rheology of drilling fluids is highly dependent on temperature and OWR. Higher shear stress is displayed when the OWR is decreased. The most pronounced increase is observed when the OWR is changed from 70:30 to 60:40.
- From the model fit analysis it was found that the Herschel-Bulkley, Robertson and Stiff, and the Unified model gives the best description of the fluids.
- Increased OWR caused the fluid to be more susceptible for dynamic sag. The fluid sample with the lowest OWR showed the lowest degree of dynamic sag, with an increasing severity of sag when the OWR was increased. This is seen in connection with the rheological measurements for the corresponding fluids.
- The fluid with the lowest water fraction displayed no signs of internal structure, which consequently led to static sag of weight material at ambient temperature.
- The elastic properties was found to decrease when the OWR of the drilling fluid increased. When the water fraction was sufficiently low, the fluid change characteristics from viscoelastic-gel to viscoelastic-liquid. The lack of structure when OWR is increased results in a more pronounced deformation upon applied stress. This was observed from the creep analysis. Stability of internal structure is more stable when the water fraction of the drilling fluid is high.
- Structural breakdown over time was observed for all fluids except the fluid with an OWR of 60:40. This was observed at angular frequency of 110 rad/s and 10 rad/s.

- The apparent yield stress in the drilling fluids was found to be low and is highly dependent on measurement technique. The fluid that displayed the highest yield stress also had the lowest OWR. The Herschel-Bulkley model and Bingham Plastic model overestimates the yield stress. The fluid with an OWR of 90:10 displayed no signs of yield stress from viscoelastic measurements and shear stress ramp.

From the performance analysis it was observed that the water fraction in oil based drilling fluids plays an important factor in connection with wellbore hydraulics and cuttings transport. The fluid with the lowest OWR imposed a larger impact on wellbore hydraulics then the remaining fluids. Annular pressure loss was 3 times higher for the 60:40 sample when it was compared to the sample which displayed the lowest frictional pressure loss. This was compared at flow rate of 1900lpm and temperature of 50°C. The onset of turbulent flow regime caused the pump pressure and annular pressure loss for the fluid sample with 80:20 and 90:10 OWR to be almost equal.
The cuttings transport simulation showed that a higher rheology caused more efficient carrying capacity of the fluids. The low OWR was the primary reason for the higher rheology. Cuttings transport capacity decreased with increasing OWR.

References

[1] Aleksandr IAkovlevich Malkin, Alexander Ya Malkin, and Avraam I Isayev. *Rheology: concepts, methods, and applications*. ChemTec Publishing, 2006.

[2] Faith Morrison. *Understanding rheology*. Oxford University Press, New York, 2001. ISBN 0-19-514166-0.

[3] M-I Swaco. *Drilling Fluids Engineering Manual, Version 2.2*. M-I Swaco - A Schlumberger Company, 2009.

[4] Bernt S Aadnoy. *Modern well design*. CRC Press, 2010.

[5] Ryen Caenn, Henry CH Darley, and George R Gray. *Composition and properties of drilling and completion fluids (6th ed.)*. Gulf Professional Publishing, 2011.

[6] American Petroleum Institute. Rheology and hydraulics of oil-well fluids, api recommended practice 13d, sixth edition. *API Recommended Practice*, 2010.

[7] Howard A Barnes. A handbook of elementary rheology. 2000.

[8] Ida Sandvold. Gel evolution in oil based drilling fluids. Master's thesis, Norwegian University of Science and Technology, 2012.

[9] Taha Sochi. Non-newtonian flow in porous media. *Polymer*, 51(22):5007–5023, 2010.

[10] Howard A Barnes. Thixotropy—a review. *Journal of Non-Newtonian Fluid Mechanics*, 70(1):1–33, 1997.

[11] Robert F. Mitchell Larry W Lake. *Petroleum engineering handbook*. Richardson, TX, Society of Petroleum Engineers, 2006.

[12] M Zamora and F Growcock. The top 10 myths, misconceptions and mysteries in rheology and hydraulics. AADE-10-DF-HO-40, AADE Fluids Conference and Exhibition, 2010.

[13] M Zamora and D Power. Making a case for aade hydraulics and the unified rheological model. In *AADE 2002 Technology Conference Drilling & Completion Fluids and Waste Management*, 2002.

[14] Marilyn Viloria Ochoa. *Analysis of drilling fluid rheology and tool joint effect to reduce errors in hydraulics calculations*. PhD thesis, Texas A&M University, 2006.

[15] PA Bern, M Zamora, KS Slater, PJ Hearn, et al. The influence of drilling variables on barite sag. *SPE*, 36670(8):887–894, 1996.

[16] RE Robertson and HA Stiff Jr. Improved mathematical model for relating shear stress to shear rate in drilling fluids and cement slurries. *Soc. Pet. Eng. J.;(United States)*, 16(1), 1976.

[17] Binh Bui, Arild Saasen, Jason Maxey, Mehmet E Ozbayoglu, Stefan Z Miska, Mengjiao Yu, and Nicholas E Takach. Viscoelastic properties of oil-based drilling fluids. *Annual Transactions of the Nordic Rheology Society*, 20, 2012.

[18] Danton Lemini. *Engineering viscoelasticity*. Springer, New York, 2013.

[19] Thomas G. Mezger. *The Rheology Handbook - For users of rotational and oscillatory rheometers*. Vincentz Network GmbH & Co KG, 2002.

[20] H. F. Brinson. *Polymer engineering science and viscoelasticity : an introduction*. Springer, New York, 2015.

[21] Thomas G. Mezger. *The Rheology Handbook - For users of rotational and oscillatory rheometers, 3rd Revised Edition*. Vincentz Network GmbH & Co KG, 2011.

[22] BT Bui, AN Tutuncu, et al. Creep-recovery test: A critical tool for rheological characterization of drilling fluids. In *Unconventional Resources Technology Conference*. Society of Petroleum Engineers, 2013.

[23] Tor H Omland, Jorunn Øvsthus, Kåre Svanes, Arild Saasen, Hans-Joachim Jacob, Terje Sveen, Helge Hodne, and Per A Amundsen. Weighting material sag. *Ann. Trans. Nord. Rheol. Soc*, 12:115–122, 2004.

[24] A Saasen, H Hoset, EJ Rostad, A Fjogstad, O Aunan, E Westgård, PI Norkyn, et al. Application of ilmenite as weight material in water based and oil based drilling fluids. In *SPE Annual Technical Conference and Exhibition*. Society of Petroleum Engineers, 2001.

[25] TR Jones. The properties and uses of clays which swell in organic solvents. *Clay Minerals*, 18(4):399–401, 1983.

[26] R Leaper, N Hansen, M Otto, et al. Meeting deepwater challenges with high performance water based mud. In *Preparcd for presentation at the AADE 2006 Fluids Conference held in Houston, Texas*, 2006.

[27] Tor Henry Omland. *Particle Settling in non-Newtonian Drilling Fluids*. PhD thesis, University of Stavanger, 2009.

[28] Ahmadi Tehrani, Mario Zamora, and David Power. Role of rheology in barite sag in sbm and obm. In *AADE 2004 Drilling Fluids Conference*, 2004.

[29] SPE Arild Saasen. Sag of weight materials in oil based drilling fluids. 2002.

[30] M.G Mims, A.N Krepp, and H.A Williams. *Drilling Design and Implementation for Extended Reach and Complex Wells, 2nd ed.* K&M Technology Group, 1999.

[31] Luc Van Puymbroeck and Henry Williams. Increasing drilling performance for erd wells using new generation hydromechanical drill oipe. *AADE–13–FTCE–01*, 2013.

[32] A Saasen, G Løklingholm, et al. The effect of drilling fluid rheological properties on hole cleaning. In *IADC/SPE Drilling Conference*. Society of Petroleum Engineers, 2002.

[33] PM Hanson, TK Trigg Jr, G Rachal, M Zamora, et al. Investigation of barite" sag" in weighted drilling fluids in highly deviated wells. In *SPE Annual Technical Conference and Exhibition*. Society of Petroleum Engineers, 1990.

[34] Arild Saasen, LIU DAWEI, and CD Marken. Prediction of barite sag potential of drilling fluids from rheological measurements. In *Drilling conference*, pages 663–671, 1995.

[35] T Omland, T Albertsen, K Taugbfl, A Saasen, K Svanes, and P Amundsen. The effect of the synthetic-and oil based drilling fluid's internal water phase composition on barite sag" paper spe 87135 presented at the 2004 iadc. In *SPE Drilling Conference, Dallas*, 2004.

[36] Ahmadi Tehrani, Andy Popplestone, and MI SWACO. Can you improve rheology and mitigate barite sag in invert emulsion fluids through brine phase treatment? AADE-07-NTCE-02, AADE National Technical Conference, Houston, 2007.

[37] Carsten Ehrhorn and Arild Saasen. Barite sag in drilling fluids. *Ann. Trans. Nordic Rheology Soc*, 4:66, 1996.

[38] Benjamin Herzhaft, Lionel Rousseau, Laurent Neau, Michel Moan, Frederic Bossard, et al. Influence of temperature and clays/emulsion microstructure on oil-based mud low shear rate rheology. *SPE Journal*, 8(03):211–217, 2003.

[39] Sharath Savari, Sandeep Kulkarni, Jason Maxey, Kushabhau Teke, and Halliburton. A comprehensive approach to barite sag analysis on field muds. AADE-13-FTCE-30, AADE National Technical Conference, Oklahoma, 2013.

[40] Howard A Barnes. The'yield stress myth?'paper–21 years on. *Applied Rheology*, 17(4):43110–44250, 2007.

[41] Richard P Jachnik. Low shear rate rheology of drilling fluids. *ANNUAL TRANSACTIONS-NORDIC RHEOLOGY SOCIETY*, 11:21–28, 2003.

[42] J Maxey, R Ewoldt, P Winter, and G McKinley. Yield stress: what is the true value. *Proceedings of the 2008 AADE-08-DF-HO-27. American Association of Drilling Engineers*, pages 1–10, 2008.

[43] Mario Zamora, Sanjit Roy, and Ken Slater. Comparing a basic set of drilling fluid pressure-loss relationships to flow-loop and field data. In *AADE 2005 National Technical Conference and Exhibition*, 2005.

Appendices

A Drilling Fluid Formulation

Table 11: Mud formulation

Oil Water Ratio	60 : 40	70 : 30	80 : 20	90 : 10
Weight [s g]	1,75	1,75	1,75	1,75
Sample volume, ml	1000	1000	1000	1000
Chemicals, [g/l]				
Base oil	330,6	387,3	443,1	498,4
Emulsifier	25,0	25,0	25,0	25,0
Clay	7,0	7,0	7,0	7,0
Alkalinity	25,0	25,0	25,0	25,0
Filter Loss Agent	10,0	10,0	10,0	10,0
Fresh Water	275,8	205,8	136,4	67,8
Salt	84,8	63,3	42,0	20,9
Weight Material	990,8	1026,6	1061,4	1095,9
Mixing date	07.01.15	07.01.15	07.01.15	07.01.15

B Rheological Measurements

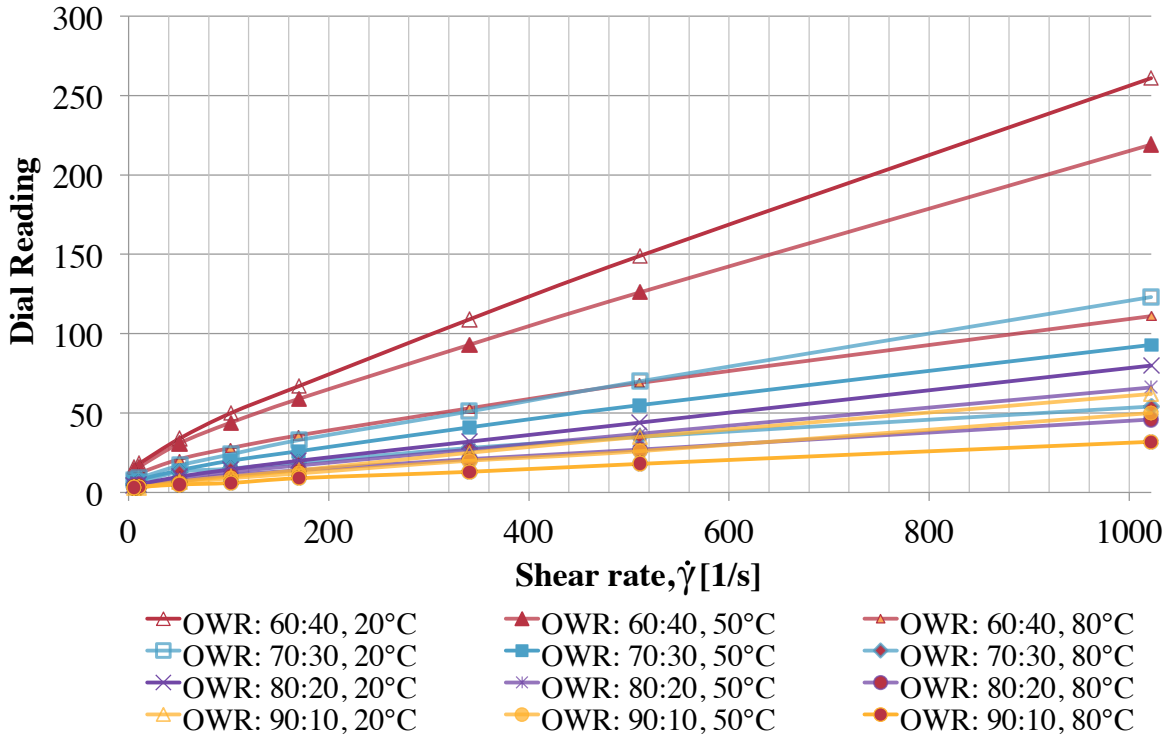

Figure 40: Rheological measurements for all fluid samples at temperature of

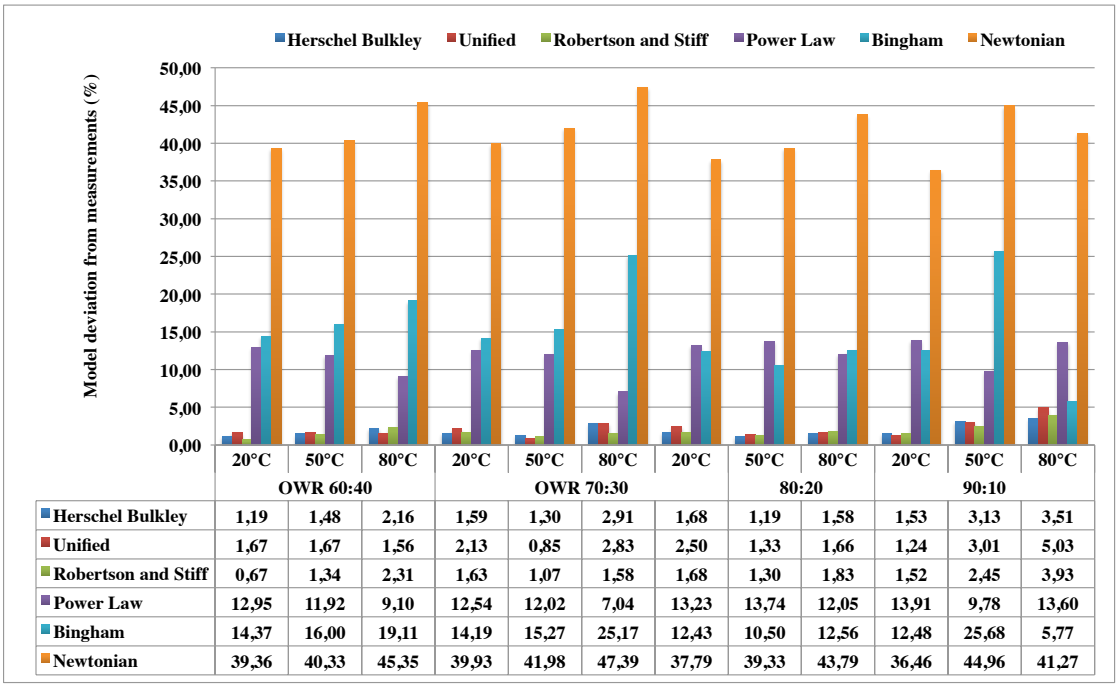

	20°C	50°C	80°C	20°C	50°C	80°C	20°C	50°C	80°C	20°C	50°C	80°C
	OWR 60:40			OWR 70:30				80:20		90:10		
Herschel Bulkley	1,19	1,48	2,16	1,59	1,30	2,91	1,68	1,19	1,58	1,53	3,13	3,51
Unified	1,67	1,67	1,56	2,13	0,85	2,83	2,50	1,33	1,66	1,24	3,01	5,03
Robertson and Stiff	0,67	1,34	2,31	1,63	1,07	1,58	1,68	1,30	1,83	1,52	2,45	3,93
Power Law	12,95	11,92	9,10	12,54	12,02	7,04	13,23	13,74	12,05	13,91	9,78	13,60
Bingham	14,37	16,00	19,11	14,19	15,27	25,17	12,43	10,50	12,56	12,48	25,68	5,77
Newtonian	39,36	40,33	45,35	39,93	41,98	47,39	37,79	39,33	43,79	36,46	44,96	41,27

Figure 41: Comparison of rheological models.

B.1 Rheological Model Comparison

C Hydraulic Simulation

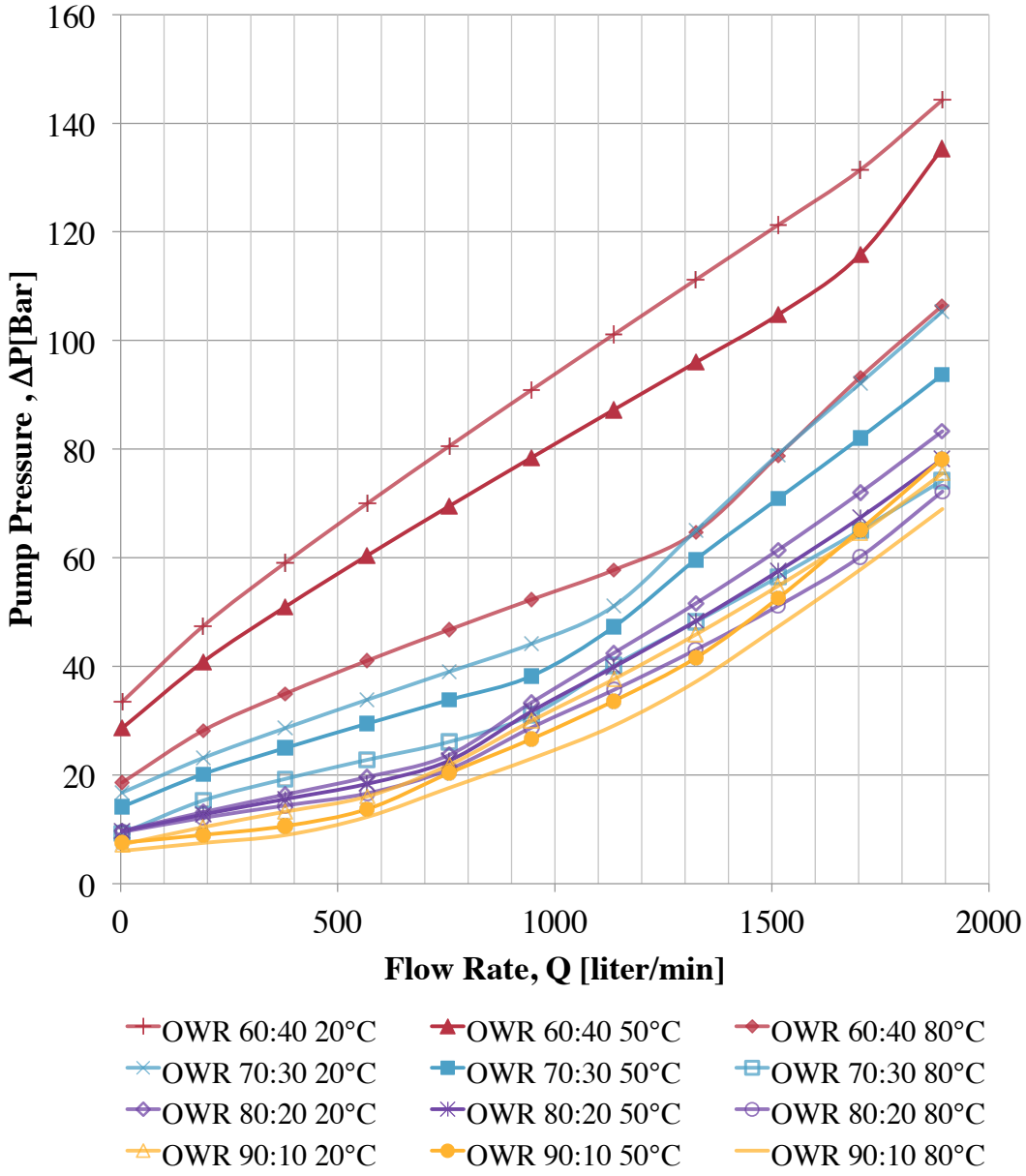

Figure 42: Total pump pressure for all fluid samples at 20°C , 50°C and 80°C. Simulation based upon the Unified rheology model and measurements given in table 3

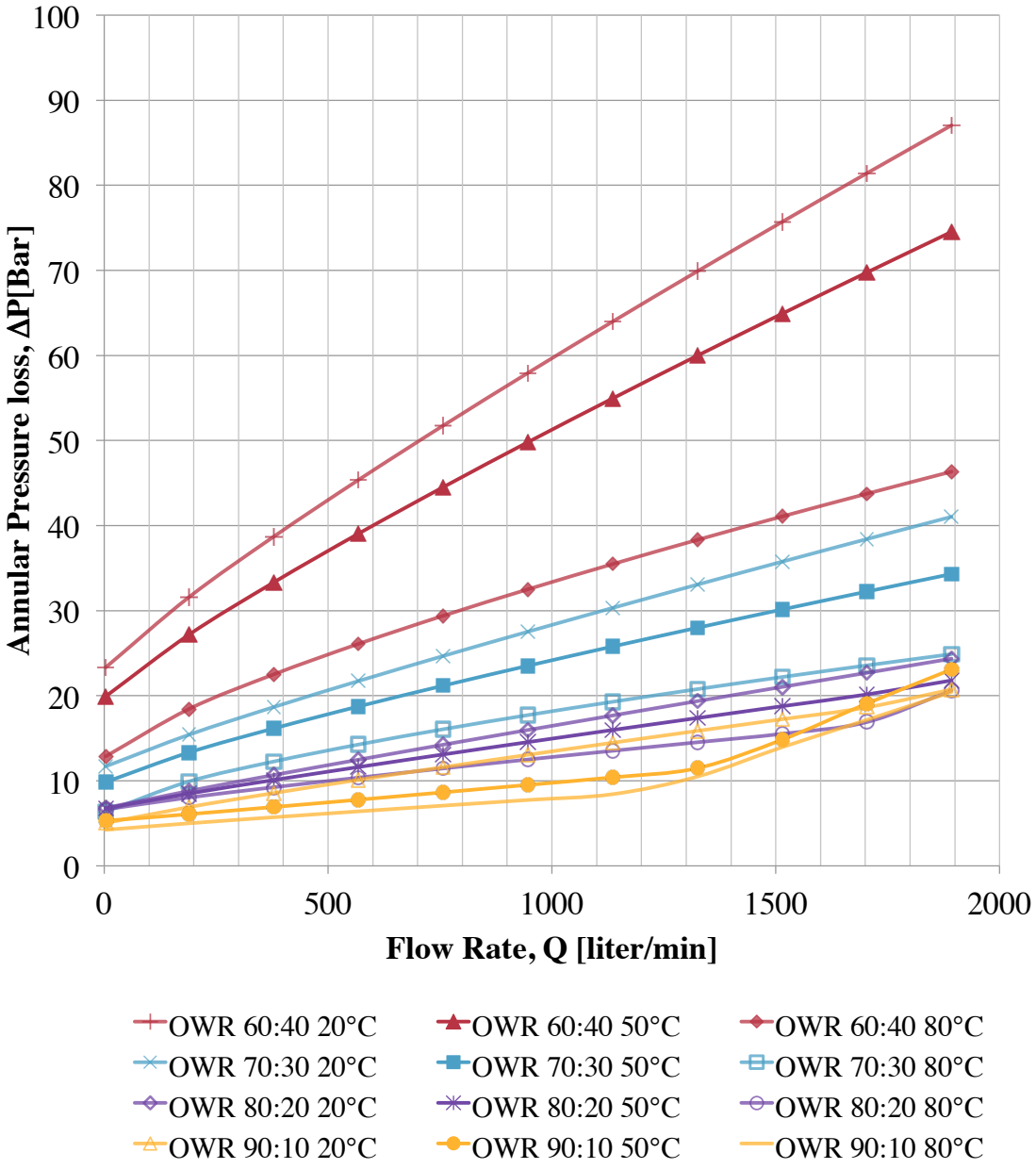

Figure 43: Total annular pressure loss simulated for all fluid samples at 20 °C, 50 °C and 80 °C. Simulation based upon the Unified rheology model and measurements given in table 3

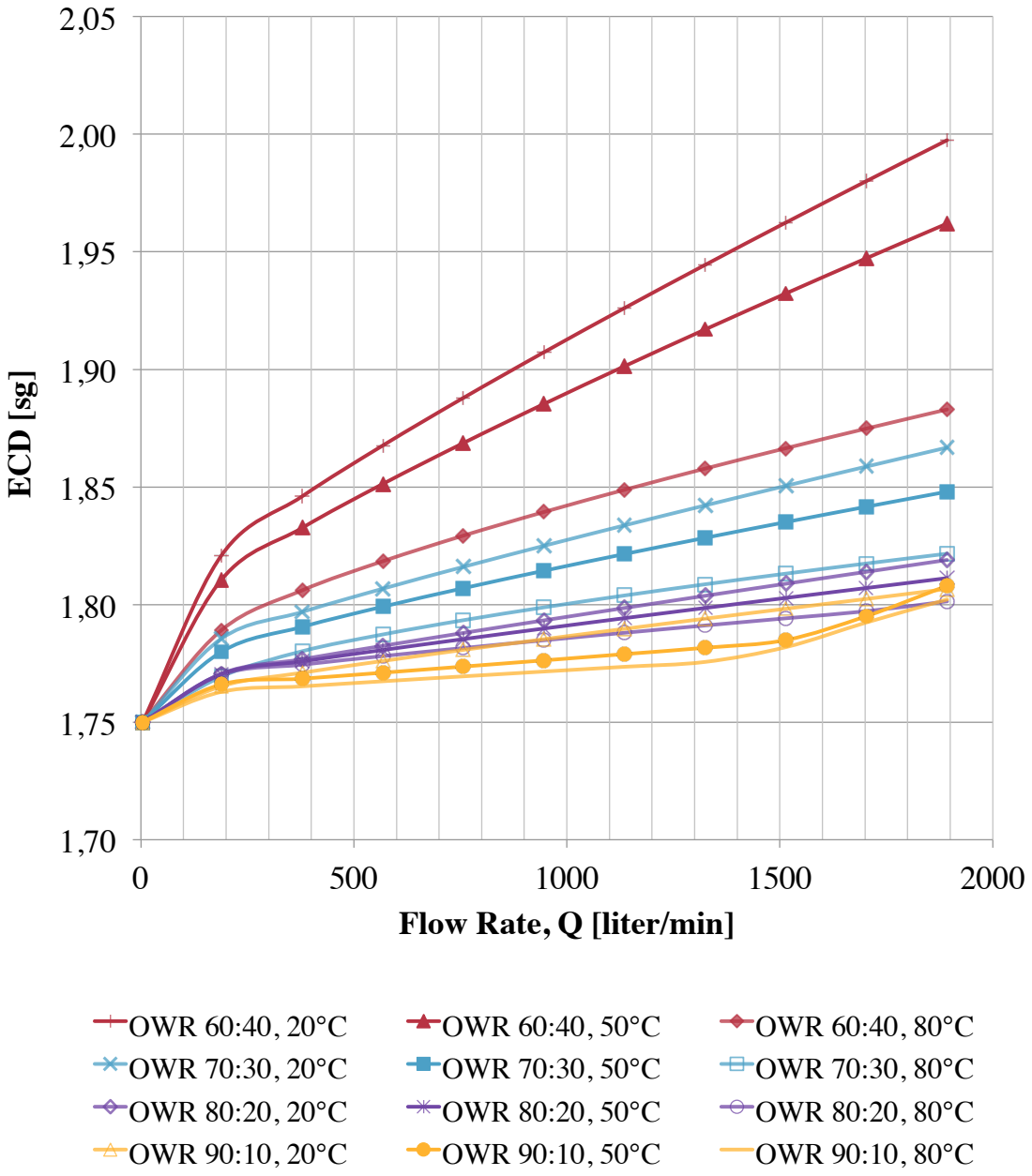

Figure 44: Calculated ECD for all fluid samples at 20 °C , 50 °C and 80 °C. Calculation based upon the annular pressure loss given in figure 43.

D Aton Paar Measurements

D.1 Amplitude Sweep

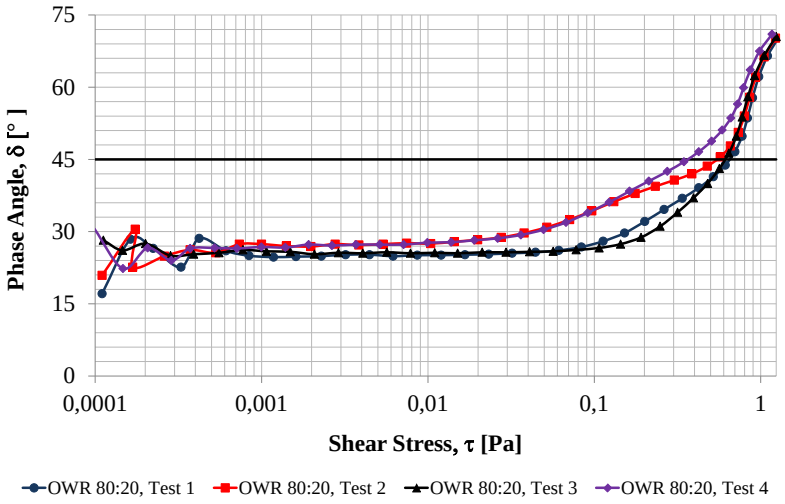

Figure 45: Phase angle vs shear stress from repeatability testing of OWR 80:20 at $20°C$, $\omega = 10\,\mathrm{rad/s}$

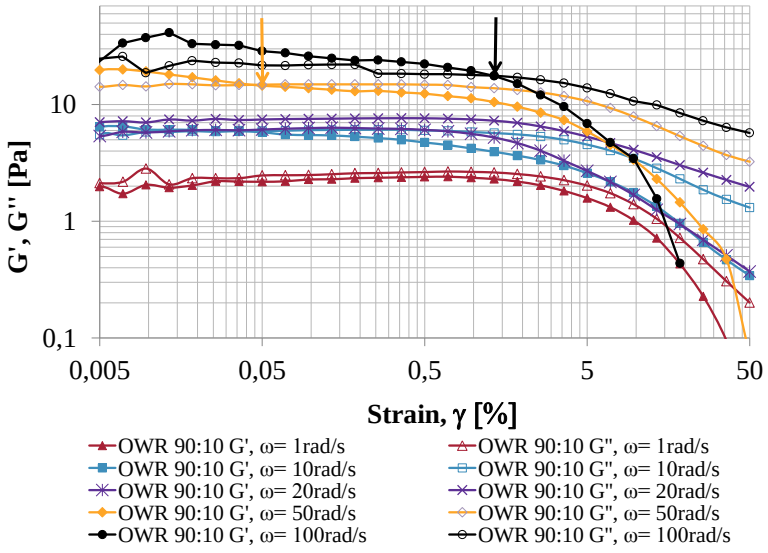

Figure 46: All amplitude sweeps performed on the 90:10 sample with increasing angular frequency. Arrows indicating crossover point.

D.2 Frequency Sweep

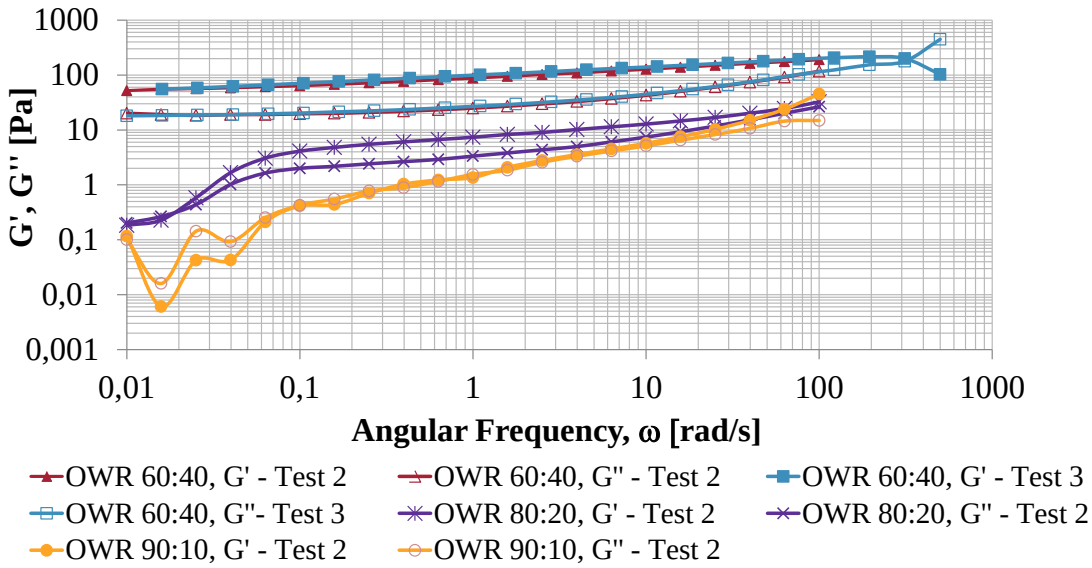

Figure 47: Frequency sweep performed outside linear range at 20°C, $\gamma = 0.1\%$ for 60:40 and $\gamma = 0.01\%$ for 90:10

D.3 Time Sweep

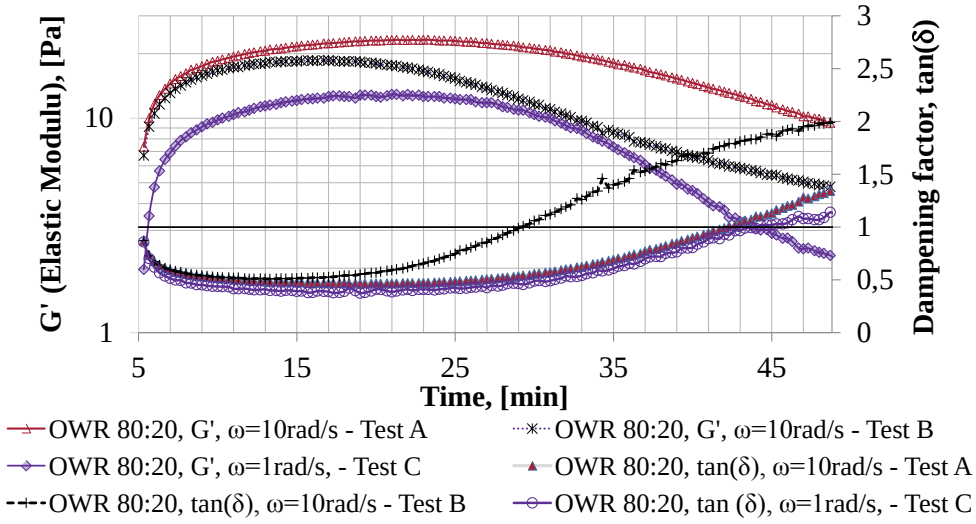

Figure 48: Time sweep performed at $\omega = 1\,\mathrm{rad/s}$ and $\omega = 10\,\mathrm{rad/s}$, $20°C$ for 80:20 sample

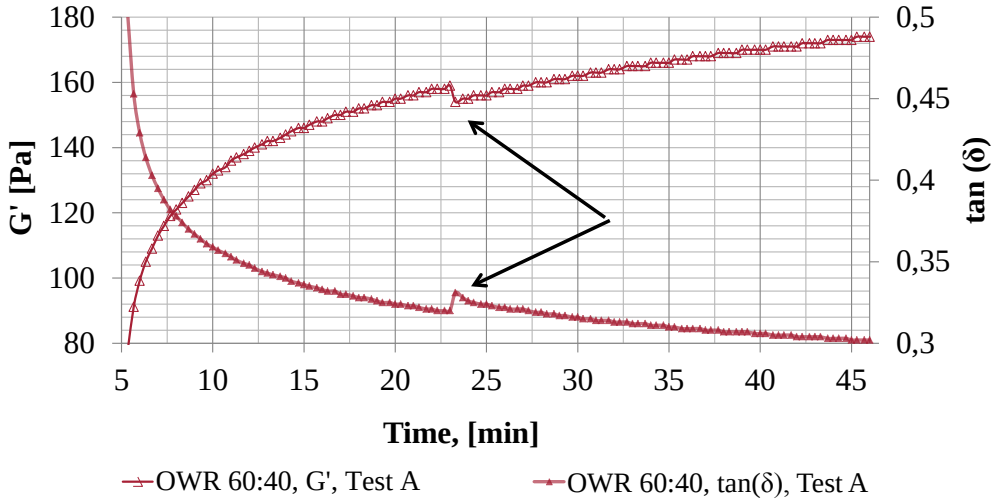

Figure 49: Erroneous time sweep measurement at $\omega = 10\,\mathrm{rad/s}$, $20°C$, $\gamma = 0.1\%$ for 60:40 sample

D.4 Temperature Sweep

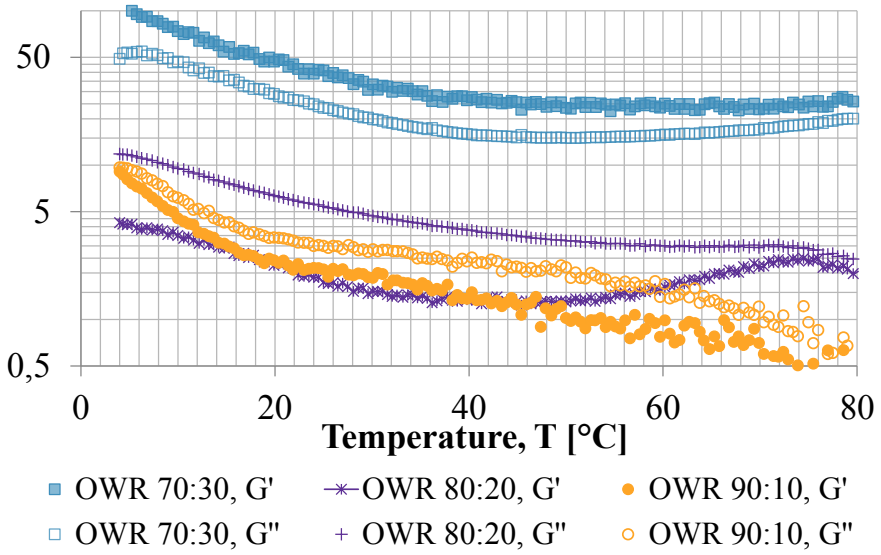

Figure 50: Temperature sweep measurements at angular frequency of $\omega = 10\,\text{rad/s}$ and $dT/dt = 0,05°\text{C/s}$. No rest period before testing commenced.

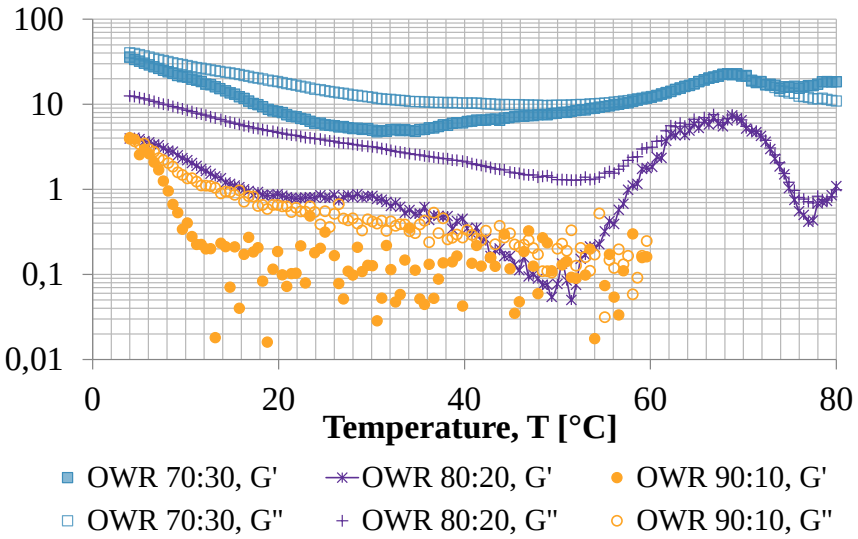

Figure 51: Erroneous temperature sweep measurements due to phase separation, at angular frequency of $\omega = 10\,\text{rad/s}$ and $dT/dt = 0,00926°\text{C/s}$.

D.5 Creep Recovery Test

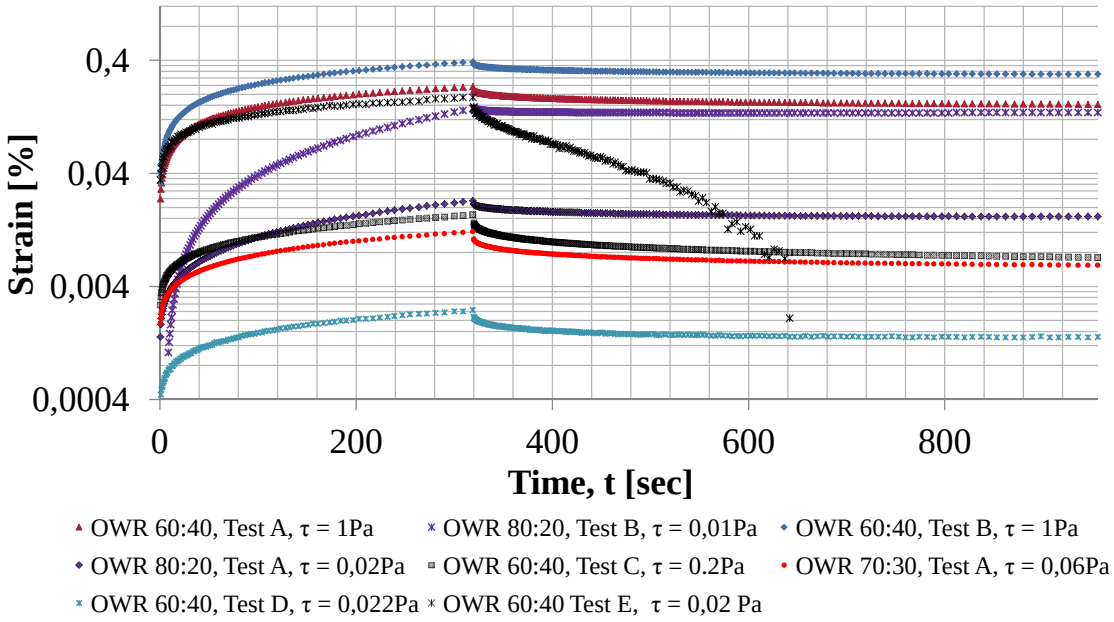

Figure 52: Creep recovery test at different magnitude of stress. Part of preliminary testing to achieve reasonable results.

D.6 Controlled Shear Stress Ramp

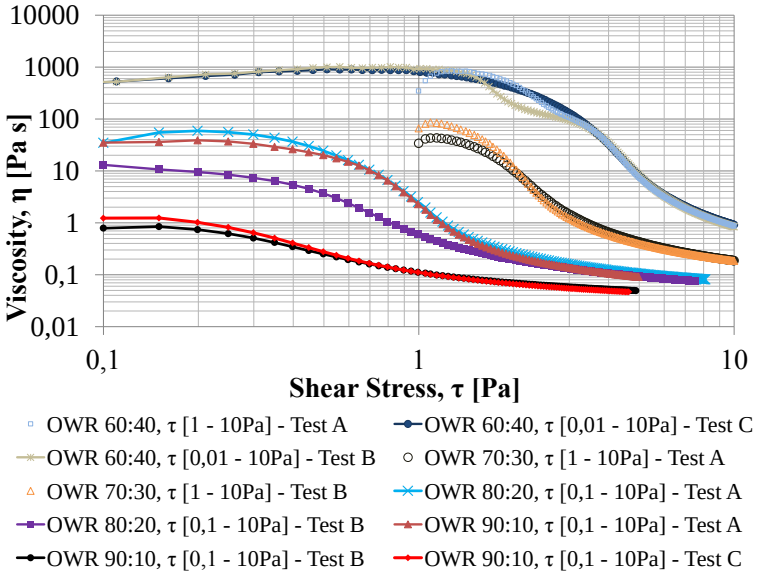

Figure 53: Controlled stress ramp for all fluids.

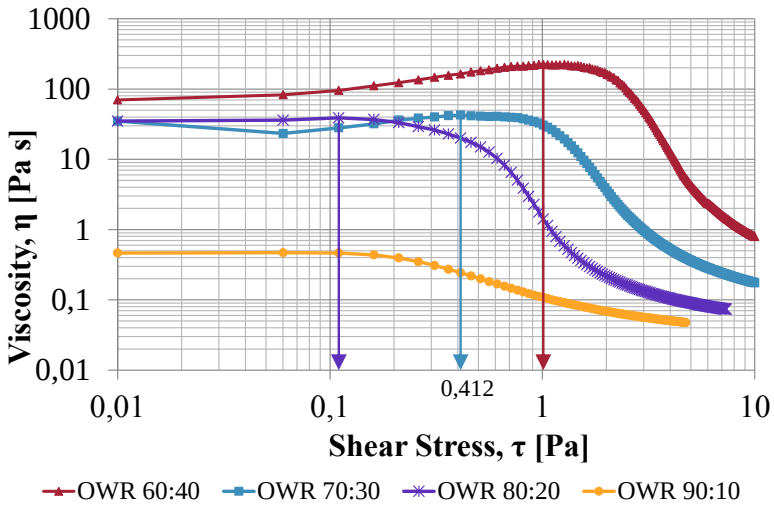

Figure 54: Controlled stress ramp for all fluids at $\tau = 0.01$Pa.

D.7 Shear rate ramp

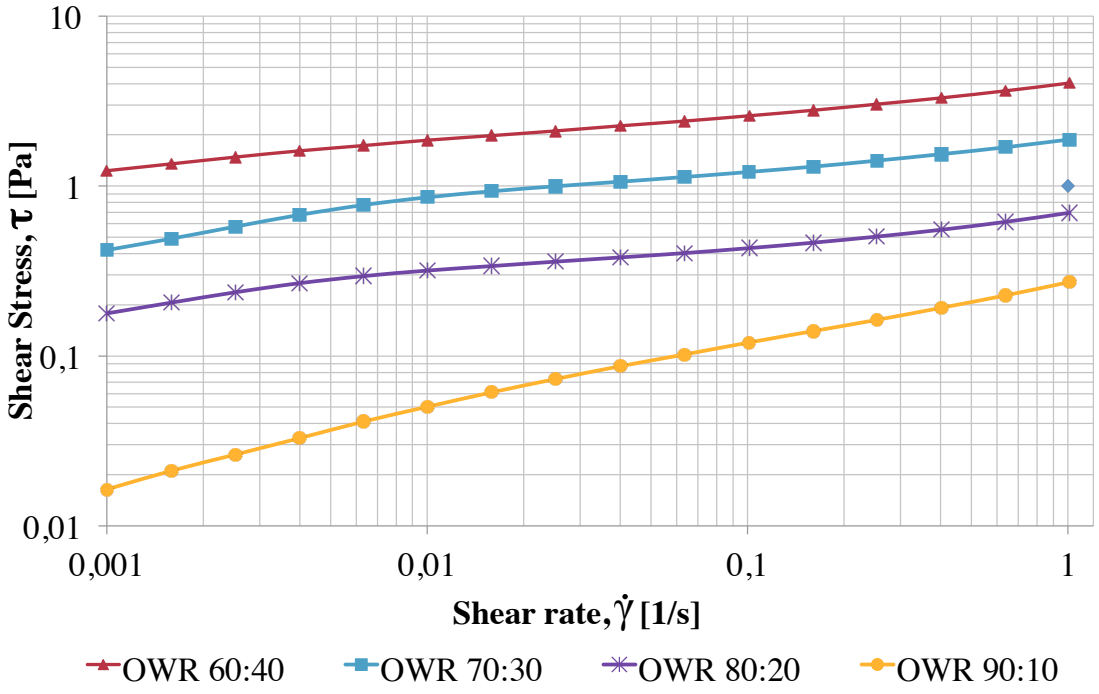

Figure 55: Low shear rate flow curves for all samples measured at 20°C. Used to evaluate yield stress in section 4.4.9.

E Summary of Unified hydraulics model used in simulation

The Unified hydraulics model can be applied to calculate frictional pressure loss in annuli and inside pipe. The equations that are being used for frictional pressure loss in pipe flow is presented first followed by the equations for annluar flow. Note that the units given in the following equations are in standard oil field units. The output values in this thesis are converted with conversion factors for the end results. The general equation is on the following form[14, 43]:

$$\tau = \tau_y + k\gamma^n$$

E.1 Pipe Flow

Plastic Viscosity

$$\eta_{pv} = \theta_{600} - \theta_{300}$$

Bingham Yield Point

$$\tau_y = 2\theta_{300} - \theta_{600}$$

Low Shear Yield Stress

$$\tau_0 = 2\theta_3 - \theta_6$$

Flow Behaviour index

$$n_p = 3.32 \log\left(\frac{2\eta_{pv} + \tau_y}{\eta_{pv} + \tau_y}\right)$$

Concisitency factor

$$K_p = \frac{\eta_{pv} + \tau_y}{511^{n_p}}$$

Geometrical factor used to calculate shear rate at wall, γ_w:

$$G = \left[\frac{(3-\alpha)n+1}{(4-\alpha)n}\right]\left[1+\frac{\alpha}{2}\right]; \qquad \alpha = 0 \quad \text{for pipe flow}$$

Mean velocity inside pipe

$$V_p = \frac{24,51Q}{d_i^2}$$

Shear rate at the wall

$$\dot{\gamma_w} = 1.6\frac{GV}{d_{hyd}}$$

where d_{hyd} is hydraulic diameter of pipe.

Shear stress at the wall

$$\tau_w = 1.066\left[\left(\frac{4-\alpha}{3-\alpha}\right)^n \tau_y + k\gamma_w^n\right]$$

Generalized reynolds number to define flow regime,

$$N_{Re_G} = \frac{\rho V_p^2}{19.36\tau_w}$$

For laminar flow regime:

$$f_{lam} = \frac{16}{N_{Re_G}}$$

For transitional flow:

$$f_{trans} = \frac{16 N_{Re_G}}{(3470 - 1370 \cdot n_p)^2}$$

For turbulent flow:

$$f_{turb} = \frac{a}{N_{Re_G}^b} \begin{cases} a = \frac{\log(n_p)+3.93}{50}. \\ b = \frac{1.75-\log(n_p)}{7}. \end{cases}$$

Fanning friction factor f:

$$f = (f_{int}^{12} + f_{lam}^{12})^{1/12}$$

where

$$f_{int} = (f_{trans}^{-8} + f_{turb}^{-8})^{-1/8}$$

Frictional pressure loss gradient

$$\left(\frac{dP}{dL}\right) = 1.076 \frac{f_p V_p^2 \rho}{10^5 D_i}; \qquad \text{[psi/ft]}$$

Pressure loss over the pipe length

$$\Delta P = \left(\frac{dP}{dL}\right) \cdot \Delta L$$

Pressure loss over bit nozzle

$$\Delta P_{nozzle}[\text{PSI}] = \frac{156 \rho q^2}{(D_{N_1}^2 + D_{N_2}^2 + D_{N_3}^2)^2}$$

Where D_N is nozzle diameter in inch

E.2 Annluar Flow

Plastic Viscosity

$$\eta_p = \theta_{600} - \theta_{300}$$

Bingham Yield Point

$$\tau_y = 2\theta_{300} - \theta_{600}$$

Low Shear Yield Stress

$$\tau_0 = 2\theta_3 - \theta_6$$

Flow Behaviour index

$$n_a = 3.32 \log\left(\frac{2\eta_{pv} + \tau_y - \tau_0}{\eta_{pv} + \tau_y - \tau_0}\right)$$

Concisitency factor

$$K_a = \frac{\eta_{pv} + \tau_y - \tau_0}{511^{n_a}}$$

Geometrical factor used to calculate shear rate at wall, γ_w:

$$G = \left[\frac{(3-\alpha)n+1}{(4-\alpha)n}\right]\left[1+\frac{\alpha}{2}\right]; \qquad \alpha = 1 \quad \text{for annular flow}$$

Mean velocity inside pipe

$$V_a = \frac{24,51Q}{d_o^2 - d_i^2}$$

Shear rate at the wall

$$\dot{\gamma_w} = 1.6\frac{GV}{d_{hyd}}$$

where d_{hyd} is hydraulic diameter of pipe.

Shear stress at the wall

$$\tau_w = 1.066\left[\left(\frac{4-\alpha}{3-\alpha}\right)^n \tau_y + k\gamma_w^n\right]$$

Generalized reynolds number to define flow regime,

$$N_{Re_G} = \frac{\rho V_a^2}{19.36\tau_w}$$

For laminar flow regime:

$$f_{lam} = \frac{24}{N_{Re_G}}$$

For transitional flow:

$$f_{trans} = \frac{16N_{Re_G}}{(3470-1370\cdot n_a)^2}$$

For turbulent flow:

$$f_{turb} = \frac{a}{N_{Re_G}^b} \begin{cases} a = \frac{\log(n_p)+3.93}{50}. \\ b = \frac{1.75-\log(n_p)}{7}. \end{cases}$$

Fanning friction factor f:

$$f = (f_{int}^{12} + f_{lam}^{12})^{1/12}$$

where

$$f_{int} = (f_{trans}^{-8} + f_{turb}^{-8})^{-1/8}$$

Frictional pressure loss gradient

$$\left(\frac{dP}{dL}\right) = 1.076\frac{f_a V_a^2 \rho}{10^5 D_o}; \qquad \text{[psi/ft]}$$

$$\Delta P[\text{PSI}] = \left(\frac{dP}{dL}\right) \cdot \Delta L$$

Pressure loss over bit nozzle

$$\Delta P_{nozzle}[\text{PSI}] = \frac{156\rho q^2}{(D_{N_1}^2 + D_{N_2}^2 + D_{N_3}^2)^2}$$

Where D_N is nozzle diameter in inch

E.3 Conversions Factors

Table 12: Conversion Factors.

Unit to change	To unit	Multiply by
PSI	Bar	0.06895
gal/min	liter/min	3.7854
feet	meter	0,3048
ppg	sg	0,12

To convert viscometer dial reading [°] to Pa:

$$1\text{dial reading} = 1,067[(\text{lb}/100\,\text{ft}^2)]$$

$$1[\text{lb}/100\,\text{ft}^2] = 0,48[\text{Pa}]$$

convert shear rate from RPM to s^{-1}

$$\dot{\gamma}[\text{s}^{-1}] = \text{RPM} \cdot 1,703$$